SURFACE-ENHANCED RAMAN SPECTROSCOPY AS A RAPID DETECTION METHOD FOR PATHOGENIC BACTERIA USING HIGHLY SENSITIVE SILVER NANOROD ARRAY SUBSTRATES

by

HSIAO-YUN CHU

(Under the Direction of YAO-WEN HUANG)

ABSTRACT

A portable SERS probe based on silver nanorod array has been developed. The substrate consists of a base layer of 500 nm Ag film and a layer of Ag nanorod array with length of ~1 μm deposited by oblique angle deposition method at a vapor incident angle of 86°. The incoming laser beam was designed to focus onto the SERS substrate at 45° incident angle to maximize SERS signal. With a fiber Raman system, a detection sensitivity of 10^{-17} moles for trans-1,2-bis(4-pyridyl)ethane molecules has been demonstrated.

SERS spectra of whole cell bacteria from several species and strains, including Gram positive and Gram negative have been obtained from this novel SERS substrate. Spectral difference between Gram types, species and strains were observed. Viable and noviable cells were also examined and significantly reduced SERS responses at major Raman bands were observed for noviable cells. The observation of SERS spectra of bacteria on single cell level excited at low incident powers (12 μW) and short collection time (10 s) was also demonstrated. SERS spectra of two different mixed cultures consisting of *E.coli* O157:H7 and *S. aureus*; *E.coli* O157:H7 and *S. typhimurium*, as well as their respective pure culture were measured. PCA was

applied to group these microorganisms based on their spectral fingerprints. The resultant PCs score plots showed correct grouping of these microorganisms, including discrimination between two pure cultures and the mixed culture in each case.

These results show that the highly sensitive silver nanorod arrays substrate is a potential analytical sensor for rapid identification of microorganisms with minimum sample preparation. In addition, SERS spectra can be utilized to identify a pure culture in a mixed cell populations via its spectral fingerprint as demonstrated by principle component analysis. This study shows that the integrated OAD silver nanorod arrays substrates and fiber Raman system has great potential as a portable and remote sensor for on-site biological or chemical detection.

INDEX WORDS: Bacteria identification, *E.coli* O157:H7, rapid method, portable sensor, silver nanorod array, surface-enhanced Raman scattering.

SURFACE-ENHANCED RAMAN SPECTROSCOPY AS A RAPID DETECTION METHOD FOR PATHOGENIC BACTERIA USING HIGHLY SENSITIVE SILVER NANOROD ARRAY SUBSTRATES

by

HSIAO -YUN CHU

B.S., Chinese Culture University, Taipei, Taiwan. 1992

M.S., The University of Georgia, Athens, GA. 1999

A Dissertation Submitted to the Graduate Faculty of The University of Georgia in Partial Fulfillment of the Requirements for the Degree

DOCTOR OF PHILOSOPHY

ATHENS, GEORGIA

2007

SURFACE-ENHANCED RAMAN SPECTROSCOPY AS A RAPID DETECTION METHOD FOR PATHOGENIC BACTERIA USING HIGHLY SENSITIVE SILVER NANOROD ARRAY SUBSTRATES

by

HSIAO-YUN CHU

Major Professor: Yao-Wen Huang

Committee: Jinru Chen
Leslie P. Jones
William S. Kisaalita
Yiping Zhao

Electronic Version Approved:

Maureen Grasso
Dean of the Graduate School
The University of Georgia
December 2007

DEDICATION

To my parents

Mr. Albert Chang-Shun Chu and Ms. Shen-Jung Lee

Their love and sacrifices make me what I am today.

ACKNOWLEDGEMENTS

I would like to express my sincere gratitude to Dr. Yao-Wen Huang for being my major advisor and for his support during my stay at UGA. I also like to express my deep appreciation to Drs. Jinru Chen, Les Jones, William Kisaalita and Yiping Zhao for serving on my advisory committee. In particular, I would like to thank Dr. Yiping Zhao for his guidance and support to this project and towards the completion of my study. The experience and knowledge I gained by working in his lab is invaluable.

I thank the National Science Foundation for funding and also the UGA engineering grant and the Food Science Department for funding my stay at UGA.

Many thanks are extended to my colleagues and friends in Food science department and in Dr. Zhao's laboratory for their help and assistance.

My deepest gratitude must go to my family. My parents, my sisters Chiao-Yun Chu, Li-Yun Chu, and my husband Scott P. Squeglia. Their caring, love, support and encouragement have lifted me through many of my difficult times and health crisis throughout my years at UGA. Finally, I want to acknowledge my unborn son, Seton Chu Squeglia to patiently wait a couple more weeks to be born, so I can finish my defense.

TABLE OF CONTENTS

Page

ACKNOWLEDGEMENTS v

LIST OF FIGURES vii

CHAPTER

1 INTRODUCTION 1

2 LITERATURE REVIEW 6

3 A HIGH SENSITIVE FIBER SERS PROBE BASED ON SILVER NANOROD ARRAYS 41

4 SILVER NANOROD ARRAY AS A SERS SUBSTRATE FOR PATHOGENIC BACTERIA DETECTION 64

5 SURFACE-ENHANCED RAMAN SPECTRA OF MIXED CULTURE: CLASSIFICATION BY PRINCIPLE COMPONENT ANALYSIS 97

6 SUMMARY AND CONCLUSIONS 119

7 FUTURE RESEARCH 122

APPENDICES 125

LIST OF FIGURES

Page

Figure 2.1: Schematic diagram showing the main components of biosensor.....12

Figure 2.2: Oblique angle deposition experimental setup 19

Figure 3.1: A typical SEM image of Ag nanorod array. The Ag nanorods have an average length of 868 ± 95 nm and an average diameter of 99 ± 29 nm. The scale bar represents 2 μm……..58

Figure 3.2: (a) The schematics of the fiber Raman setup for SERS measurement. (b) Photograph of SERS probe. (c) The schematic of the tilting Ag nanorods parallel to the incident plane at 45° incident angle relative to surface normal. 59

Figure 3.3: Typical SERS spectrum of bare substrate. The spectrum was collected at an excitation wavelength of 785 nm, incident laser power of 52 mW on the substrate and collection time of 10 s. 60

Figure 3.4: SERS spectra of BPE deposited on Ag nanorod substrate. The amount of adsorbed BPE on substrate was calculated to be from 10^{-17} to 10^{-16} moles. The spectra were collected at an excitation wavelength of 785 nm, incident laser power of 52 mW on the samples and collection time of 10 s. Spectra were offset for clarity.....61

Figure 3.5: Log- log plot of the integrated band areas at 1200 cm^{-1} in the SERS spectra of BPE against the number of moles of BPE deposited onto the Ag nanorod substrate surface. Spectra were collected from 5 spots for each application of BPE at an excitation wavelength of 785 nm, incident laser power of 52 mW on the samples and collection time of 10 s. The average intensities were plotted and the error bars represent the standard deviation values. 62

Figure 3.6: Plot of the integrated band areas at 1200 cm^{-1} in the SERS spectra of BPE as a function of time. The concentrations of BPE were from 10^{-6} to 10^{-5} M. Distilled water was used as solvent. The BPE solution was sucked out of the liquid cell before the next higher concentration was added. The elapsed time for each concentration was 80 min. The spectra were collected at an excitation wavelength of 785 nm, incident laser power of 96 mW on the samples and collection time of 10 s. 63

Figure 4.1: Raman spectra of (A) TSB medium; (B) *E. coli* O157 (10^8 CFU/ml) in TSB. Incident laser powers of 69 mW and collection time of 10 s were used to obtain these spectra. Spectra were vertically offset (30%) for clarity. 85

Figure 4.2: Raman spectra of (A) PBS; (B) *E. coli* O157 (10^8 CFU/ml) in PBS. Incident laser powers of 69 mW and collection time of 10 s were used to obtain these spectra. Spectra were vertically offset (30%) for clarity. 86

Figure 4.3: Raman spectra of (A) DI water; (B) *E. coli* O157 in DI water. Incident laser powers of 69 mW and collection time of 10 s were used to obtain these spectra. Spectra were vertically offset (10%) for clarity. 87

Figure 4.4: SERS spectra of (a) *S. typhimurium* and (b) *E. coli* O157:H7 normalized to the peak intensity of the most intense are overlapped in order to demonstrate the SERS signal reproducibility from different area of the same substrate. Spectra were collected from several spots on different substrates. Incident laser powers of 35 mW and collection time of 10 s were used to obtain these spectra. The standard deviation spectrum for each species is shown at the bottom of each panel.....88

Figure 4.5: A SEM image of *E. coli* bacteria on a silver nanorod array substrate. The scale bar represents 2 μm. Since the cells did not appear to have lysed, the shifts observed in the SERS spectra are a product of cell wall biochemistry or other chemical components external to the cell. 89

Figure 4.6: SERS spectra of four bacterial species obtained on silver nanorod array substrates. EC, *E. coli* O157:H7; ST, *S. typhimurium*; SA, *Staphylococcus aureus* and SE, *Staphylococcus epidermidis*. Incident laser powers of 24 mW and collection time of 10 s were used to obtain these spectra. Spectra were offset vertically for display clarity.....90

Figure 4.7: SERS spectra of the *E. coli* strains. EC, *E. coli* O157:H7; DH, *E. coli* DH 5σ; GE, generic *E. coli*. Incident laser powers of 69 mW and collection time of 10 s were used to obtain these spectra. Spectra collected from multiple spots for each strain were baseline corrected and normalized to the most intense band. Spectra were offset vertically for display clarity. 91

Figure 4.8: The average SERS signal of generic *E. coli* (GE), *E. coli* O157:H7 (EC) and *E. coli* DH 5α (DH) between 400-800 cm^{-1}. Incident laser powers of 69 mW and collection time of 10 s were used to obtain these spectra. Spectra collected from multiple spots for each strain were baseline corrected and normalized to the most intense band.....92

Figure 4.9: The average SERS signal of generic *E. coli* (GE), *E. coli* O157:H7 (EC) and *E. coli* DH 5α (DH) between 800-1100 cm^{-1}. Incident laser powers of 69 mW and collection time of 10 s were used to obtain these spectra. Spectra collected from multiple spots for each strain were baseline corrected and normalized to the most intense band.....93

Figure 4.10: SERS spectra of viable *E. coli* O157:H7 and nonviable *E. coli* O157:H7. Incident laser powers of 14 mW and collection time of 10 s were used to obtain these spectra. Spectra were offset vertically for display clarity.....94

Figure 4.11: SERS spectra of viable and nonviable *E. coli* DH 5α. Incident laser powers of 14 mW and collection time of 10 s were used to obtain these spectra. Spectra were offset vertically for display clarity. 95

Figure 4.12: Raman microscope measurement. Bacteria imaging under 50× microscope objective, (a) single *E. coli* O157:H7 two-three cell chain contributing to the SERS spectrum (b) a multiple cell cluster contributing to the SERS spectrum. SERS spectra of single *E. coli* O157:H7 two-three cell chain and a multiple cell cluster are offset vertically for display clarity. Incident laser powers of 12 μW and collection time of 10 s were used to obtain these spectra.....96

Figure 5.1: Typical SERS spectra of two bacterial species and its mix culture obtained on silver nanorod array substrates. EC, *E. coli* O157:H7; ST, *S. typhimurium*; Mix, mix culture of *E. coli* O157:H7 and *S. typhimurium*. Incident laser powers of 28 mW and collection time of 10 s were used to obtain these spectra. Spectra were offset vertically for display clarity.....112

Figure 5.2: The average SERS response for each of the samples between 500-900 cm^{-1}. EC, *E. coli* O157:H7; ST, *S. typhimurium*; Mix, mix culture of *E. coli* O157:H7 and *S. typhimurium*. Incident laser powers of 28 mW and collection time of 10 s were used to obtain these spectra. 113

Figure 5.3: The average SERS response for each of the samples between 1200-1800 cm^{-1}. EC, *E. coli* O157:H7; ST, *S. typhimurium*; Mix, mix culture of *E. coli* O157:H7 and *S. typhimurium*. Incident laser powers of 28 mW and collection time of 10 s were used to obtain these spectra. 114

Figure 5.4: Typical SERS spectra of two bacterial species and its mix culture obtained on silver nanorod array substrates. EC, *E. coli* O157:H7; SA, *Staphylococcus aureus*; Mix, mix culture of *E. coli* O157:H7 and *Staphylococcus aureus*. Incident laser powers of 24 mW and collection time of 10 s were used to obtain these spectra. Spectra were offset vertically for display clarity. 115

Figure 5.5: The average SERS response for each of the samples between 400-900 cm^{-1}. EC, *E. coli* O157:H7; SA, *Staphylococcus aureus*; Mix, mix culture of *E. coli* O157:H7 and *Staphylococcus aureus*. Incident laser powers of 24 mW and collection time of 10 s were used to obtain these spectra. 116

Figure 5.6: (A) PCA scores plot of *E. coli* O157:H7 (EC); and *S. typhimurium* (ST) pure cell samples; (B) PCA scores plot of pure cell samples and their mixed cell samples (M). The PCA model was constructed using the spectral range from 400-1800 cm^{-1}. 117

Figure 5.7: (A) PCA scores plot of *E. coli* O157:H7 (EC); and *S. aureus* (SA) pure cell samples; (B) PCA scores plot of pure cell samples and their mixed cell samples (M). The PCA model was constructed using the spectral range from 400-1800 cm^{-1}. 118

CHAPTER 1

INTRODUCTION

Recently, there has been a renewed interest in the detection methods of bacteria, especially those species that are involved in foodborne diseases, water contamination, clinical cases and biological warfare. It is largely as a result of increased incidences of *Escherichia coli* O157:H7, *Salmonella* outbreaks, the spread of the antibiotic-resistant *Staphylococcus aureus*, and the use of anthrax (*Bacillus anthracis*) as a source of bioterrorism in the United States. The development of alternative detection method to identify pathogens rapidly, nondestructively and distinctively has major benefit to epidemic outbreak and bioterrorism prevention. Conventional microbiological methods for the presence of microorganisms often involve pre/enrichment and isolation of presumptive colonies of bacteria on solid media, and final confirmation by biochemical and/or serological identification. Thus, they are laborious and time consuming. To overcome these disadvantages, molecular and immunological techniques such as PCR and ELISA have been commonly adopted in pathogen detection. Biosensor technology based on antibodies- antigen interaction or DNA to provide specificity also draws a lot of interest. However, certain reagents still require for these techniques and there is limitation for discriminating viable and nonviable cells for DNA based methods.

Over the years, new techniques in chemical and biological sensing have set new stage for pathogen detection. One of the alternative approaches towards the rapid identification of pathogens is based on spectroscopic techniques due to its ability to detect pathogens nondestructively. Fourier transform infrared spectroscopy is starting to become an accepted technique in microbiology. For its vibrational spectroscopic counterpart, Raman spectroscopy, the potential is equally. In contrast to infrared spectroscopy, Raman spectroscopy offers other advantages for aqueous samples because water itself does not significantly affect Raman spectra. It has been used to obtain highly structured information on bacteria (Nelson et al., 1992 and Wu

et al., 2001), even at the single bacterial cell level (Alexander et al., 2003). Although Raman sensitivity is low in comparison to IR spectroscopy, it can be greatly increased by the surface-enhanced Raman scattering.

Surface-enhanced Raman spectroscopy (SERS) has been used as an analytical tool to observe trace amount of chemical and biological molecules due to its capability of giving real-time molecular vibrational information under ambient conditions. In addition to signal enhancement, SERS has a fluorescence-quenching effect (Kneipp et al., 2002). This is extremely valuable when investigating microorganisms, which often exhibit fluorescence background under excitation in the near-infrared to visible regions. We believe SERS to be a sensitive analytical tool that can be used to study low concentration of bacteria and provide fingerprinting capability to discriminate among different bacteria. The main challenge with SERS is in the ability to generate reproducible substrates with the correct surface morphology that provide maximum SERS enhancements, without which, reproducible spectra and quantitative analysis is difficult.

Silver nanorod substrates prepared by the oblique angle deposition (OAD) technique have previously been shown to provide SERS enhancement factors of ~10^8 and have also been shown to be SERS active (Chaney et al., 2005). Very recently, the OAD prepared SERS substrates demonstrated its potential to distinguish between viruses (Shanmukh et al., 2006). The OAD technique offers an easy and inexpensive way for the fabrication of silver nanorod arrays for high sensitivity SERS applications. The SERS substrates produced by OAD have the advantages of uniformity and reproducibility.

The overall objectives of this work were to develop a SERS-based sensor using silver nanorod substrates fabricated by OAD technique and to integrate the SERS-based sensor with a fiber optic Raman spectroscopy as a potential portable pathogen sensor. There are three research

chapters in this work. The first research chapter dealt with investigation of the sensitivity of the silver nanorod substrate integrated into a specially designed portable SERS probe, a molecular probe, trans-1,2-bis(4-pyridyl)ethane was used. The second chapter objective was to distinguish different species and strains of bacteria based on their SERS spectral variation obtained on the novel silver nanorod array. Viable cells and nonviable cells were also compared. The objective of the last chapter was to study the capability of Ag nanorod substrates in differentiating pure culture from mixed culture based on their SERS fingerprints. Principle component analysis was also applied for classification of the samples.

References

Alexander, T. A. Pellegrion, P. M. and Gillespie, J. B. "Near-infrared surface-enhanced Raman scattering mediated detection of single optically trapped bacterial spores," Appl. Spectrosc. 57, 1340-1345 (2003).

Chaney, S. B. Shanmukh, S. Dluhy, R. A. and Zhao, Y.- P. "Aligned silver nanorod arrays produce high sensitivity surface-enhanced Raman spectroscopy substrates," Appl. Phys. Lett. 87, 031908.1-3 (2005).

Kneipp, K. Haka, A. S. Kneipp, H. Badizadegan, K. Yoshizawa, N. Boone, C. Shafer-Peltier, K. E. Motz, J. T. Dasari, R. R. and Feld, M. S. "Surface-enhanced Raman spectroscopy in single living cells using gold nanoparticles," Appl. Spectrosc. 56, 150-154 (2002).

Nelson, W. H. Manoharan, R. and Sperry, J. F. "UV Resonance Raman studies of bacteria," Appl. Spectrosc. Rev. 27, 67-124 (1992).

Shanmukh, S. Jones, L. Driskell, J. Zhao, Y.-P. Dluhy, R. and Tripp, R. A. "Rapid and sensitive detection of respiratory virus molecular signatures using a silver nanorod array SERS substrate," Nano Lett. 6, 2630-2636 (2006).

Wu, Q. Hamilton, T. Nelson, W. H. Elliott, S. Sperry, J. F. and Wu, M. "UV Raman spectral intensities of E. coli and other bacteria excited at 228.9, 244.0 and 248.2 nm," Anal. Chem. 73, 3432-3440 (2001).

CHAPTER 2

LITERATURE REVIEW

Importance of Foodborne Pathogen

Rapid pathogen detection and identification is increasingly becoming important on the wake of national concern over bioterrorism, especially those pathogens that are involved in food poisoning, water contamination and biological warfare. Food processing quality control and food material supply chain control are among our national security interests. The interest in rapid detection has also increased as a result of heighten consumer awareness and concerns over unexpected foodborne disease outbreaks. Contamination of foods by bacterial pathogens (such as *Escherichia coli*, *Salmonella typhimurium*, *Campylobacter jejuni*, etc.) results in numerous foodborne diseases. The Centers for Disease Control (CDC) estimates that foodborne diseases cause approximately 76 million illnesses, 325,000 hospitalizations, and 5,000 deaths in the United States each year (Mead et al., 1999). Known pathogens are estimated to cause about 72% of all food-borne deaths. The estimated economic costs of foodborne illness caused by *Salmonella* and *E.coli* O157:H7 was approximately 2.9 billion dollars in 2006 (ERS, 2007). Recent examples of the foodborne outbreaks are; the *E. coli* O157:H7 contaminated spinach infected hundreds of people from 26 states and resulted in three deaths in 2006; and the *Salmonella* outbreak linked to Peter Pan Peanut butter in 2007.

In the past twenty years, *Escherichia coli* O157:H7 has become a very important bacterium especially in regard to its significance in causing diseases for human. It was first recognized as a cause of illness in 1982 during an outbreak of severe bloody diarrhea and is one of hundreds of strains of the bacterium Escherichia coli. Although most strains are harmless and live in the intestines of healthy humans and animals, this particular strain produces a powerful toxin and can cause severe illness. In United States, an estimated 73,000 cases of infection, 2100 hospitalizations and 61 deaths occur each year. Infection often leads to bloody diarrhea, and

occasionally to kidney failure. Most illness has been associated with eating undercooked, contaminated ground beef. Person-to-person contact in families and child care centers is also an important mode of transmission. Infection can also occur after drinking raw milk and after swimming in or drinking sewage-contaminated water. *E. coli* O157:H7 is a Gram-negative rod-shaped bacterium producing Shiga toxin(s). Although the exact infectious dose is unknown, it has been estimated to be around 10-100 organisms (Feng and Weagant, 1998). The low infectious dose of this pathogen enables that cross-contamination can occur readily and can involve a diverse range of vehicles. The serious nature of the symptoms of hemorrhagic colitis and hemolytic uremic syndrome caused by *E. coli* O157:H7 place this foodborne pathogen in a category apart from those typically cause only mild symptoms.

Salmonellosis is one of the most commonly reported infections in the United States. The centralization of food industries' production and large-scale distribution has doubled the salmonellosis incidence in the past two decades, highlighting the importance of *Salmonella spp*. as the leading cause of foodborne bacterial diseases in humans (Altekruse et al., 1997). *Salmonella Typhimurium* is among the most common *Salmonella* serotypes causing salmonellosis infections in the US. Typhoid fever caused by *S. typhimurium* leads to 16.6 million cases and 600,000 deaths annually, with the vast majority of cases occurring in Southeast Asia, Africa and South America (Shangkuan and Lan, 1998). *Salmonella* is readily transmitted through the faces of people or animals. The integrated meat and poultry production and processing industries render raw poultry and meats principal vehicles of human foodborne salmonellosis. Like *E. coli* O157:H7, *Salmonella Typhimurium* is also Gram-negative rod-shaped, motile bacterium. The infective dose, depends on age and health of host, and strain differences, has been estimated to be as few as 15- 20 cells.

Established Methods for Pathogen Detection

Conventional bacterial identification methods usually include a morphological evaluation of the microorganism as well as tests for the microorganism's ability to grow in various media under a variety of conditions. Conventional methods generally have four distinct phases: 1) preenrichment, to allow growth of all organisms; 2) selective enrichment, to allow growth of the organism under investigation and to increase bacterial population to a detectable level; 3) isolation, by using selective agar plates; and 4) conformation, serological and biochemical tests to confirm the identification of a particular pathogenic organism. While these methods can be sensitive, inexpensive and give both qualitative and quantitative information on the number and the nature of the microorganisms tested, they are greatly restricted by assay time, with initial enrichment needed in order to detect pathogens which typically occur in low numbers in certain foods and in water.

Though the conventional culture method has been the gold standard, newer technologies have been used for bacterial detection. For example, the polymerase chain reaction (PCR) can be used to amplify small quantities of genetic material to determine the presence of bacteria. It is based on the isolation, amplification and quantification of a short DNA sequence. Target nucleic segments of defined length and sequence are amplified by repetitive cycles of strand denaturation, annealing, and extension of oligonucleotide primers by the thermostable DNA polymerase. The PCR method is extremely sensitive, a single cell or viral particle can be detected in about an hour compared with conventional methods that may require days or even weeks. However, a major disadvantage for PCR is that the amount of DNA sequence known for a given organism may be limited, and the DNA sequence must be unique for the target organism (Newton and Graham, 1997). Other problems associated with DNA based methods, such as the

sensitivity of the polymerase enzyme to environmental contaminants, difficulties in quantification, the generation of false positives through the detection of naked nucleic acids, non-viable microorganisms, or contamination of samples in the laboratory (Toze, 1999).

Immunological detection dependent on antibody-antigen recognition and interactions has been successfully employed for the detection of cells, spores, viruses and toxins (Iqbal et al., 2000). There are many commercial immunoassays available for the detection of a wide variety of microbes and their products. Enzyme-linked immunosorbent assay (ELISA) test is the most established technique nowadays as well as the source of inspiration for many biosensor applications. ELISA combines the specificity of antibodies and the sensitivity of simple enzyme assays by using antibodies or antigens coupled to an easily assayed enzyme. While DNA-based detection may be more specific and sensitive than immunological-based detection, the later is more robust and has the ability to detect not only contaminating organisms but also their biotoxins that may not be expressed in the organism's genome. However, one of the disadvantages of ELISA method is the long incubation time required for each ELISA step. Also, the sensitivity of ELISA methods is insufficient for direct measurement of bacteria and other microorganisms in the original samples. Especially for those biological sample contains very low numbers of pathogenic bacteria. Even though immunological-based and nucleic acid-based detection have greatly decreased assay time compared to conventional culture techniques, they still lack the ability to detect microorganisms in "real-time".

Nanobiosensor

A biosensor is a device that consists of a biological recognition element or bio-receptor and a signal transducer. When the analyte interacts with the bio-receptor, the biological event

elicits a physicochemical change at the bio-interface, which is converted by the transducer to an measurable signal (either electronic or optical). The output from the transducer is then processed and finally displayed as a measurable signal in real time (Chaplin and Burcke, 1990). Figure 2.1 illustrates the schematic of a typical biosensor. The most common types of bio-receptor/analyte complexes are based on: (1) antibody/antigen interactions, (2) nucleic acid interactions, (3) enzymatic interactions, (4) cellular interactions (e.g. microorganisms, proteins) and (5) interactions using biomimetic materials (e.g. synthetic bio-receptors). The most prevalent signal transduction methods include: (1) optical measurements (e.g. luminescence, absorption, scattering, etc.), (2) electrochemical (e.g. potentiometric, amperometric, etc.) and (3) mass-sensitive measurements (e.g. surface acoustic wave, microcantilever, microbalance, etc.). Biosensors show great potential especially in the area of clinical diagnostics, food analysis and environmental monitoring because they allow the detection of a broad spectrum of analytes in complex sample matrices with minimum sample pretreatment (Feng, 1992; Alvarez-Icaza and Bilitewski, 1993; Deshpande and Rocco, 1994).

Biosensors can also be classified into two broad categories: sensors for direct detection of the target analyte and sensors with indirect detection. Direct detection biosensors are based on direct measurement of physical phenomena occurring during the biochemical reactions on a transducer surface. Signal parameters such as changes in pH, oxygen consumption, ion concentrations, potential difference, current, resistance, or optical properties can be measured by electrochemical or optical transducers. Indirect detection biosensors are those that involve a preliminary biochemical reaction to produce a product before detecting by a sensor. Indirect detection usually requires labeling of the product to facilitate the detection.

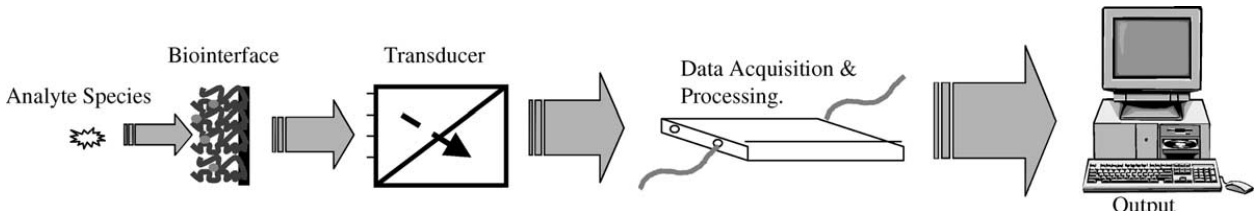

Fig. 2.1. Schematic diagram showing the main components of a biosensor (adapted from Chaplin and Burcke, 1990).

Nanotechnology is the creation and utilization of materials, devices, and systems through the control of matter on the nanometer scale (1 billionth of a meter-length scale). The significance of nanotechnology is based on the fact that some structures smaller than 100 nm have new properties and behaviors that are not exhibited by the bulk matter of the same composition. Nanostructures that are smaller than the characteristic lengths associated with the specific phenomena often display new chemical and physic properties that depend on the size (Riu et al., 2006). The unusual properties and behaviors of nanostructure usually not found in bulk material propel the development of novel devices and applications previously unavailable. One of the applications of nanotechnology is in the development of improved chemical and biological sensors with dimensions on the nanometer scale. Nanosensors of various types have made significant progress in their development and their applications in environmental analysis and clinical diagnostics (Kewal, 2005). To achieve stable, direct, and reproducible screening and detection, the integration of biological systems and nanostructured materials requires information to be induced across the interface in a consistent and reproducible format. The advances in the field of nanotechnology and processing have provided fabrication and strategies to reproducibly develop nanostructured materials that project tremendous potential towards the development of

new sensor designs with unique capabilities. Sensors utilizing optical output are especially attractive as they allow direct label-free and real time detection. Raman spectroscopy has numerous applications in various fields, and is of our primary interest. Thus we focus our discussion on Raman spectroscopy, in particular surface-enhanced Raman spectroscopy, and its application in bacterial detection in the following.

General Aspects of Raman Spectroscopy

Spontaneous Raman Scattering

When light is incident on matter, it can interact with the atoms or molecules in several ways. Photons can be absorbed or can be scattered. When light is scattered from a molecules, most photons are elastically scattered. The scattered photons have the same energy (wavelength) as the incident photons. However, a small fraction of light (approximately 1 out of 10^6-10^8 photons) is scattered at optical frequencies different from the frequency of the incident photons. The incident photons interact with the molecules in such a way that energy is either gained or lost so that the scattered photons are shifted in frequency. Such inelastic scattering is called Raman scattering. Raman scattering can occur due to changes in vibrational, rotational, or electronic energy of a molecules. The observation of Raman scattering is in some cases limited by the excitation of fluorescence, which typically exhibits an intensity that is several orders of magnitude stronger than Raman scattering. This occurrence is critical in investigations of biomolecules because they often contain fluorophores, which fluoresce when excited with light in the visible range. This problem can be addressed by extending the excitation wavelength to the near infrared region, where fluorescence background is reduced and photochemical changes in sample is less likely to occur (Chase and Parkinson, 1988).

As an optical spectroscopy, the Raman scattering effect can be applied non-invasively under ambient conditions. Measuring a Raman spectrum does not require special sample preparation techniques. Optical fiber probes are used to bring excitation laser light to the sample and transport scattered light to the spectrograph, therefore enable remote detection of Raman signals. The main advantages of Raman spectroscopy are its capability to provide rich information about the molecular structure of the sample and it does not suffer from water interference as water is very weak scatterer. Recently, sophisticated data analysis techniques based on multivariate analysis have made it possible to exploit the full information content of Raman spectra and to draw conclusions about the chemical structure and composition of very complex systems such as biological materials.

However, the application of Raman spectroscopy for trace analysis has been limited by the fact that the Raman cross section is inherently small. Because of the extremely small Raman cross sections, typically at least ~10^8 molecules are necessary to generate a measurable normal Raman scattering signal (Kneipp et al, 1999). With only 1 in 10^8 incident photons resulting in Raman scattering, a large number of molecules are required to achieve adequate conversion rates from excitation laser photons to Raman photons, limiting the detection of molecules in cells or tissue with very low concentration. Besides, certain biological systems exhibit high fluorescence quantum yields. Raman spectra collected with a visible laser from biological samples can often be plagued with fluorescence, which exhibits much broader Raman peaks, can dominate the sharp spectra and often need to be removed mathematically. To further enhance Raman efficiencies to enable trace level detection, surface-enhanced Raman scattering (SERS), the phenomenon of a strongly increased Raman signal from molecules attached to metallic nanostructures, is often employed.

Surface-Enhanced Raman Scattering

The effect of drastically enhanced Raman signals from molecules adsorbed on an electrochemically roughened silver surface was discovered by Fleischmann et al (1974). The surface enhancement effect generally can be explained by two major mechanisms; (1) electromagnetic (EM) enhancement, sometime referred to as the field effect, and (2) chemical enhancement, sometime referred to as first layer effect or charge transfer effect (CT) (Moskovits, 1985). Electromagnetic enhancement, thought to contribute more to the overall magnitude of enhancement, takes place at the surface of the metal where the molecule experiences enhanced local optical fields caused by excitation of electromagnetic resonances. The redistribution and concentration of electromagnetic energy coupled with the incoming electric field from the incident radiation, generates a larger spectroscopic signal for an analyte "caught" in both fields. To achieve the EM effect, analyte molecule is not required to be in contact with the metallic surface but can be located anywhere within the range of the enhanced local field. A roughen silver surface can induce a SERS enhancement factor of 10^6, whereas a smooth silver surface produces only 10-400 fold Raman enhancement (Udagawa et al., 1981). For isolated single colloidal silver spheroids (10-100 nm diameter), maximum values for electromagnetic enhancement has been calculated to be on the order of 10^6-10^7 (Wang and Kerker, 1981, Zeman and Schatz, 1987). The dependence of the SERS enhancement on surface roughness exhibits different excitation profiles for different surface preparations. In general, there is an optimal size of roughness for each type of surface structure. Because the strength of the local electromagnetic field at the surface has its maximum in the direction perpendicular to the surface, vibrational modes from changes in the polarizability of the adsorbate that are perpendicular to the surface will be preferentially enhanced. The normal direction of the electromagnetic field, in

combination with the fact that the electromagnetic effect strongly decreases with the distance from the surface, allows one to determine the adsorbate's orientation with respect to the average surface normal and the nature of the functional groups close to the surface (Creighton, 1983; Moskovits, 1985).

Chemical enhancement is thought to take place at sites of atomic-scale roughness on the metal surface and involves electronic coupling (an exchange of electrons) between the metal substrate and the adsorbed molecules, resulting in an electronic enhancement. A major difference between the electromagnetic and chemical effects is the fact that the chemical effect contribution to SERS is necessarily short-ranged (0.1-0.5 nm). This mechanism depends on the adsorption site, the geometry of bonding, and the energy levels of the adsorbate molecule. For specific adsorbate-surface systems, the enhancements may be large. The contribution of charge-transfer processes to SERS has been estimated to be approximately $10\text{-}10^3$ (Persson, 1981; Adrian, 1982). Experimental data have shown that adsorption of molecules to local defect sites on smooth metal surface results in an approximately 15-65 fold enhancement of the Raman signal for pyridine (Jiang and Campion, 1987). Chemical enhancement can provide useful information on chemisorption interactions between metal and adsorbate. However, this enhancement is not a general mechanism and is applicable only to specific adsorbate-metal surface systems. Additional enhancement can be provided by closely spaced interacting particles, or by sharp features and large curvature regions which may exist on silver and gold nanostructure.

In order to optimize the electromagnetic surface enhancement effect, the chosen laser excitation wavelength should be in resonance with the broad band of the surface plasmon vibrations of the select metal. For silver and gold, the surface plasmon bands are typically in the visible (500-700 nm) to near-infrared region (700-1300 nm) (Chen et al., 1980). Near-infrared

(NIR) excitation has additional spectroscopic application; the fluorescence background from analytes and impurities that are adsorbed on the metallic substrates can be reduced at longer wavelength excitation. The quenching of fluorescence, which occurs as a result of charge transfer and radiationless energy transfer to the metal surface, can efficiently reduce the luminescence from the adsorbed molecules and allow the detection of excellent vibrational spectra over wide frequency ranges from minimum amounts of substances (Kerker, 1984).

SERS-Active Substrates

The metal substrates used for SERS generally fall into several groups: noble metals (e.g., Ag, Cu and Au), free-electron-like metals (e.g., Al) and transition metals (e.g., Ni). Since the morphology of the metallic structure plays a major role in determining the magnitude of signal enhancement and sensitivity of detection, different types of substrates have been used. The SERS substrates usually have a metallic fine structure with dimensions of the order of nanometers. The necessary roughness can be achieved in a number of ways: electrochemical (oxidation and reduction of electrodes), photochemical (photoreduction of adsorbates on electrodes, single crystals or powder surfaces), lithography (grating structures on Ag surfaces or uniformly shaped Ag microstructures on an array of silica posts), vapor deposition (clusters of a few metal atoms surrounded by a matrix), mechanical polishing (use of different-sized abrasives), chemical reduction (metal colloids produced in aqueous solution or deposited on rough or flat surfaces) and evaporation (vacuum deposition of metallic films on smooth insulating or metallic substrates).

Various forms of nanostructure have been studied for the SERS effects, for example; a random distribution of roughness features produced by oxidation reduction on a metal electrode (Stacy et al., 1983), evaporation of thin metal film on a flat substrate (Kovacs et al. 1986), rough

metallic surfaces by chemical etching (Carron et al., 1991), silver films on TiO_2 (Sudnik et al. 1996), colloidal silver nanoparticles (Nie and Emory, 1997), silver nanoparticle arrays fabricated by nanosphere lithography (Jensen et al. 2000), electro-deposition of silver on silver films at high potential (Suer et al., 2000), aligned monolayer of silver nanowires (Tao et al., 2003). Roughen metal electrodes were the first SERS-active surface discovered and have been mostly used for theoretical study because the experimental conditions can be adjusted more easily to support the EM and CT models. Metal colloidal particles are widely used due to the ease of formation and manipulation, and the dependence of the enhancement on particle size and shape. However, analyte-induced coagulation of the colloidal dispersion often causes instability of the entire system, and the SERS activity of a given analyte usually depends on the preparation protocols. Metal nanoparticle films and nanostructured substrates were then developed and used as SERS-active media for a wide variety of areas, especially in applications requiring reproducible results. Many of these substrate preparation methods still face the obstacle of reproducing substrates of the correct surface morphology to provide maximum SERS enhancements. Without uniformity and good reproducibility of the metal substrates, the attainment of reproducible spectra remains a major challenge for SERS.

Nanostructure Fabrication using Oblique Angle Deposition

Oblique angle deposition technique (OAD) is a simple modification of conventional physical vapor deposition methods. OAD involves positioning the substrate at a specific angle such that incident metal vapour atoms are deposited on a substrate at a large incident angle (>70°) with respect to the surface normal of the substrate. This process results in the preferential growth of isolated nanocolumnar structures on the substrate tilted towards the direction of the

vapour source. Directional columnar growth is a result of surface diffusion and atomic shadowing effects that occur at the substrate surface (Abelmann and Lodder, 1997). During the initial stages of thin film deposition by vapor, adatoms condense onto the substrate and form individual separated islands or nuclei (Kaiser, 2002). As the incident vapour proceed to arrive on the substrate at a oblique angle, the initial nucleated islands will act as shadowing centers, all the taller islands will capture more atoms than the shorter ones do (shadowing effect), resulting in the formation of columns growing in the direction of the vapour source. The experimental setup of OAD is illustrated in Figure 2.2

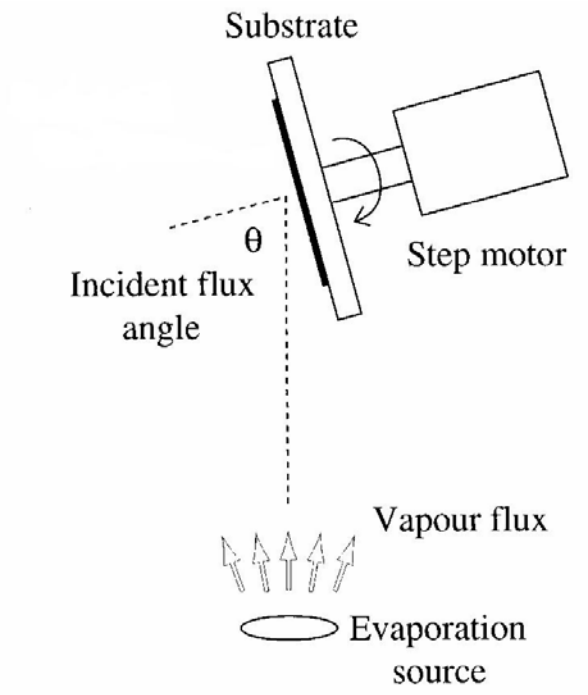

Fig. 2.2. Oblique angle deposition experimental setup

The major advantages of OAD technique include: a) control over the size, shape, and density of the nanostructures by varying the deposition conditions such as the incident vapor flux angle, temperature and the duration and rate of deposition; b) a wide variety of elements can be used to form these nanostructures as long as the material used can be evaporated; c) any standard

physical vapor deposition system equipped with a holder capable of rotation in the polar and azimuthal directions can be utilized. By rotating the substrate at controlled speeds in an azimuthal direction, it is possible to produce complex and unique nanostructure designs (Zhao et al., 2003).

Silver nanorod substrates prepared by the OAD technique with length of ~868 nm, diameter of ~99nm, and tilting angle of 73° have previously been shown to provide SERS enhancement factors of $>10^8$ for the molecular probe, trans-1,2-bis(4-pyridyl)ethane (BPE) (Channey et al. 2005; Zhao et al., 2006). The silver nanorod arrays fabricated by OAD generate large SERS response with maximum SERS intensity observed at around 45° incident angle. The maximum SERS intensity is about five times the intensity at the surface normal (Liu et al., 2006). The OAD technique offers a flexible, easy and inexpensive way for the fabrication of silver nanorod arrays for high sensitivity SERS applications. Very recently, OAD fabricated silver nanorod arrays substrate has been used as a SERS active substrate to distinguish between viruses and even different strains of viruses (Shanmukh et al., 2006).

Application of SERS Active Substrates in Bacteria Detection

The potential of SERS for studying biomolecules was exploited since the early eighties. SERS spectra have been measured from amino acids and peptides, also from 'large' molecules such as proteins, DNA and RNA. For DNA and RNA, it can take hours until stable and strong SERS spectra appear. This might indicate that these relatively large molecules need a long time to achieve stationary adsorption states on SERS-active sites of the surface which allowed a strong SERS enhancement (Kneipp et al., 1991). SERS can also be applied to the analysis of more complex structures than proteins, such as whole bacteria. A key problem in application of

SERS is developing SERS active substrates that provide reproducible and large enhancement factors and are compatible to biological environment. Silver and sometimes gold have been used to generate SERS active substrates for applications in biological science. Various forms of SERS substrates have been used to obtain spectra for bacteria, such as, bacteria coated by silver metal deposits, bacteria co-deposited with silver colloid aggregates on inert substrates, bacteria in silver and gold colloid solutions, and bacteria placed on electrochemically roughened metal surfaces. In the following, we discuss examples of bacteria detection by SERS.

Bacteria Coated by Silver Metal Deposits

One of the most common SERS substrates used for biological system is colloidal silver particles. Efrima and Bronk (1998) reported SERS spectra of *Escherichia coli* obtained after depositing nanocolloidal silver particles on the outer cell wall (an external coating) of *E. coli*. The silver colloid-bacteria combination was achieved by soaking washed bacteria in 0.05 M sodium borohydride. After serial of centrifugation, the bacteria were re-suspended in silver nitrate solution. This resulted a smaller than 0.05μm of thickness of the silver coating at the bacterial wall. Intense surface-enhanced Raman signals were observed at 514.5 nm excitation using 1-2 mW power for these silver coated *E. coli* bacteria. The same procedures were also applied to study of *Bacillus megaterium*. The SERS spectra of *B. megaterium* were essentially the same as for *E. coli*, reflecting the basic similarity of cell and cell wall chemical composition for even very different bacterial species. Zeiri et al. (2002) extended the work, spreading the silver nanocolloid coated bacterial cells on microscope slides and dried them overnight to obtain SERS spectra. The silver particles were prepared by an adaptation of the method of Lee and Meisel (1982), producing nanoparticles of silver by trisodium citrate-reduction of silver nitrate. They obtained SERS spectra of *E. coli* and *Acinetobacter calcoaceticus* RAG-1, *Pseudomonas*

aeruginosa YS-7, and *B. megaterium* as well as riboflavin (RF). The SERS spectra of all four different bacteria and RF were quite similar, suggesting that the spectra were selective and sensitive to a specific molecular species, which dominated the spectra and which presented in all these tested bacteria. In 2004, Zeiri et al. reported additional spectra of *E. coli*, *A. calcoaceticus* RAG-1, and flavin adenine dinucleotide (FAD), which is a coenzyme for many proteins present in practically all bacteria. The spectra of *E. coli* and FAD were very similar for excitation at 514.5 nm as were the spectra for *E. coli* and RAG-1. They concluded that the spectra for the mixture of bacteria and silver particles were dominated by flavins located in the plasma membrane of the cell.

Bacteria Co-deposited with Silver Colloid Aggregates on Inert Substrates

Jarvis and Goodacre (2004) used citrate-reduced silver colloidal particles to obtain SERS spectra of 21 isolates from patients with urinary tract infection. To assess the discrimination of bacteria at the subspecies level, seven *E. coli* isolates were also investigated. The bacteria/silver colloid mixtures were deposited on CaF_2 disks and SERS spectra were collected using a Renishaw 2000 Raman microscope equipped with a 785 nm laser. Cluster analysis was performed to classify genus-level (six different types) and strain level of seven *E. coli* isolates. Subtle quantitative differences in raw spectra of *E. coli* isolate and *Enterococcus spp*. (ENTC90) isolates were found. This work showed that there were differences in SERS spectra when sampled from the same batch. They suggested this was the result of the large size of the bacteria relative to the colloidal Ag particles, and because of the heterogeneity of the cell envelope. In a separated report, Jarvis et al. (2004) extended their study and developed a scanning electron microscope (SEM) with a Raman spectroscopy interface and obtained reproducible bacterial SERS spectra by depositing silver coated bacterial samples on a dry surface. With the

magnification afforded by SEM, SERS active regions of the sample matrix (where both the biomass and the silver colloidal particles were present) were revealed and reproducible spectra were obtained. SERS spectra were collected utilizing this approach with 532 nm excitation and $NaBH_4$-reduced silver colloid substrates. SERS spectra of *Bacillus subtilis* B0014T and *E. coli* UB5201 were investigated. Upon visual inspection of the spectra, there was little to distinguish between the *B. subtilis* and *E. coli*. Principle component analysis was then applied to classify between these two microorganisms and two separate clusters for *B. subtilis* and *E. coli* were clearly resolved. In these two studies, single colony of bacterial samples was mixed with a small aliquot of silver colloid, the detection limits or concentration of the bacterial samples was not determined.

Kahraman et al. (2007) investigated the influence of experimental conditions on SERS spectra of *E. coli* and *B. megaterium* by varying the pH of the silver colloidal solution before mixing with the bacteria samples. They also increased the concentration of the colloidal silver solution to increase the possibility of acquiring reproducible SERS spectra. The results showed that the natural sample preparation of pH, which was around 9, was sufficient to produce quality spectra and there was no need for pH adjustment. Increasing concentration of colloidal solution improved the reproducibility of the spectra. Similar to Jarvis's approach in sample preparation, five micro liters of bacteria sample was added into 100 μL silver colloid solution before small aliquot of mixture was deposit onto a CaF_2 disk; both 514 and 830 nm wavelength laser were used to acquire the spectra. This study did not report the concentration nor the detection limits of the bacterial samples, the spectral similarity and difference between two different bacteria was not addressed.

Bacteria in Silver Colloid Solutions

Since the uniformly deposition of nanoparticles on bacteria is yet to be achieved, and the deposition of metal coated bacteria on a surface could lead to greater discrepancy. Numbers of researches had look into the detection of bacterial species in aqueous colloid suspensions.

Sengupta et al. (2005[a, b]) used the mixture of bacteria and silver colloidal suspension to obtain signal enhancement and reported that a specific narrow range of volume ratios was required to minimize the fluorescence from the analyte. They also studied the adsorption rate of the silver colloid particles on the bacteria by varying the pH and the concentration of bacteria suspensions. To explore the parameters affecting the binding rate, the normalized peak height changes of the major peak at 1355 cm^{-1} (relative to the water peak at 1635 cm^{-1}) was plotted as function of time for different optical densities of *Salmonella typhimurium*. The results showed that the more diluted bacterial suspensions (OD600 < 2), the peak height increased with time, but at higher optical densities (OD600 > 2), the peak height decreased with time. The time dependent spectra for *E. coli* (OD600 = 3.4) as function of pH (pH = 3.25, 8 and 9.74) was measured. The rate of evolution was found to be much faster at pH = 3.25 than under basic conditions. Their results suggested that, at acidic pH and at higher volume ratios of colloid particles to bacteria, aggregation of the colloidal particles increased the deterioration of the Raman signal, and the experimental parameters must be controlled to obtain reproducible SERS data. The optimized parameters of silver colloid solution to aqueous bacterial suspension were then studied and applied to obtain SERS spectra of Arctic psychro-active marine bacteria (marine bacteria/silver colloid ratio = 1:100) and mesophillic bacteria (*E. coli*/silver colloid ratio = 1:50) with 514.5 nm excitation. The results found no difference between five different Arctic sea-ice bacterial strains,

but difference between the mesophillic bacteria (*E. coli* and *P.aerigunosa*) and the psychro-active marine bacteria was observed (Laucks et al., 2005).

Moskovits and Michaelian (1978) reported that water spectra in a broad range (0 to 2,000 cm^{-1}) were dominated by a broad water librational envelope (the rotational oscillations of water molecules) that extends to 1,640 cm^{-1}. They assigned an intramolecular scissoring mode to a broad band at about 1,635 cm^{-1}, librational modes to bands at 470, 570, 760, and the broad band between 1,000 and 2100 cm^{-1}. The presence of a relatively high background could mask the bacterial fingerprints and prevented reliable detection at low concentration levels of pathogens. To investigate the sensitivity of SERS technique for pathogen detection in aqueous medium; the SERS spectra of diluted concentrations of *E.coli* suspensions (10^2-10^5cfu/mL, with a ratio of 1:50 *E.coli* /silver colloidal solution) was corrected for the broad librational OH at 1,635 cm^{-1} and reproducible spectra for *E. coli* concentrations as low as approximately 10^3 CFU/ml was obtained (Sengupta et al., 2006).

Gold Colloids as SERS Substrate

Montoya et al (2003) used antibodies conjugated with gold nanoparticles (12 nm) as a SERS active substrate. The gold conjugated antibody binds to certain surface antigens on Salmonella enteriditis to obtain signal enhancement. At 10^7 CFU/ml concentration, strong SERS response was observed. However, at concentration 10^6 CFU per mL and lower, SERS signal got lost in a high background noise. Goeller and Riley (2007) presented spectra of *E. coli* evaluated by Raman spectroscopy in the presence of gold colloids (60nm) to stimulate the SERS effect. Upon addition of gold colloids, a substantial increase in intensity was observed; however, the locations of the spectral feature had shifted so it was not feasible to compare with the colloid-free spectra. Using the peak at 1449 cm^{-1} (which they assigned to carbohydrates) as an indicator, the

limit of detection appeared to be approximately 10^6 CFU/mL for hydrated bacteria. A more detailed study utilizing gold colloids (~80nm) covered SiO_2 substrates showing enhancement factors of 10^4 for both *E. coli* and *Bacillus anthracis*, and that bacterial signatures were strongly amplified on the substrates (Premasiri et al., 2005). The SERS spectra were found to be less congested and showed better differentiation than the normal Raman spectra of the bacteria at 785 nm excitation wavelength, They also reported that quality Raman spectra of single bacterium was made possible by this gold particles aggregate covered glass chips. A unique detection system based on the simultaneous exploitation of the optical trapping and SERS phenomena had been reported (Alexander et al., 2003). The SERS substrates used in this study were based on gold colloids (60nm) bound to a 3-aminopropyltriethoxysilane derivatized glass. The light from a 787 nm laser diode was used to trap and simultaneously excited the SERS of an individual bacillus spore. Comparison of normal Raman and SERS spectra revealed not only enhancement of the Raman features but also the appearance of other features absent in the normal Raman spectra. Results indicated that spectral features measured using this method was possible to discriminate between two *Bacillus stearothmophilus* strains.

Bacteria on Other Forms of SERS Substrate

Guzelian et al (2002) used electrochemically roughened gold SERS substrate with 784 nm excitation to investigate the individual components of bacteria and concentrated on nucleic acids, amino acids, and peptides. In the study of intact cells, the SERS response from various species (*E.coli*, *Pseudomonas aeruginosa*, *Listeria monocytogenes*, *Bacillus subtilis*, and *Bacillus cereus*) showed a number of similarities as well as some differences. In addition, the data showed spectral differences from viable and nonviable *Bacillus cereus* cells.

Escoriza et al (2006[a]) used normal Raman spectroscopy to study the metabolic changes found in the growth phases of *E. coli* and *Staphylococcus epidermidis*. Samples of bacteria in deionized water were deposited on aluminum-coated slides and dried prior to Raman analysis. The cells were washed in deionized water to remove the growth media, which fluoresced and would interfere with the Raman signal. Spectra throughout the growth cycle: lag, exponential, stationary and decay phases was measured. Although, *E. coli* and *S. epidermidis* shared very similar SERS spectra, both bacteria exhibited changes of intensities in specific spectral bands over the course of time of the experiments. Principal component analysis indicated that spectra can be grouped according to growth phases. In another study, Escoriza et al (2006[b]) used FALCON™ Raman Chemical Imaging Microscope to view the interested regions of waterborne bacteria filtered on a Whatman aluminum membrane or a silver membrane and to acquire Raman signal. The filtering approaches for water sampling showed significant background interference from Aluminum and silver membranes therefore reduced the sensitivity of this method and prevented low bacteria cell detection (10^7 cells/membrane and lower).

Silver film over nanosphere (AgFON) substrates has been used to exploit the rapid detection of *Bacillus subtilis* spores (Zhang et al., 2005). AgFON substrate was fabricated by drop of carboxyl-functionalized polystyrene latex nanosphere (diameter ~ 600 nm) onto a piranha solution cleaned glass substrate before silver film (thickness ~ 200 nm) was vacuum deposited onto the spheres. Calcium dipicolinate (CaDPA), a biomarker for bacillus spores, was efficiently extracted by sonication in nitric acid and detected by SERS with a portable battery-operated Raman spectrometer. This technique demonstrated a sensitivity of 10^4 bacillus spores. Gold film over nanosphere (AuFON) substrate (D = 400nm with 200 nm gold film) and gold island films was used to measure SERS spectra of *E.coli* (Jones et al., 2003). Their preliminary

results demonstrated that Au-island films showed no enhancement for the bacteria while the AuFONS spectrum reproducibly showed some amount of enhancement. It should be noted that the surface of the AuFONS can be characterized with spots that are better than others. Stacking of spheres can result in "hot" spots where enhancement was increased, or strong interference by the SERS spectrum of the latex spheres could also be present.

Data Analysis for Classification and Identification of Microorganisms

To classify and identify microorganisms based on vibrational spectroscopy, it is not necessary to identify all band intensities, frequencies, and bandwidths in a spectrum and assign them to specific molecular compounds. Spectra can be evaluated as spectroscopic fingerprints of the samples. Chemometrics or multivariate statistical techniques can be employed for the analysis of the whole spectrum, in a similar approach as in pattern recognition procedures. Chemometrics is the use of mathematical and statistical methods to improve the understanding of chemical information and to correlate quality parameters or physical properties to analytical instrument data (Lavine, 1998). Chemometric techniques highlight the minute spectral differences and can objectively differentiate between similar spectra. It has been applied to spectroscopy, such as IR and normal Raman spectra analysis. Multivariate data such as the spectra data generated from a Raman experiment consist of the results of observations of many different variables (wavenumbers) for a number of objects (e.g. samples of different microorganisms). Each wavenumber may be considered as constituting a different dimension, such that if there are n wavenumbers, each object may be assumed to reside at a unique position in an abstract entity referred to as n-dimensional hyperspace. Since this hyperspace is difficult to visualize, multivariate analysis is applied to simplify or reduce dimensionality. In other words, a

large body of data can be summarized by means of relatively few parameters, which provide a graphical display with minimal loss of information, therefore allowing human to visualize and interpret the data. Within chemometrics, there are two main strategies to analyze multivariate data, unsupervised learning and supervised learning algorithms (Ellis and Goodacre, 2006).

Unsupervised learning algorithms can help understanding the similarity of one sample to another (e.g. bacteria) based on their collected Raman fingerprints with a cluster analysis. The reduction of the Raman data has typically been carried out using principal components analysis (PCA) or hierarchical cluster analysis (HCA). PCA is a well-known technique for reducing the dimensionality of multivariate data while preserving most of the variance, and is used to identify correlations amongst a set of variables and to transform the original set of variables to a new set of uncorrelated variables called principal components (PCs). These PCs are then plotted and clusters in the data can be visualized. Since these PCs maintain all the variance of the original data, therefore when multivariate data set such as spectra applied, permits the identification of the similarities and difference among different spectra. HCA employs a calculated distance between the objects in either the original data or a derivative (e.g. the PCs) to construct a similarity matrix using a suitable similarity coefficient.

Supervised techniques, on the other hand, require a prior knowledge of the sample identity. The basic idea behind supervised learning is that there are some patterns (e.g. Raman fingerprints) which have desired responses previously known, such as the identity of a micro-organism, which has been decided by conventional approaches. These two types of data (the representation of the objects and their responses in the system) form pairs that are conventionally called inputs (x-data) and outputs/targets (y-data). The goal of supervised learning is to find a model or mapping that will correctly associate the inputs with the outputs. With a set of well-

characterized samples, a model can be developed so that it can predict the identity of unknown samples. Example of supervised method is artificial neural networks (ANNs). Combination of objective and subjective methods can be used. Pre-selecting spectral regions based on visual inspection of the spectra and using these regions in cluster analysis is a common approach (Maquelin et al., 2002).

Potentials and Considerations of SERS as an Analytic Tool in Biological System

Molecules of interest can be detected and characterized using SERS spectra by using an optical label or by their own intrinsic surface enhanced Raman spectra. The technique relying on molecules' own intrinsic surface enhanced Raman scattering is particularly desirable because optical labeling is avoided; thus, enable a label free direct detection. In many cases, the adsorption of molecules on the metal surface would result in formation of new and fast relaxation channels for the electronic excitation of the target molecules, therefore, quenching the fluorescence signals. The fluorescence quenching ability gives SERS analytical advantage in complex chromophore environments.

The positions as well as the widths and shapes of the spectral lines give information about the vibrational, rotational, and electronic properties of molecules. These parameters reflect the structure of the molecules and also their interaction with the surroundings. With the rational use of known frequencies and selection rules, identification is often possible by Raman spectroscopy. The fingerprinting properties of the Raman spectra allow identification of molecules even in a mixture of many substances. However, due to the non-uniform enhancement level for different vibrations and also due to the interaction between molecule and metal surface,

a SERS spectrum can show deviations from the normal spectrum of the molecule. Nevertheless, in most cases, a SERS spectrum can still provide fingerprint of the molecule.

While SERS has proved to be a valuable tool for the detection of Raman spectra for low concentrations, few published papers reported on the application of SERS for quantitative analysis of certain substances. Quantitative analytical applications of SERS are often compromised by the experimental difficulties in measuring intensities with a precision and reproducibility. A major problem lies in the difficulty in reproducing SERS amplification processes, which can be explained by the extreme sensitivity of the enhancement on the metal structures. Only slight variations of parameters such as cluster sizes and shapes in a colloidal solution could produce changes in the enhancement factors by several orders of magnitude. Additionally, the combinations of different enhancement mechanisms can result in different enhancement factors for different molecules or molecular vibrations. Temperature, pH, ageing of solutions and laboratory practices also can affect the enhancement. Nonetheless, optimal experimental parameters and careful selection of reproducible SERS substrates still can make quantitative analysis possible.

Limitations of SERS are associated with the fact that target molecules have to be attached to or in close proximity to SERS active substrates such as nano-sized silver or gold structures. Based on the theory that electromagnetic field enhancement contributes more to the overall magnitude of SERS enhancement, it should be possible to achieve SERS effect for each molecule. However, SERS enhancement can not be observed for all molecules. There seems to be a molecular selectivity of the effect that can not be explained yet. SERS seems to work well with molecules with lone pair electrons or pi clouds. The effect was first discovered with pyridine. In 1986 Seki published a list with 544 references of molecules considered to be

surface-enhanced. These data reveals aromatic nitrogen or oxygen containing compounds, such as aromatic amines or phenols, and other electron-rich functionalities such as carboxylic acids are strongly SERS active. This is not surprising as these species promote strong adsorption on the metal surface. Fortunately, many molecules of biological interest are SERS active. Therefore, SERS should be applicable for relatively many biological systems. Combinations of fingerprinting capabilities, sensitive detection limits with careful considerations of experimental parameters and choice of reproducible substrates, opens up exciting perspectives for SERS as a spectroscopic tool.

Conclusions

SERS combines the structural information content of Raman spectroscopy with ultrasensitive detections capability. Although the reproducibility and uniformity of some substrates can be a little bit challenging, the sampling is very flexible. From a problem solving standpoint, SERS is not yet well-developed. Much work needs to be done on the applicability to real life complex matrix samples. The development of standardized SERS active surfaces on a routine basis to become more reproducible and more easily prepared will expand analytical applications, so as to spread the use of this spectroscopic tool in biological diagnostic laboratory. Further development in integrating SERS active substrate with probes or optical fibers and in portable instrumentation will open horizons for remote in situ sensing for environmental and biological applications.

References

1. Abelmann, L. and Lodder, C. Oblique evaporation and surface diffusion. Thin Solid Films 1997, 305, 1-21.
2. Adrian, F. J. Charge transfer effects in surface-enhanced Raman scattering. J. Chem. Phys. 1982, 77, 5302-5314.
3. Alexander, T.A., Pellerino, P. M. and Gillespie, J. B. Near-infrared surface-enhanced Raman scattering mediated detection of single optically trapped bacterial spores. Appl. Spectros. 2003, 57, 1340-1345.
4. Altekruse, S.F., Cohen, M.L., and Swerdlow, D.L. Emerging foodborne diseases. Emerging Infectious Diseases. 1997, 3, 285-294.
5. Alvarez-Icaza, M. and Bilitewski, U. Mass production of biosensors. Anal. Chem. 1993, 65, 525A–533A.
6. Carron, K. T., Gi, X. and Lewis, M. L. A surface enhanced Raman spectroscopy study of the corrosion-inhibiting properties of benzimidazole and benzotriazole on copper. Langmuir 1991, 7, 2-4.
7. Chaney, S. B., Shanmukh, S., Dluhy, R. A. and Zhao, Y.-P. Aligned silver nanorod arrays produce high sensitivity surface-enhanced Raman spectroscopy substrates. Appl. Phys. Lett. 2005, 87, 031908.1-3.
8. Chaplin, M. F., and Burcke, C. Enzyme technology. 1st ed. England: Cambridge University Press, 1990.
9. Chase, D.B. and Parkinson, B.A. Surface-enhanced Raman spectroscopy in the near-infrared. Appl. Spectrosc., 1988, 42, 1186-1187.

10. Chen, C.Y., Davoli, I., Ritchie G., and Burstein, E. Giant Raman scattering and luminescence by molecules adsorbed on Ag and Au metal island films. Surf. Sci., 1980, 101, 363-366.
11. Creighton, J.A. Surface Raman electromagnetic enhancement factors for molecules at the surface of small isolated metal spheres: the determination of adsorbate orientation from SERS relative intensities. Surf. Sci. 1983, 124, 209-219.
12. Deshpande, S.S., and Rocco, R.M. Biosensors and their potential use in food quality-control. Food Technol. 1994, 48 (6), 146–150.
13. Economic Research Service, Food-borne illness cost calculator. United States Department of Agriculture. Link: http://www.ers.usda.gov/data/foodborneillness/. 2007.
14. Efrima, S. and Bronk, B.V. Silver colloids impregnating or coating bacteria. J. Phys. Chem. B. 1998, 102, 5947-5950.
15. Ellis, D. I. and Goodacre, R. Metabolic fingerprinting in disease diagnosis: biomedical applications of infrared and Raman spectroscopy. Analyst 2006, 131, 875-885.
16. Escoriza, M. F., Vanbriesen, J. M., Sewart, S. and Maier, J. Studying bacterial metabolic states using Raman spectroscopy. Appl. Spectrosc. 2006a, 60, 971-976.
17. Escoriza, M. F., Vanbriesen, J. M., Sewart, S., Maier, J. and Treado, P. J. Raman spectroscopy and chemical imaging for quantification of filtered waterborne bacteria. J. Microbiol. Methods. 2006b, 66, 63-72.
18. Feng, P. Commercial assay systems for detecting foodborne Salmonella: a review. J. Food Protect. 1992, 55, 927–934.
19. Feng, P. and Weagant, S.D. in Diarrheagenic Escherichia coli, Bacteriological Analytical Manual, 8th edn. 1998.

20. Fleischman, M., Hendra, P. J., and McQuillan, A. J. Raman spectra of pyridine adsorbed at a silver electrode. Chem. Phys. Lett. 1974, 26, 163-166.

21. Goeller, L. J. and Riley, M. R. Discrimination of bacteria and bacteriophages by Raman spectroscopy and surface-enhanced Raman spectroscopy. Appl. Spectrosc. 2007, 61, 679-685.

22. Guzelian, A. A., Sylvia, J. M., Janni, J. A., Clauson, S. L. and Spencer, K. M. SERS of whole cell bacteria and trace levels of biological molecules. Proc. SPIE. 2002, 4577, 182-192.

23. Iqbal, S.S., Mayo, M. W., Bruno, J. G., Bronk, B. V., Batt, C.A., and Chambers, P. A review of molecular recognition technologies for detection of biological threat agents. Biosens. Bioelectron. 2000, 15, 549–578.

24. Jarvis, R.M. and Goodacre, R. Discrimination of bacteria using surface-enhanced Raman spectroscopy. Anal. Chem. 2004, 76, 40-47.

25. Jarvis, R.M. Brooker, A. and Goodacre, R. Surface-enhanced Raman spectroscopy for bacterial discrimination utilizing a scanning electron microscope with a Raman spectroscopy interface. Anal. Chem. 2004, 76, 5198-5202.

26. Jensen, T. R., Malinsky, M. D., Haynes, C. L. and Van Duyne, R. P. Nanosphere lithography: tunable localized surface plasmon resonance spectra of silver nanoparticles. J. Phys. Chem. B. 2000, 104, 10549-10556.

27. Jiang, X. and Campion, A. Chemical effects in surface-enhanced Raman scattering: pyridine chemisorbed on silver adatoms on Rh (100) Chem. Phys. Lett. 1987, 140, 95-100.

28. Jones, J. P., Fell, N. F., Alexander, T., Dorschner, K., Tombrello, C., Reis, B. R., and Fountain, III LTC A. W., Surface-enhanced Raman substrate optimization for bacterial identification. Proc. SPIE. 2003, 5071, 205-211.
29. Kahraman, M., Yazici, M. M., Sahin, F., Bayrak, O.F., and Culha, M. Reproducible surface-enhanced Raman scattering spectra of bacteria on aggregated silver nanoparticles. Appl. Spectrosc. 2007, 61, 479-485.
30. Kaiser, N. Review of the fundamentals of thin-film growth. Appl. Optics. 2002, 41, 3053 -3060.
31. Kerker, M. Electromagnetic model for surface-enhanced Raman scattering (SERS) on metal colloids. Acc. Chem. Res., 1984, 17, 271-277.
32. Kewal, K. J. Nanotechnology in clinical laboratory diagnostics, Chin. Chim. Acta 2005, 358, 37-54.
33. Kneipp, K., Pohle, W. and Fabian, H. Surface enhanced Raman spectroscopy on nucleic acids and related compounds adsorbed on colloidal silver particles. J. Mol. Struct. 1991, 244, 183–192.
34. Kneipp, K., Kneipp, G., Itzkan, I., Dasari, R. R., and Feld, M. S. Ultrasensitive chemical analysis by Raman spectroscopy. Chem. Rev. 1999. 99, 2957-2975.
35. Kovacs, G.J., Loutfy, R.O., Vincett, P.S., Jennings, C., and Aroca, R. Distance dependence of SERS enhancement factor from Langmuir-Blodgett monolayers on metal island films: evidence for the electromagnetic mechanism. Langmuir 1986, 2, 689-694.
36. Laucks, M. L., Sengupta, A., Junge, K., Davis, E. J. and Swanson, B. D. Comparison of psychro-active marine bacteria and common mesophillic bacteria using surface-enhanced Raman spectroscopy. Appl. Spectrosc. 2005, 59, 1222–1228.

37. Lavine, B. K. Chemometrics. Anal. Chem. 1998,70, 209R–228R.

38. Lee, P.C. and Meisel, D. Adsorption and surface-enhanced Raman of dyes on silver and gold sols. J. Phys. Chem. 1982, 86, 3391-3395.

39. Liu, Y. J., Fan, J. G., Shanmukh, S., Dluhy, R. A. and Zhao, Y.-P. Angle dependent surface enhanced Raman scattering obtained from a Ag nanorod array substrate. Appl. Phys. Lett. 2006, 89, 173134.1-3.

40. Maquelin, K., Kirschner, C., Choo-Smith, L.-P., Van den Braak, N., Endtz, H. Ph., Naumann, D. and Puppels, G. J. Identification of medically relevant microorganisms by vibrational spectroscopy. J. Microbiol. Methods, 2002, 51, 255–271

41. Mead, P.S., Slutsker, L., Dietz, V., McCaig, L.F., Bresee, J.S., Shapiro, C., Griffin, P.M., and Tauxe, R. V. Food-related illness and death in the United States. Emerging Infectious Diseases. 1999, 5, 607-625.

42. Montoya, J. R., Armstrong, R. L., and Smith, G. B. Detection of Salmonella using surface enhanced Raman scattering. Proc. SPIE. 2003, 5085, 144–152.

43. Moskovits, M. and Michaelian K. H. A reinvestigation of the Raman spectrum of water. J. Chem. Phys. 1978, 69, 2306–2311.

44. Moskovits, M. Surface-enhanced spectroscopy. Rev. Mod. Phys. 1985, 57, 783-826.

45. Nie, S. M. and Emory, S. R. Probing single molecules and single nanoparticles by surface-enhanced Raman scattering. Science 1997, 275, 1102-1106.

46. Newton, C. R. and Graham, A. PCR. 2nd edn., Bios Scientific, Oxford, 1997.

47. Persson, B.N.J. On the theory of surface-enhanced Raman scattering. Chem. Phys. Lett. 1981, 82, 561-565.

48. Premasiri, W. R., Moir, D. T., Klempner, M. S., Krieger, N., Jones, G. and Ziegler, L. D. Characterization of the surface enhanced Raman scattering (SERS) of bacteria. J. Phys. Chem. B. 2005, 109, 312-320.

49. Riu, J., Maroto, A., and Rius. F.X. Nanosensors in environmental analysis. Talanta, 2006, 69, 288-301.

50. Seki, H. Raman spectra of molecules considered to be surface enhanced. J. Electron. Spectrosc. Relat. Phenom. 1986, 39, 289-310.

51. Sengupta, A., Laucks, M.L., Dildrine, N., Drapala, E., and Davis, E. J. Bioaerosol characterization by surface-enhanced Raman spectroscopy (SERS). J. Aerosol. Sci. 2005a, 36, 651–664.

52. Sengupta, A., Laucks, M. L., and Davis, E. J. Surface-enhanced Raman spectroscopy of bacteria and pollen. Appl. Spectrosc. 2005b, 59, 1016–1023.

53. Sengupta, A., Mujacic, M. and Davis, E. J. Detection of bacteria by surface-enhanced Raman spectroscopy. Anal. Bioanal. Chem. 2006, 386, 1379-1386.

54. Shangkuan, Y. H. and Lan, H. C. Application of radom amplified polymorphic DNA analysis to differentiate strains of Salmonella typhi and other Salmonella species. J. Appl. Microbiol., 1998, 85,693-702.

55. Shanmukh, S., Jones, L., Driskell, J., Zhao, Y.-P., Dluhy, R. and Tripp, R. A. Rapid and sensitive detection of respiratory virus molecular signatures using a silver nanorod array SERS substrate. Nano Lett. 2006, 6, 2630-2636.

56. Stacy A.A. and Van Duyne R.P. Surface enhanced raman and resonance raman spectroscopy in a non-aqueous electrochemical environment: tris(2,2′-

bipyridine)ruthenium(II) adsorbed on silver from acetonitrile. Chem. Phys. Lett. 1983, 102, 365-370

57. Sudnik, L. M., Norrod, K. L., and Rowlen, K. L. SERS-active Ag films from photoreduction of Ag+ on TiO2. Appl. Spectrosc. 1996, 50, 422-424.
58. Suer, G., Nickel, U. and Schneider, S. Preparation of SERS-active silver film electrodes via electrocrystallization of silver. J. Raman Spectrosc. 2000, 31, 359-363.
59. Tao, A., Kim, F., Hess, C., Goldberger, J., He, R., Sun, Y., Xia, Y. and Yang, P. D. Langmuir-Blodgett silver nanowire monolayers for molecular sensing using surface-enhanced Raman spectroscopy. Nano Lett. 2003, 3, 1229-1233.
60. Toze, S. PCR and the detection of microbial pathogens in water and wastewater. Water Res. 1999, 33, 3545–3556.
61. Udagawa, M., Chou, C., Hemminger, J., and Ushioda, S. Raman scattering cross section of adsorbed pyridine molecules on a smooth silver surface. Phys. Rev. B 1981, 23, 6843-6846.
62. Wang, D. S. and Kerker, M. Enhanced Raman scattering by molecules adsorbed at the surface of colloidal spheroids. Phys. Rev. B 1981, 24, 1777-90.
63. Zeiri, L., Bronk, B.V., Shabtai, Y., Czégé, J., and Efrima, S. Silver metal induced surface enhanced Raman of bacteria. Colloids Surfaces A. 2002, 208, 357-362.
64. Zeiri, L., Bronk, B.V., Shabtai, Y., Eichler, J. and Efrima, S. Surface-enhanced Raman spectroscopy as a tool for probing specific biochemical components in bacteria. Appl. Spectrosc. 2004. 58, 33-40.

65. Zeman, E. J., and Schatz, G. C. An accurate electromagnetic theory study of surface enhancement factors for Ag, Au, Cu, Li, Na, AL, GA, In, Zn, and Cd. J. Phys. Chem. 1987, 91, 634-643.

66. Zhang, X., Young, M. A., Lyandres, O., and Van Duyne, R. P. Rapid detection of an anthrax biomarker by surface-enhanced Raman spectroscopy. J. Am. Chem. Soc 2005, 127, 4484-4489.

67. Zhao, Y. - P., Ye, D. X., Wang, G. C. and Lu, T. M. Designing nanostructures by glancing angle deposition. Proc. SPIE. 2003, 5219, 59-73.

68. Zhao, Y.-P., Chaney, S. B., Shanmukh, S. and. Dluhy, R. A. Polarized surface enhanced Raman and absorbance spectra of aligned silver nanorod arrays. J. Phys. Chem. B 2006, 110, 3153-3157.

CHAPTER 3

A HIGH SENSITIVE FIBER SERS PROBE BASED ON SILVER NANOROD ARRAYS[1]

[1]HsiaoYun Chu, Yongjun Liu, Yaowen Huang, and Yiping Zhao. 2007. *Optic Express.* 15:12230-12239.

Reprinted here with permission of publisher

Abstract

A portable fiber SERS probe has been developed based on Ag nanorod array fabricated by oblique angle deposition. The incoming laser beam was designed to focus onto the Raman substrate at 45° incident angle in order to maximize surface enhanced Raman scattering signal. With a fiber Raman system, a detection sensitivity of 10^{-17} moles for trans-1,2-bis(4-pyridyl)ethane molecules has been demonstrated. This Raman probe can also be used for in situ measurement for samples in aqueous solution. Such a fiber probe has great potential as a portable and remote sensor for on-site biological or chemical detection.

OCIS codes: (040.1240) Arrays; (130.3120) Integrated optics devices; (170.5660) Raman spectroscopy; (130.6010) Sensors

1. Introduction

Surface-enhanced Raman spectroscopy (SERS) has been used as an analytical tool to observe trace amount of chemical and biological molecules due to its capability of giving real-time molecular vibrational information under ambient conditions [1,2]. It has the advantages of using extremely small amount of analyte without amplification or manipulation of the samples, and the extremely short time frame for acquisition of the spectra. SERS requires minimal sample preparation and is non destructive to sample which allows real time analysis and great potential for multi components analysis. The well-known enhancement effect for SERS arises from either the adsorption or close proximity of an analyte onto a metal substrate [3]. The morphology of the metallic structure plays a major role in determining the magnitude of signal enhancement and sensitivity of detection. Early SERS substrates included a random distribution of roughness features produced by oxidation reduction on a metal electrode [4] or evaporation of thin metal film on a flat substrate [5]. Various forms of nanostructure have been explored to enhance SERS effects, such as rough metallic surfaces by chemical etching [6], silver films on TiO_2 [7], colloidal silver nanoparticles [8], silver nanoparticle array fabricated by nanosphere lithography [9], electro-deposition of silver on silver films at high potential [10], aligned monolayer of silver nanowires [11]. However, many of these methods are either expensive or time consuming, and it is not easy to make reproducible substrates of the correct surface morphology to provide maximum SERS enhancements. Without uniformity and good reproducibility of the metal substrates, the attainment of reproducible spectra remains a major challenge for SERS. We had previously demonstrated that silver nanorod substrate fabricated by oblique angle deposition (OAD) with length of ~868 nm, diameter of ~99nm, and tilt angle of 73° has achieved SERS enhancement factors of approximately 10^8 for the molecular probe trans-1,2-bis(4-pyridyl)ethane

(BPE) [12,13]. The silver nanorod arrays fabricated by OAD generate large SERS response with maximum SERS intensity observed at around 45° incident angle. The maximum SERS intensity is about five times the intensity at the surface normal [14]. Very recently, we also demonstrated that this SERS substrate can be used to distinguish between viruses and even different strains of viruses [15]. Thus, the OAD technique offers an easy and inexpensive way for the fabrication of silver nanorod arrays for high sensitivity SERS applications. It can be easily implemented in the laboratory. The deposition procedure is straightforward and inexpensive. The SERS substrates produced by OAD have the advantages of uniformity and reproducibility.

Despite its extremely high and unique sensitivity, the application of SERS has not been incorporated into the development of practical in situ analytical tool for real-time sensing or detecting. Usually SERS measurement is carried out by a conventional Raman scattering spectrometer, which is bulky, expensive, and not easily accessible. For portable and remote applications, the ideal SERS sensor systems would be field-deployable, small and compact in size with very high sensitivity, selectivity and multiplexing ability. In addition, the need for easily fabricated SERS-active sensors that can be used in solution is essential for the application of SERS in in situ analyses. In this paper, we report our special design of a portable SERS probe with a slit sample holder which allowing the laser beam focus onto the sample with 45° incident angle, hence achieving the maximum SERS effect. Combining this custom designed SERS probe with a fiber Raman system, we demonstrated the SERS intensity is dependent on the concentration with a sensitivity of 10^{-17} moles on the OAD fabricated silver nanorod arrays using trans-1,2-bis(4-pyridyl)ethane (BPE) as the molecular probe. These results show the potential use of the SERS probe as a sensitive, remote and portable sensor for in situ SERS analyses.

2. Experimental

Silver nanorod substrates were fabricated by OAD technique using a custom-designed electron beam/sputtering evaporation (E-beam) system (Torr International, New Windsor, NY) that has been described previously [12]. Glass microscopic slides (Gold Seal® Catalog No.3010) were used as the base platform for silver nanorod arrays deposition. The glass slides were cleaned with Piranha solution before loading into the E-beam system. A base layer of 500 nm silver film was first deposited onto the glass slides before arrays of Ag nanorod (length of approximately 1 μm) was deposited on the silver base layer by OAD at a vapor incident angle of 86°. The deposition rate was 0.3 nm/s, and the deposition pressure was approximately 1×10^{-6} Torr. The film thickness was monitored by a quartz crystal microbalance positioned at normal incidence to the vapor source direction. Figure 3.1 shows a typical scanning electron microscope (SEM) image of silver nanorod surface. Average length of the silver nanorods was 868 ± 95 nm and the average diameter was 99 ± 29 nm. The average density of the nanorods was approximately 13 ± 0.5 rods/μm^2. The average tilting angle of the nanorods was ~73° with respect to the substrate normal.

The SERS detection system is shown in Fig. 3.2. The fiber Raman system used in this study was the HC-10HT Raman Analyzer (Enwave Optronics Inc., Irvine, CA). This system was made up of a diode laser, spectrometer, integrated Raman probe head for both excitation and collection, and separate excitation and collection fibers. The excitation source was a frequency stabilized, narrow linewidth near IR diode laser with a wavelength of 785nm. The excitation laser beam coupled to a 100 μm fiber was focused onto the substrate through the Raman probe head and was unpolarized at the sample. The focal length of the Raman probe was 6 mm, and the laser beam spot size was 100 μm. The Raman signal from the substrate was collected by the

same Raman probe head and was coupled to a 200 μm collection fiber, which delivered the signal to the spectrometer equipped with a charge coupled device (CCD) detector (Fig. 3.2(a)).

We designed a portable silver nanorod substrate based SERS probe with a 45° slit to achieve the optimum experimental configuration and ensure maximum SERS scattering response from silver nanorod arrays as shown in Fig. 3.2(b). This cylinder shape custom-designed probe measures 7.4 cm in length and 2 cm in diameter. The front of the probe opens with a cylindrical hole that is 9.8 mm in diameter for connecting with the commercial Raman Analyzer. At 3.2 cm into the SERS probe, there is a glass sealed widow protecting the Raman head probe from liquid or vapor. Right next to the sealed window is the liquid or vapor cell with an inlet. Following the liquid cell is a slit to hold the substrate which makes the incoming laser beam focus onto the substrate at 45° incident angle to the substrate surface normal. The distance between the sealed window and the center of the silt is around 5.2 mm so that the laser beam could focus on the substrate. The silver nanorod substrates prepared by OAD technique were placed into the SERS probe through the open slit, facing the fiber optic Raman probe head. This arrangement allowed the focal length remained fixed and the investigated spot on the sample could be adjusted by moving the substrate along in the open slit. The tilting plane of the silver nanorods was parallel to the incident plane at 45° incident angle relative to surface normal (Fig. 3.2(c)). Through the SERS fiber probe, SERS signal could be obtained by the Raman Analyzer.

The molecular probe used in this study was trans-1,2-bis(4-pyridyl) ethene (BPE, 99.9+%, Sigma). BPE solutions were prepared by sequential dilution in HPLC grade methanol (Aldrich). For each concentration, a 2μl drop of BPE solution was applied onto the silver nanorod substrate and allowed to dry before the acquisitions of data. SERS spectra were collected from multiple

points across the substrate. The power at the sample surface was measured with a power meter (Thorlabs Inc., Newton, NJ) and was 52 mW (λ = 785 nm).

3. Results and discussion

3.1 SERS probe detection limit of BPE

The SERS signals were acquired by the fiber Raman system at an excitation wavelength of 785 nm. Figure 3.3 shows the representative SERS spectrum of the as-grown bare silver nanorod substrate. A broad peak was seen around 1360 cm^{-1}. Vapor deposited silver films and electrochemically reduced silver electrodes have been reported to exhibit backgrounds due to graphitic carbonaceous adsorption onto the substrate during deposition [16]. The peak around 1360 cm^{-1}, ascribed to disorder in the carbon chains [17], was probably contaminants from the fabrication process and/or storage in ambient environment. Such background signals are commonly found in SERS. Similar spectra from multiple spots on the same silver nanorods substrate or from different substrates showed no difference in peak position and the intensity remained unaffected under laser irradiation.

BPE was chosen as the molecular probe because of its high Raman scattering cross section, its ability to adsorb strongly and irreversibly onto a silver substrate, and its lack of resonant enhancement in the visible region [18]. Besides being centrosymmetric, BPE is photo stable and exhibits very intense SERS spectra using relatively modest laser powers [19]. In order to study the concentration of BPE in connection with SERS intensity, the SERS response of the silver nanorod substrate for nominal surface coverage of BPE was measured. Increasing amounts of BPE were consecutively applied onto the silver nanorod substrate and SERS spectra were collected for each application of BPE. Collecting multiple spectra from a single spot can cause

loss of SERS intensity as a result of sample degradation or the molecules bleached on the spot. To avoid such possible artifacts in the data, spectra were obtained from 5 spots on the same substrate. One drop of 2µl BPE solutions with different concentrations, 10^{-7} M, 10^{-6} M, 10^{-5} M, 10^{-4} M and 10^{-3} M was subsequently applied onto the silver nanorod substrate, where it spread over a geometric sample area on the silver substrate measured a diameter of approximately 1.2 cm. The estimated BPE molecular coverage on the surface ranged from 1.5×10^{-4} (at 2µl of 10^{-7} M) to 1.5 (at 2µl of 10^{-3} M) monolayer, assuming 7×10^{14} BPE molecules per cm^2 in a monolayer [20], thus, the amount of analyte excited in the laser spot were approximately from 1.4×10^{-17} to 1.4×10^{-13} moles. For the lowest concentration, it corresponds to ~ 84 BPE molecules/Ag nanorod. Figure 3.4 shows the SERS spectra of different amount of adsorbed BPE, from 1.4×10^{-17} to 1.4×10^{-16} moles, on the silver nanorod substrate. All spectra show the characteristic peaks of BPE at around 1200 cm^{-1}, 1610 cm^{-1} and 1640 cm^{-1}, corresponding to ethylenic C=C stretching mode, pyridine ring C=C stretching, and the whole ring C=C stretching mode, respectively [19]. The broad peak around 1360 cm^{-1} from substrate background remained unchanged during the study. Thus, it does not present as a significant interference peak in the BPE spectra. The results in Fig. 3.4 demonstrated that the integrated SERS probe could detect approximately 14 attomole of BPE on silver nanorod array prepared by the OAD method with good signal-to-noise ratio spectra.

Figure 3.5 shows the integrated band areas of the 1200 cm^{-1} peak plotted against the moles of BPE put down on the silver nanorod substrate in a log-log scale. The 1200 cm^{-1} peak of BPE was chosen for the quantification due to its relative insensitivity to molecular orientation on a silver surface [19]. As shown in Fig. 3.5, the Raman intensity increases as the BPE molecules adsorbed on the Ag nanorod substrate increases. The SERS signal from BPE increase over 3

orders of magnitude (14 attomoles to 14 femtomoles), after which point the further increase in Raman intensity was barely remarkable. This reflects that the saturation of the intensity occurred between the estimated surface coverage of ~0.7 and 1.5 monolayer. It has been established that, on silver surface, maximum enhancement is observed when a monolayer of the adsorbate molecule is formed on the surface [21,22]. According to the fast decay of the local electromagnetic field as moving away from the metallic surface, SERS spectra are optimized when a single layer of molecules is adsorbed on the substrate [23]. Though not the dominant role, interadsorbate interactions have been found to play some role in determining the coverage dependence [24]. Depending on the size and shape of the particles, interadsorbate interactions can either decrease or increase the intensity. Decrement in the SERS response often occurs at high surface coverage could be attributed to these intermolecular interactions. Though different model molecules and different substrate structures were used, the common observation in coverage dependence studies suggested the SERS intensity dependence can be established in a certain range of concentrations and surface coverage.

A comparison study of sensitivity on different SERS substrates reported detection limit between 270 and 0.4 femtomole for BPE. These differences depended on the substrates with the lowest detection of 0.4 femtomole found on vapor deposited annealed silver film (~5 nm) and a reduction in the SERS response occurred at coverage greater than ~ 0.01 monolayer [20]. Another study reported approximately 50-200 μM detection limits for BPE on etched silver foil and vapor deposited silver film [25]. In this study of SERS probe detection of BPE, our results showed that the portable probe has a sensitivity of 14 attomole for BPE. We also demonstrated the concentration dependent of Raman intensities of BPE on the OAD fabricated silver nanorod array. It is difficult to make direct comparisons between various substrates based on the literature

since the available data were acquired with different instruments, exposure time and environmental conditions. However, unlike most SERS measurement carried out by a bulky Raman spectrometer which is not feasible for remote function, our SERS probe provides the advantage of easy implementation, mobility and compact size for real-time, on-site field application.

3.2 SERS signal of BPE as function of time

Response time and stability of the SERS signal with time are two important analytical parameters. In order to utilize our integrated SERS probe fiber Raman system for in situ measurement, the time evolution of the SERS signal of aqueous BPE on the silver nanorod substrate was studied. Distilled water was used as a solvent instead of methanol because methanol evaporates much faster than water; therefore, it is unsuitable for long observation time. A fresh silver nanorod substrate was first secured onto the SERS probe through the 45° slit. Then 50 μl of 10^{-6}M BPE aqueous solution was applied to the substrate through the liquid inlet, the diameter of the sample area on the substrate submerged in the liquid cell was measured to be about 7 mm. The SERS spectra were collected at a 10 min interval as BPE accumulated on the surface over a period of 80 min. BPE solution was sucked out of the liquid inlet before the next higher concentration was added. Figure 3.6 shows the plot of the integrated band areas at 1200 cm^{-1} in the SERS spectra of BPE as a function of time.

The data shown in Figure 3.6 indicate the equilibrium of the BPE molecules between the water and the substrate was reached in 60 min after the addition of 10^{-6}M BPE. Though a higher laser power was used to acquire higher intensity for the in situ measurement, the substrate was only exposed to the laser beam during the spectra acquisition to avoid photodecomposition of the

analyte. Any substrate surface heating that may have been caused by the incident laser beam would have been dispersed instantly since the substrate was in contact with the liquid medium, which served as a heat sink. Furthermore, when any photodecomposition of the sample occurred at the substrate surface, the decomposed sample molecule could have diffused into the sample solution while being replaced by another BPE molecule from the solution. The increasing SERS signals over the first 80 min elapsed time indicate that BPE molecules were not thermally degraded with time. As expected, the Raman intensity increased when the higher concentration of BPE solution (10^{-5}M) was added on the substrate. In 10 min after adding the BPE solution (10^{-5}M), the SERS signal appeared to be on a slight decline.

In the study of SERS effect of BPE on gold particle arrays, Félidj et al reported that by immersing the array into 10^{-5}M BPE solution, where single layer of absorbed molecules occurred, yielded the maximum Raman intensity [26]. Increasing or decreasing this concentration in the solution lead to a weakening of the Raman signal. Assuming over time, BPE ultimately accumulated at the geometric surface area which the applied sample spread, the estimated BPE molecular coverage on the surface could have been as high as 1.1 monolayer (50 μl of 10^{-5}M BPE, assuming 7×10^{14} BPE molecules per cm^2 in a monolayer). In Fig. 3.6, the slight decline of the addition of BPE solution (10^{-5}M) reflects the saturation of the Raman intensity as increasing BPE adsorbed on the surface and suggests that the single layer occurred. This result coincides with the observation from Félidj et al. The high surface coverage could explain the descent in the SERS response, considering the Raman enhancement arises mainly from the electromagnetic amplification of the local field that exponentially decreases as moving away from the surface. Another possibility for the slow decline of the SERS signal is that photodegradation of BPE molecules might have occurred at this point and caused the decay of

the Raman signals. Moreover, some BPE molecules could have been lost through the dynamic equilibrium with surfaces, thus producing a smaller final concentration.

It is known that solvents induce morphology changes of silver island films. The change in surface tension at the silver surface, resulting from the adsorbed solvent, could greatly perturb the morphology. Roark et al. reported thin silver film morphology changes by dip coating solvent on the surface and found the intensity of the SERS of BPE adsorbed to the silver films increased [27]. The mechanism by which solvent induced morphology changes appears to be associated with the mechanical aspect of dip-coating, as well as changes in the surface tension, but is not due to significant loss of metal from the substrate. Li et al found the formation of infinite regular silver rings on a thin silver island film after immersing in water for 30 min and then blow dried with nitrogen gas [28]. As the water evaporated, capillary forces drew the nanorods together and contributed to the morphology changes on the substrate. In our study, nanorod array was immersed in the aqueous BPE solution throughout the measurement period. Sealing the liquid cell with plastic Parafilm wrap delayed the evaporation of water, therefore preventing the capillary force changing the morphology of silver nanorod substrate. We focus our attention on the in situ measurement of the SERS response of aqueous BPE on the silver nanorod substrate. Over all, our data shows the concentration dependent SERS signal of BPE on the silver nanorod substrate in an aqueous environment. Our special design of the SERS probe is an adequate sample holder for performing in situ analyses.

4. Conclusions

We have created a portable SERS probe which can be easily incorporated with a fiber Raman system. We demonstrated the concentration dependent of Raman intensities on the OAD

fabricated silver nanorod array using BPE as molecular probe and observed a sensitivity of 14 attomole for BPE. Furthermore, we tested the response time and stability of the in situ SERS signal of BPE in a water solution on the silver nanorod substrate. Our present experiment indicates that SERS probe can be integrated into a fiber Raman system for in situ measurements and can act as a portable and remote sensor for accurate and rapid real-time SERS measurements. It has great potential as a multiplexing system for chemical and biological sensing, such as environmental pollution, chemical and biological warfare agent detection, virus or bacteria detection, etc. This is an important development for practical SERS applications because of the possibility of using low-power laser, inexpensive substrate and compact size sensor for field applications.

Acknowledgements

This research was supported by funding from the National Science Foundation (ECS0304340 and ECS070178) and the UGA Engineering Grant. The authors thank Ruth Ann Morrow for her feedback on the manuscript.

References

1. T. Vo-Dinh, "Surface-enhanced Raman spectroscopy using metallic nanostructures," Trends Analyt. Chem. **17,** 557-582 (1998).
2. C.R. Yonzon, D. A. Stuart. X. Zhang, A. D. McFarland, C. L. Haynes, and R. P. Van Duyne, "Towards advanced chemical and biological nanosensors-An overview," Talanta, **67,** 438-448 (2005).
3. M. Fleischmann, P. J. Hendra, and A. J. McQuillan, "Raman spectra of pyridine adsorbed at a silver electrode," Chem. Phys. Lett. **26,** 163-166(1974).
4. A.A. Stacy and R.P. Van Duyne, "Surface enhanced raman and resonance raman spectroscopy in a non-aqueous electrochemical environment: tris(2,2′-bipyridine)ruthenium(II) adsorbed on silver from acetonitrile," Chem. Phys. Lett. **102,** 365-370 (1983).
5. G.J. Kovacs, R.O. Loutfy, P.S. Vincett, C. Jennings, and R. Aroca, "Distance dependence of SERS enhancement factor from Langmuir-Blodgett monolayers on metal island films: evidence for the electromagnetic mechanism," Langmuir **2,** 689-694 (1986).
6. K. T. Carron, X. Gi, and M. L. Lewis, "A surface enhanced Raman spectroscopy study of the corrosion-inhibiting properties of benzimidazole and benzotriazole on copper," Langmuir **7,** 2-4 (1991).
7. L. M. Sudnik, K. L. Norrod, and K. L. Rowlen, "SERS-active Ag films from photoreduction of Ag+ on TiO2," Appl. Spectrosc. **50,** 422-424 (1996).
8. S. M. Nie, and S. R. Emory, "Probing single molecules and single nanoparticles by surface-enhanced Raman scattering," Science **275,** 1102-1106 (1997).

9. T. R. Jensen, M. D. Malinsky, C. L. Haynes, and R. P. Van Duyne, "Nanosphere lithography: tunable localized surface plasmon resonance spectra of silver nanoparticles," J. Phys. Chem. B **104,** 10549-10556 (2000).
10. G. Suer, U. Nickel, and S. Schneider, "Preparation of SERS-active silver film electrodes via electrocrystallization of silver" J. Raman Spectrosc. **31,** 359-363 (2000).
11. A. Tao, F. Kim, C. Hess, J. Goldberger, R. R.He, Y. G. Sun, Y. N. Xia, and P. D. Yang, "Langmuir-Blodgett silver nanowire monolayers for molecular sensing using surface-enhanced Raman spectroscopy," Nano Lett. **3,** 1229-1233 (2003).
12. S. B. Chaney, S. Shanmukh, R. A. Dluhy, and Y.- P. Zhao, "Aligned silver nanorod arrays produce high sensitivity surface-enhanced Raman spectroscopy substrates," Appl. Phys. Lett. **87,** 031908.1-3 (2005).
13. Y.-P. Zhao, S. B. Chaney, S. Shanmukh, and R. A. Dluhy, "Polarized surface enhanced Raman and absorbance spectra of aligned silver nanorod arrays," J. Phys. Chem. B **110,** 3153-3157 (2006).
14. Y. J. Liu, J. G. Fan, S. Shanmukh, R. A. Dluhy, and Y.-P. Zhao, "Angle dependent surface enhanced Raman scattering obtained from a Ag nanorod array substrate," Appl. Phys. Lett. **89,** 173134.1-3 (2006).
15. S. Shanmukh, L. Jones, J. Driskell, Y.-P. Zhao, R. Dluhy, and R. A. Tripp, "Rapid and sensitive detection of respiratory virus molecular signatures using a silver nanorod array SERS substrate," Nano Lett. **6,** 2630-2636 (2006).
16. C. E. Taylor, S. D. Garvey, and J. E. Pemberton, "Carbon contamination at silver surfaces: surface preparation procedures evaluated by Raman spectroscopy and X-ray photoelectron spectroscopy," Anal. Chem. **68,** 2401-2408 (1996).

17. Y. W. Alsmeyer, and R. L McCreery, "Surface-enhanced Raman spectroscopy of carbon electrode surfaces following silver electrodeposition," Anal. Chem. **63,** 12891295 (1991).

18. R. P. Van Duyne, J. C. Hulteen, and D. A. Treichel, "Atomic force microscopy and surface-enhanced Raman spectroscopy. I. Ag island films and Ag film over polymer nanosphere surfaces supported on glass," J. Chem. Phys. **99,** 2101-2115 (1993).

19. W. -H. Yang, J. Hulteen, G.C. Schatz, and R. P. Van Duyne, "A surface-enhanced hyper-Raman and surface-enhanced Raman scattering study of trans-1,2-bis(4-pyridyl)ethylene adsorbed onto silver film over nanosphere electrodes. Vibrational assignments: experiment and theory," J. Chem. Phys. **104,** 4313-4323 (1996).

20. K. L. Norrod, L. M. Sudnik, D. Rousell, and K. L. Rowlen, "Quantitative comparison of five SERS substrates: sensitivity and limit of detection," Appl. Spectrosc. **51,** 994-1001 (1997).

21. P.N. Sanda, J.M. Warlaumont, J.E. Demuth, J.C. Tsang, K. Christmann, and J.A. Bradley, "Surface-enhanced Raman scattering from pyridine on Ag(111)," Phys. Rev. Lett. **45,** 1519-1523 (1980).

22. U.K. Sarkar, A.J. Pal, S. Chakraborti, and T.N. Misra, "Classical and chemical effects of SERS from 2,2':5,2" terthiophene adsorbed on Ag-sols," Chem. Phys.Lett. **190,** 59-63 (1992).

23. M. Moskovits, "Surface-enhanced spectroscopy," Rev. Mod. Phys. **57,**783-825 (1985).

24. E. J. Zeman, K. T. Carron, G. C. Schatz, and R. P. Van Duyne, "A surface enhanced resonance Raman study of cobalt phthalocyanine on rough Ag films: theory and experiment," J. Chem. Phys. **87,** 4189-4200 (1987).

25. R. J. Dijkstra, A. Gerssen, E. V. Efremov, F. Ariese, U. A. T. Brinkman, and C. Gooijer, "Substrates for the at-line coupling of capillary electrophoresis and surface-Raman spectroscopy," Anal. Chim. Acta. **508,** 127-134 (2004).

26. N. Félidj, S. Lau Truong, J. Aubard, G. Lévi, J. Krenn, A. Hohenau, A. Leitner, and F. Aussenegg, "Gold particle interaction in regular arrays probed by surface enhanced Raman scattering," J. Chem. Phys. **120,** 7141-7146 (2004).

27. S. E. Roark, D. J. Semin, A. Lo, R. Skodje, and K. L. Rowlen, "Solvent-induced morphology changes in thin silver films," Anal. Chim. Acta. **307,** 341-353 (1995).

28. X. Li, W. Xu, H. Jia, X. Wang, B. Zhao, B. Li, and Y. Ozaki, "Water-induced morphology changes in an ultrathin silver film studied by ultraviolet-visble, surface-enhanced Raman scattering spectroscopy and atomic force microscopy," Thin Solid films **474,** 181-185 (2005).

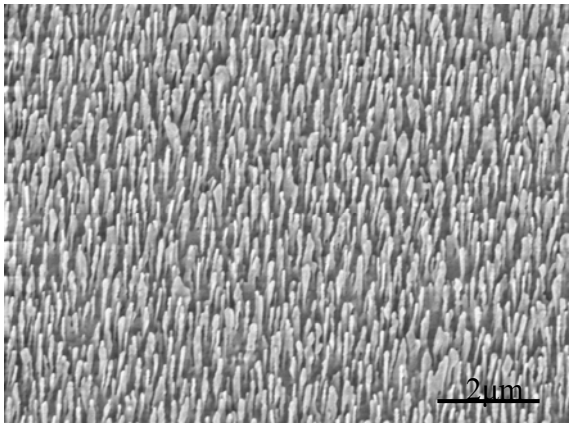

Fig. 3.1. A typical SEM image of Ag nanorod array. The Ag nanorods have an average length of 868 ± 95 nm and an average diameter of 99 ± 29 nm. The scale bar represents 2 μm.

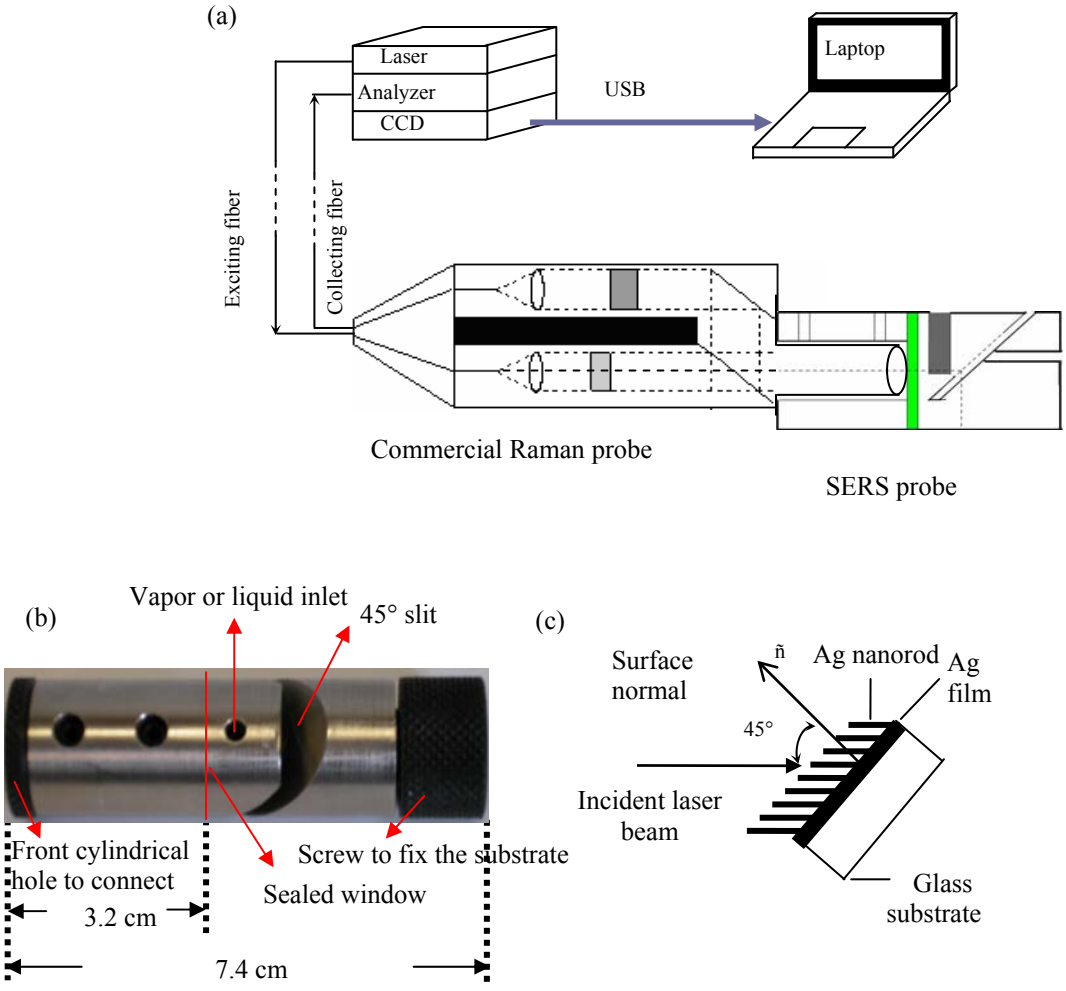

Fig. 3.2. (a) The schematics of the fiber Raman setup for SERS measurement. (b) Photograph of SERS probe. (c) The schematic of the tilting Ag nanorods parallel to the incident plane at 45° incident angle relative to surface normal.

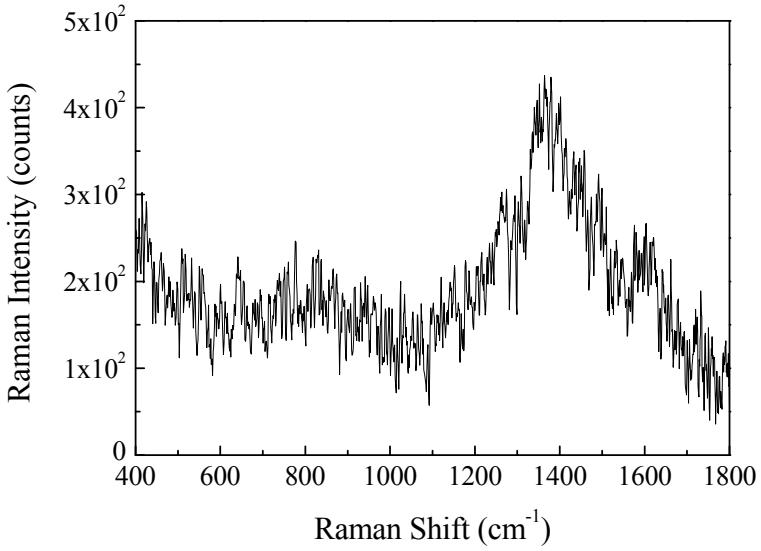

Fig. 3.3. Typical SERS spectrum of bare substrate. The spectrum was collected at an excitation wavelength of 785 nm, incident laser power of 52 mW on the substrate and collection time of 10 s.

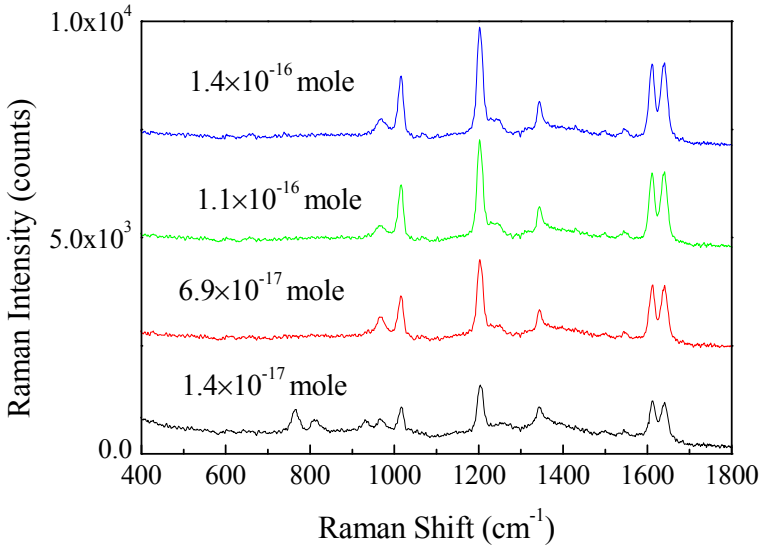

Fig. 3.4. SERS spectra of BPE deposited on Ag nanorod substrate. The amount of adsorbed BPE on substrate was calculated to be from 10^{-17} to 10^{-16} moles. The spectra were collected at an excitation wavelength of 785 nm, incident laser power of 52 mW on the samples and collection time of 10 s. Spectra were offset for clarity.

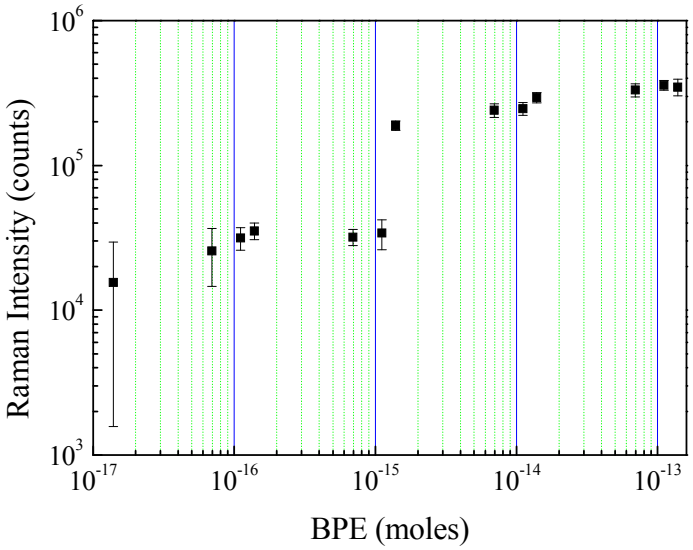

Fig. 3.5. Log- log plot of the integrated band areas at 1200 cm^{-1} in the SERS spectra of BPE against the number of moles of BPE deposited onto the Ag nanorod substrate surface. Spectra were collected from 5 spots for each application of BPE at an excitation wavelength of 785 nm, incident laser power of 52 mW on the samples and collection time of 10 s. The average intensities were plotted and the error bars represent the standard deviation values.

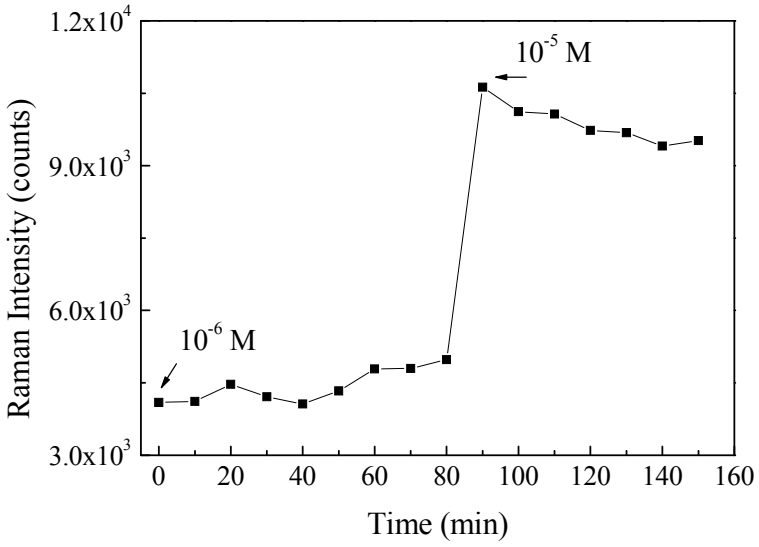

Fig. 3.6. Plot of the integrated band areas at 1200 cm^{-1} in the SERS spectra of BPE as a function of time. The concentrations of BPE were from 10^{-6} to 10^{-5} M. Distilled water was used as solvent. The BPE solution was sucked out of the liquid cell before the next higher concentration was added. The elapsed time for each concentration was 80 min. The spectra were collected at an excitation wavelength of 785 nm, incident laser power of 96 mW on the samples and collection time of 10 s.

CHAPTER 4

SILVER NANOROD ARRAY AS A SERS SUBSTRATE FOR FOODBORNE PATHOGENIC BACTERIA DETECTION[1]

[1]HsiaoYun Chu, Yaowen Huang, and Yiping Zhao. To be submitted to *Applied Spectroscopy*.

ABSTRACT

Surface enhanced Raman scattering (SERS) using novel silver nanorod array substrates has been used for the detection of pathogenic bacteria. The substrate consists of a base layer of 500 nm silver film first deposited onto a glass slide and a layer of silver nanorod array with length of ~1 μm deposited by OAD method at a vapor incident angle of 86°. Spectra from whole cell bacteria, Generic *Escherichia coli*, *Escherichia coli* O157:H7, *E. coli* DH 5α, *Staphylococcus aureus*, *Staphylococcus epidermidis* and *Salmonella typhimurium* have been obtained. This novel SERS active substrate can detect spectral differences between Gram types, different species and strains. Viable and nonviable cells have also been examined and significantly reduced SERS responses at major Raman bands were observed for nonviable cells. The SERS spectra of bacteria on single cell level excited at low incident powers (12 μW) and short collection time (10 s) was also demonstrated on this silver nanorod substrate. These results indicate that the SERS-active silver nanorod arrays substrate is a potential analytical sensor for rapid identification of microorganisms with a minimum sample preparation procedure.

INTRODUCTON

The potential risk for deliberate contamination of the environment, food and agricultural products has recently increased due to the global war on terrorism, making biosensing as an important issue for several federal agencies. The current trend is to decentralize large stationary laboratory facilities such that tests can be performed anywhere and under field conditions. Consequently, the development of portable, rapid and sensitive biosensors with on-the-spot interpretation of results is gaining momentum. In the food safety point of view, real-time microbial detection and source identification are becoming increasingly important due to the growing consumer concerns over foodborne disease outbreaks and economic loss from the outbreaks. The Centers for Disease Control (CDC) estimated that foodborne diseases cause approximately 76 million illnesses, 325,000 hospitalizations, and 5,000 deaths in the United States each year. Known pathogens account for an estimated 14 million illnesses, 60,000 hospitalizations, and 1,800 deaths. [1] The most recent foodborne outbreaks include the *E. coli* O157:H7 contaminated spinach and *Salmonella* outbreak linked to Peter Pan® Peanut butter in 2006.

The conventional culture method recommended by the USDA for detection and identification of foodborne pathogens usually requires three general steps: enrichment, colony isolation, and confirmation. Although conventional culturing is the most sensitive detection methodology available, it is time-consuming and requires extensive manual labor. Other methods including polymerase chain reaction (PCR), antibody-based systems and mass spectrometry have been developed as a diagnostic tool to detect pathogens; however, these approaches have fundamental restriction that limit the use outside of a laboratory. False negative/ false positive identification with PCR method, [2] the multi-steps, chemical reagents required for procedures for

immunoassay, and the expensive, non-portable mass spectrometry [3], make these methods neither fast nor robust enough for field detection.

The research directions for improvement of analytical methods obviously falls on 1) the reduction or elimination of the sample preparation procedure, 2) continual and routine analysis of large numbers of samples with minimum reagent usage and cost, 3) ease to operate under most conditions and 4) short data accumulation time. An alternative approach that satisfies most of the above requirements is spectroscopic techniques that are specific, noninvasive, nondestructive, and can be performed very rapidly. Similar to infrared (IR) spectroscopy, Raman spectroscopy provides detailed information about the material under investigation, often at the molecular level. Raman spectroscopy enjoys advantages over IR such as less interference from water bands in aqueous samples and selection rules that result in fewer spectral bands and thus simpler spectra. It has been used to obtain highly structured information on bacteria, [4, 5] even at the single bacterial cell level. [6] Although Raman sensitivity is low in comparison to IR spectroscopy, it can be greatly increased by the surface-enhanced Raman scattering.

The effect of drastically enhanced Raman signals rely on either the adsorption or close proximity of a molecule to a metal substrate. [7] When the analyte is in close proximity to the metal, the energy from the plasmon resonance may be coupled into bonds of the molecule of interest resulting in an enhancement of the Raman signal of several orders of magnitude. [8, 9] Surface-enhanced Raman spectroscopy has been used as an analytical tool to observe trace amount of chemical and biological molecules due to its capability of giving real-time molecular vibrational information under ambient conditions. In addition to signal enhancement, SERS has a fluorescence-quenching effect. [10] This is extremely valuable when investigating microorganisms,

which often exhibit a fluorescence background under excitation in the near-infrared to visible regions.

The substrate can take the form of a roughened metal surface, a colloidal solution, or a roughened electrode. The morphology of the metallic structure plays a major role in determining the magnitude of signal enhancement and sensitivity of detection.[11] Early SERS substrates included a random distribution of roughness features produced by oxidation reduction on a metal electrode [12], or evaporation of thin metal film on a flat substrate.[13] Various forms of nanostructure have been explored to enhance SERS effects, for example; rough metallic surfaces by chemical etching [14], silver films on TiO_2 [15], colloidal silver nanoparticles [16], silver nanoparticle arrays fabricated by nanosphere lithography [17], electro-deposition of silver on silver films at high potential [18], and aligned monolayer of silver nanowires.[19] Among them, silver colloids have been used intensely because of their ability to provide the greatest SERS enhancement, and in some cases, these colloids have proven to be capable of trace component/single-molecule detection.[20] However, metal colloidal substrates have both reproducibility and stability issues, as colloid particles might vary from batch to batch and tend to aggregate and to precipitate in solutions over time.[21-24] This is because the laser has to strike the sample at a point where the SERS substrate and analyte are both present and in the appropriate geometry (the so-called "hot spot") to achieve maximum enhancement. Other substrate preparation methods are either expensive or time consuming, and it is not easy to make reproducible substrates of the correct surface morphology to provide maximum SERS enhancements. Without uniformity and good reproducibility of the metal substrates, the attainment of reproducible spectra remains a major challenge for SERS.

Oblique angle deposition (OAD) is a physical vapor deposition technique that overcomes some of the difficulties and disadvantages of the previously mentioned deposition methods. This method involves positioning the substrate at a specific angle such that the vapor from the source is incident on the substrate close to the grazing angle. This process results in the preferential growth of nanorods on the substrate in the direction of deposition. The resulting surface morphology can be attributed to the fact that nanostructures are grown from initial metal nucleation sites due to a shadowing effect causing the growth of the nanorod arrays aligned in a specific direction. The major advantages of this technique include: a) control over the size, shape, and density of the nanostructures by varying the deposition conditions such as the incident vapor deposition angle, temperature and the duration and rate of deposition; b) a wide variety of elements can be used to form these nanostructures as long as the material used can be evaporated; c) any standard physical vapor deposition system equipped with a holder capable of rotation in the polar and azimuthal directions can be utilized. By rotating the substrate at controlled speeds in an azimuthal direction, it is possible to produce complex and unique nanostructure designs. [25] Silver nanorod substrates prepared by the OAD process have previously been shown to provide SERS enhancement factors of $> 10^8$ and have also been shown to be SERS active [26]. Very recently, the OAD prepared SERS substrates demonstrated its potential to distinguish between viruses.[27] The OAD technique offers an easy, straightforward and inexpensive way for the fabrication of silver nanorod arrays for high sensitivity SERS applications. The SERS substrates produced by OAD have the advantages of uniformity and reproducibility.

The overall objective of this study was to evaluate the ability of silver nanorod arrays as a SERS substrate to rapidly detect pathogenic bacteria. We also examined the ability of SERS to

differentiate between different bacterial species, strains and between viable and nonviable cells based on their characteristic SERS spectra. Finally, we explored the possibility to obtain single cell level Raman spectra on these silver nanorod substrates.

EXPERIMENTAL METHODS

Fabrication of Substrates

The SERS active substrate used to obtain spectra was silver nanorod arrays fabricated by OAD technique using a custom-designed electron beam/sputtering evaporation (E-beam) system (Torr International, New Windsor, NY) that has been previously described. [26] Glass microscopic slides (Gold Seal® Catalog No.3010) were used as the base platform for silver nanorod arrays deposition. The glass slides were cleaned with Piranha solution (80% sulfuric acid, 20% hydrogen peroxide), and rinsed with DI water. The substrates were then dried with a stream of nitrogen gas before loading into the E-beam system. A base layer of Ti (20nm) and silver film (500 nm) were first evaporated onto the glass slides at normal angle to the surface at a rate of ~1.0 Å/s and 3.0-4.0 Å/s, respectively. The substrates were then rotated with computer controlled motors to 86˚ with respect to the surface normal. Ag nanorods were grown at this oblique angle in which the deposition rate was ~3.0 Å/s, and the deposition pressure was approximately 1×10^{-6} Torr. The film thickness was monitored by a quartz crystal microbalance positioned at normal incidence to the vapor source direction.

This deposition conditions resulted in optimal SERS substrates with an average nanorod length of 868 ± 95 nm and the average diameter of 99 ± 29 nm. The average density of the nanorods was approximately 13 ± 0.5 rods/μm^2 with an average tilting angle of ~73° with respect to the substrate normal. Prior to data collection the substrates were stored in a relatively

clean environment at room temperature to avoid any changes in surface morphology due to temperature or atmospheric humidity.

Bacterial Samples

The following bacteria were used in the analyses: Generic *Escherichia coli* (ATCC 29993), *Escherichia coli* O157:H7 (ATCC 43888), *Staphylococcus aureus* (ATCC 6538) and *Staphylococcus epidermidis* (ATCC 33501) were obtained from American Type Culture Collection (Rockville, MD). *Salmonella typhimurium* 1925-1 poultry isolate and *E. coli* DH 5α were provided by the Department of Food Science and Technology, The University of Georgia. Bacterial cells were grown in trypticase soy broth (TSB, Difco, Detroit, Mich) over night at 37 °C with 240 rpm shaking. This growth procedure routinely yielded a stock culture containing ~10^9 colony forming units (CFU)/ml at stationary phase. Bacterial populations were determined by the conventional surface plate count method using plate count agar (PCA, Difco). Following incubation, the cultures were washed three times with sterilized deionized (DI) water before re-suspending in DI water. Desired dilutions were made in sterilized DI water.

SERS Measurements

SERS spectra were acquired using a HRC-10HT Raman analyzer system (Enware Optronics Inc. Irvine, CA). This system consists of a diode laser, spectrometer, integrated Raman probe head for both excitation and collection, and separate delivery and collection fibers. The excitation source was a frequency stabilized, narrow linewidth near IR diode laser with a wavelength of 785nm. The excitation laser beam coupled to a 100 μm fiber was focused onto the substrate through the Raman probe head and was unpolarized at the sample. The focal length of the Raman probe was 6 mm and the diameter of the laser spot was 0.1 mm. The Raman signal from the substrate was collected by the same Raman probe head and was coupled to a 200 μm

collection fiber which delivered the signal to the spectrometer equipped with a charge coupled device (CCD) detector. The laser power at the sample varied and was monitored with a power meter (λ = 785 nm, Thorlabs Inc., Newton, NJ). The spectral collection time was 10s. A 2.0-μL aliquot of intact bacteria sample was applied to the Ag nanorod array substrate and allowed to bind at room temperature prior to spectrum acquisition. SERS spectra were collected from multiple spots across the substrate and from multiple substrates. Generally, solution spot sizes were 2 mm in diameter meaning concentrations of a culture solution containing ~10^8 CFU/ml corresponded to the excitation of roughly 500 cells on the laser spot.

Data Analysis

Enwave Raman analyzer software (Enware Optronics Inc. Irvine, CA) was used for instrument control and data collection. The spectral coverage is ~200 to 2400 cm^{-1} with 785 nm excitation. ASCII data were exported from the Raman analyzer software into Origin software 7.0 version (OriginLab Corporation, Northampton, MA) for spectra processing, including plotting, baseline correction, normalization and peak detection.

RESULTS AND DISCUSSION

SERS of Background Media

In pathogens, Raman signatures arise predominantly from phenotypic information, including contributions from proteins, nucleic acids (DNA and RNA), lipids, carbohydrates, and endogenous biomolecules. In order to detect and identify pathogens of interest, it is essential to ensure the observed Raman signatures specific to target microorganisms, but not specific to the environment associated with those microorganisms (e.g., growth media and metabolic products). To examine whether media confound SERS bacterial background signal, spectra from different

media and *E. coli* inoculated media were compared. Fig. 4.1 shows the spectra of TSB medium and *E. coli* in TSB medium. There were no significant spectral differences between TSB and bacteria cells in TSB. Fig. 4.2 shows the spectra of 0.01 M phosphate buffered saline (PBS) and *E. coli* in PBS. Other than a weak bank around 730 cm^{-1}, there were no significant spectral features observed without separation of bacteria cells. The chemical components and/or metabolic byproducts in the media could have interfered or overlapped the spectral features of microorganisms. To purify *E. coli* cells, wash steps (in DI water) followed by centrifugation were then incorporated prior to spectra collection. After samples were washed and centrifuged, significant differences in spectral features were readily visible (Fig. 4.3). Therefore, it was necessary to incorporate additional separation technique, such as washing and centrifugation, into a bacterial detection and identification procedure based on SERS. Consequently, bacteria purification steps were included in the sample preparation procedures in all our further studies.

SERS Reproducibility

As mentioned earlier, the morphology of the metallic structure plays a major role in determining the magnitude of signal enhancement and sensitivity of detection. The major obstacle to the widespread use of SERS for analytical applications is to produce sensitive and uniform substrates for reproducible SERS effect. One way to measure the SERS spectral reproducibility with silver nanorod array substrates is illustrated in Figure 4.4. SERS spectra collected from separate spots on the substrate and from different substrates, were normalized with respect to the most intense band in each spectrum and are displayed in Figure 4.4. Looking at the overlaid spectra, it is clear that there is a good spot-to-spot reproducibility. At the same time, from the stacked spectra it is obvious that the spectra of *E. coli* and *S. typhimurium* obtained on the silver nanorod substrates have a high degree of reproducibility. Corresponding

standard deviation spectra for these data sets are also displayed in this figure. The relative standard deviation of these spectra for each of these species is ~6% at 735 cm^{-1} and 1328 cm^{-1} (maximum signal). Our results demonstrate high degree of reproducibility achieved with these SERS substrates. The small variation observed between individual spectra of a particular species could be attributed to the slight inhomogeneous surface morphology. In addition, some spectral differences may result from the molecular orientation of the components of the bacteria on substrate surface and from the molecular interaction with metal surfaces.

SERS of Bacteria: Species Specificity

To determine the capability of SERS to distinguish between different bacteria species, Raman spectra of four bacterial species, Gram-negative *E. coli* O157:H7 and *Salmonella typhimurium*, Gram-positive *Staphylococcus aureus* and *Staphylococcus epidermidis* were obtained. Since SERS probes molecules close to the metal surface structures, in the case of intact cells, the SERS response is expected to be dominated by the outer surface structures or molecules secreted by the cell. We report several bacterial species where intact, viable cells had been deposited on the silver nanorod array substrates. Figure 4.5 shows an SEM image of *E. coli* O157:H7 on a substrate. Figure 4.6 plots the SERS spectra of the four species of bacteria in the 400-1800 cm^{-1} region. Variations in band frequencies reflect compositional and structural differences in the bacterial species while differences in peak intensities could be a result of slight differences in the morphology of the SERS substrates. To remove spectral discrepancies caused by the substrates, each SERS spectrum was normalized with respect to its most intense peak. These spectra were acquired with ~24 mW of incident laser power and 10 s collection time. These results demonstrate that SERS spectra of bacteria with good signal-to-noise ratio spectra

can be readily obtained when cells are placed on these silver nanorod array substrates and excited by low laser power at 785 nm.

The SERS spectra in Figure 4.6 were arranged from top to bottom according to their Gram stain classifications, with bacteria belong to the same Gram type adjacent to each other. Spectral differences ascribed to different Gram types, such as *S. typhimurium* and *S. aureus*, could be discerned by naked eyes, while spectral differences attributed to closely relative species are not immediately striking. For example, SERS spectra of *S. aureus* and *S. epidermidis* exhibit clear similarities, though, on closer inspection, there are subtle quantitative differences in their relative intensities. Qualitatively, numbers of major spectral bands, such as bands at ~735, 1330 and 1450 $cm^{-1,}$ are found to be common to all these species, although their relative intensities vary. There are also differences, such as bands at ~ 550 and ~1030 cm^{-1} significant to *E. coli* O157:H7 and *S. typhimurium*, a band at ~1090 cm^{-1} unique for *S. aureus* and *S. epidermidis*, and differences among the spectra in the 800-1100 cm^{-1} region.

At this point, molecular level interpretation of SERS vibrational features has not been universally established yet, but based on the spectral position; we can make some general statement. In bacteria detection, Raman signatures from proteins, phospholipids, nucleic acids, and carbohydrates are anticipated to contribute to these spectra. The ubiquitous strong SERS band at ~735 cm^{-1} and the broad band at ~1330 cm^{-1}, for example, have been attributed to the nucleic acid base adenine in previous SERS studies of nucleic acid components and bacterial components.[28, 29] Since SERS technique is most sensitive to the outer bacterial cell layer, molecules and functional groups that are in the immediate proximity of the metal surface should predominate in a SERS measurement. Molecular components of the cell wall and membrane should favor over nucleic acids that are located internally in SERS band assignment. Therefore,

the ~735 cm^{-1} can not be straightforwardly explained by the presence of adenine containing compounds on the outer surface of bacterial cells. Another possibility is the secretion of small molecules by the cell. On the other hand, phospholipids and polysaccharides also have bands in this region and are significant components of cell membrane structures.[30] Another Raman signature common to all these four species at ~1450 cm^{-1} can be attributed to the CH_2 deformation mode of proteins. [31]

To match some of the other bands to characteristic functional groups, the broad band at ~550 cm^{-1} observed in both the spectra of *E. coli* O157:H7 and *S. typhimurium* can be assigned to carbohydrate. [32] The strong band at ~930 cm^{-1} may have some contribution from the background signal of the substrate, though this band had been assigned to C-C stretching modes in proteins. [33] The small band at 1030 cm^{-1} can be attributed to carbohydrate. [32] A band at ~1090 cm^{-1} unique for *S. aureus* and *S. epidermidis*, had been associated with protein.[31] Vibrational bands in the 930-1130 cm^{-1} region have also been previously assigned to membrane phospholipids and proteins. [30] The band at ~1600 cm^{-1} seen in all the spectra is most likely from the substrate. It should be noted that blank Ag nanorod SERS substrates produced by using OAD methods normally have background contributions that have previously been attributed to carbonaceous material adsorbing onto the substrate during the fabrication of the SERS substrate and storage in ambient conditions. [34] Such background signals are commonly encountered in SERS, and they were found to remain unchanged throughout the studies and exposure to laser radiation did not affect their position.

Considering the more evident difference in their cell envelope biochemistry (Gram negative versus Gram positive), the assumption was that these spectra would be quite difference. This does not seem to be the case from our observation, the fact that these spectra share several

similar key bands suggesting the possibility that SERS comes from a small number of SERS-promoting molecules which are prevalent in all cell surface. Zeiri et al. [21] reported that spectra measured for four different bacterial strains, representing both Gram-negative and Gram-positive bacteria, were essentially identical. The authors suggested that silver colloid particles bind only to certain specific groups on the bacterial cell wall (e.g., flavins). The cell walls of both Gram positive and negative bacteria contain a ubiquitous component called peptidoglycan, which is a polymer of disaccharide (glycan) cross-linked by short chains of amino acids. The glycan backbone is made up of alternating molecules of N-acetylglucosamine (NAG) and N-acetylmuramic acid (NAM). There has been report of SERS spectra of NAG showing an intense peak at~730 cm^{-1}; [22] which could explain the ever-present peak at~735 cm^{-1} in our spectra of both Gram negative and positive bacteria. Though there is potential to obtain chemical information from these SERS spectra, they are difficult to interpret. Although resources for standard Raman spectra of biological materials are slowly becoming available and can be useful, it is not always the case that peaks expressed in a Raman spectrum will also be observed in the SERS spectrum of the same sample. Obviously in a complex multi-component system such as a bacterial cell, there could be any number of SERS-active vibrational modes present thus, peak attributions should remain cautious and tentative, unless composition of the cells and their model compounds are thoroughly examined and independent references are employed. Nevertheless, the combination of differences and similarities among the spectra allow the potential use of SERS to distinguish bacterial species.

Strain Specificity

Since SERS could detect and differentiate among different species, it was important to determine if different strains of the same species could be distinguished on these silver nanorod

substrates. *E. coli* O157:H7, generic *E. coli* and *E. coli* DH 5α were analyzed to explore this possibility. SERS analysis of these three strains of *E. coli* and their respective spectra are displayed in Figure 4.7 Based on the finding for *E. coli* O157:H7 (Figure 4.6), the observation was that primary SERS bands should attribute to surface protein, membrane phospholipids and polysaccharides. The sharp band at ~ 735 and the broad bands at 1330 and ~1450 cm^{-1} in the spectra are common to all three strains. Although, the closely related chemical composition and structure of the *E. coli* strains would give rise to similar SERS spectra, minor but noticeable difference were expected in the spectra for different *E. coli* strains. Each spectrum displayed in Figure 4.7 was an average of 6 spectra. While all these *E. coli* samples shared some similar characteristic peaks, the relative band widths and intensities of these peaks in the spectra are quite different. This effect can be observed in the spectral 400-800 cm^{-1} region of, and again in the 800-1100 cm^{-1} region, which shows intensity differences as well as frequency shifts in the spectra among different strains. Figures 4.8 and figure 4.9 highlight regions within the spectra where differences are apparent. For example, differences on the ratio of peak intensities for the ~735 cm^{-1}, 1030 cm^{-1} and 1330 cm^{-1} bands can be readily observed. The spectral structure in this frequency range is likely due to nucleic acids or carbohydrate, protein and phospholipids [22, 30]. It is likely that the observed spectral differences relate to the composition of these components present on bacterial cell surfaces. Other possible causes were in the nature of orientation and/ or binding of surface proteins and or surface carbohydrates of particular bacteria cells on the SERS substrate. Although the basis of most of these bands can be traced from one spectrum to the next, the overall vibrational signature of each strain is unique, allowing fingerprinting potential for bacterial strain identification purposes.

Viability Specificity

Another important aspect for identifying pathogens is the ability to distinguish between viable and nonviable cells. Figure 4.10 shows spectra of viable and nonviable cells of *E. coli* O157:H7. The nonviable cells were prepared by boiling the bacteria in a hot water bath for 10 min at 100 °C. The dead cells show a significantly reduced SERS response at those characteristic bands of ~550 $cm^{-1,}$ 735 cm^{-1}, 1330 cm^{-1} and 1450 cm^{-1} that are present in the viable cells. Measurements from heat treated *E. coli* DH 5α was also obtained. Significantly reduced SERS responses at major bands from heat treated *E. coli* DH 5α were also observed (Fig. 4.11). High temperatures may produce changes in the outer cell layers of bacteria. In Gram negative bacteria, damage to the outer membranes occurs when cells are subjected to a mild heat shock. Heating may significantly denature and cause conformational changes in the outer membrane proteins of Gram negative bacteria. [35] Heat could also release carbohydrates from cells and separate surface associated carbohydrates from the cell. [36] Therefore, some variations in the spectra are expected upon heat treatment due to the changes of the structure of the adsorbed molecules or the orientation of the adsorbates. Another possibility is that if SERS bands are due to small molecules produced by the cells, the production of molecules apparently would stop upon cell death. This result is encouraging when considering possible applications of SERS in pathogen detection where the differentiation between viable and nonviable cells is imperative.

SERS Sensitivity

Up to this point, all the spectra were obtained through a HRC-10HT Raman analyzer system with a 100 μm diameter laser. Typically, a drop of 2 μL of bacteria solution (~10^8 CFU/ml) was applied on the substrate forming a spot size of 2 mm in diameter which corresponds to roughly 500 cells excited under the laser spot. To further explore the sensitivity of

SERS technique, SERS spectra of bacteria at the single cell level were observed on our silver nanorod array substrates. A Renishaw Raman microscope, with an approximately 1 μm laser spot, was used to observe the scattering excited by a 785 nm diode laser and a 12 μW laser power. Images of bacterial cells (*E. coli* O157:H7) obtained under a 50× microscope objective are provided in Figure 4.12. The area under the focal laser region is highlighted by a circle. Figure 4.12a shows an isolate cell chain, consisting of 2-3 cells, where the laser beam was focused. A cluster with congested multiple cells is shown in Figure 4.12b. The associated Raman spectrum, after exposing the area to the 1 μm laser beam for 10 s, is shown in Figure 4.12c. The SERS spectrum of the isolated cell chain is quite similar to that of the more congested cells. All the major bands, ~735, 1330, and 1450 cm^{-1}, match with what we observed from the more concentrated samples (estimated ~500 cells excited under the 100 μm laser spot in Fig. 4.7). Most bands correspond to functional groups in the main constituents of a microbial cell, proteins, carbohydrates, lipids, and nucleic acids which we have described in detail in an earlier section of this report (Species Specificity). These results show the ability to observe Raman signatures of bacteria on a single cell level using the silver nanorod substrate. Non-SERS Raman spectra of a single bacterial cell (*Clostridium beijerinckii*) obtained by a confocal microscopy have been reported. [37] However, longer illumination times (3 min) and higher incident laser power (8 mW) was required compared to the considerably low incident power (12 μW) and short illumination time (10s) employed in our study.

CONCLUSIONS

A diagnostic method that can identify pathogens rapidly and distinctively with minimum sample preparation has major benefits to prevention of epidemic outbreak and

bioterrorism. The SERS method presented here is of practical interest, as it only requires simple sample preparation consisting of washing the cells and drying on a SERS substrate. No chemical reagents are necessary to specifically label target microorganisms; the spectra contain information on all major substances present in bacterial cells. We have demonstrated that good signal-to-noise and reproducible Raman spectra of bacteria when the microorganisms were placed on the silver nanorod array substrate. We evaluated these SERS substrates as potential bioanalytical sensors for bacterial identification. The bacterial SERS fingerprints show clear distinctions between different species and strains; also the ability to distinguish between nonviable and viable cells was presented. The ability to quickly obtain high quality Raman spectra of single bacterial cell would be useful for distinguishing dangerous pathogens in a mixture. The speed, specificity and ease of implementation of SERS technique represents a valuable alternative to current bacterial diagnostic tools and provides the possibility of portable pathogen sensors for on-site food inspection.

ACKNOWLEDGEMENTS

This research was supported by funding from the National Science Foundation (ECS0304340 and ECS070178).

REFERENCES

1. P.S. Mead, L. Slutsker, V. Dietz, L.F. McCaig, J.S. Bresee, C. Shapiro, P.M. Griffin, and R. V. Tauxe, Emerging infectious diseases. **5,** 607 (1999).
2. C. A. Batt, in Listeria, Listeriosis, and Food Safety, T. Ryser and E. H. Marth, Eds. (Marcel Dekker, New York, 1999), 2nd ed., p. 261.
3. S. Vaidyanathan, D. B. Kell, and R. Goodacre, J. Am. Soc. Mass Spectrom. **13,** 118 (2002).
4. W. H. Nelson, R. Manoharan, and J. F. Sperry, Appl. Spectrosc. Rev. **27,** 67 (1992).
5. Q. Wu, T. Hamilton, W. H. Nelson, S. Elliott, J. F. Sperry, and M. Wu, Anal. Chem. **73,** 3432 (2001).
6. T. A. Alexander, P. M. Pellegrion, and J. B. Gillespie, Appl. Spectrosc. **57,** 1340 (2003).
7. M. Fleischmann, P. J. Hendra, A. J. McQuillan, Chem. Phys. Lett. **26,** 163 (1974).
8. M. Moskovits, Rev. Mod. Phys. **57,** 783 (1985).
9. A. Campion, and P. Kambhampati, Chem. Soc. Rev. **4,** 241 (1998).
10. K. Kneipp, A. S. Haka, H. Kneipp, K. Badizadegan, N. Yoshizawa, C. Boone, K. E. Shafer-Peltier, J. T. Motz, R. R. Dasari, and M. S. Feld, Appl. Spectrosc. **56,** 150 (2002).
11. Z. Q. Tian, B. Ren, and D. Y. Wu, J. Phys. Chem. B **106,** 9463 (2002).
12. A.A. Stacy and R.P. Van Duyne, Chem. Phys. Lett. **102,** 365 (1983).
13. G. J. Kovacs, R. O. Loutfy, P. S. Vincett, C. Jennings, and R. Aroca, Langmuir **2,** 689 (1986).
14. K. T. Carron, X. Gi, and M. L. Lewis, Langmuir **7,** 2 (1991).
15. L. M. Sudnik, K. L. Norrod, and K. L. Rowlen, Appl. Spectrosc. **50,** 422 (1996).
16. S. M. Nie, and S. R. Emory, Science **275,** 1102 (1997).

17. T. R. Jensen, M. D. Malinsky, C. L. Haynes, and R. P. Van Duyne, J. Phys. Chem. B **104,** 10549 (2000).

18. G. Suer, U. Nickel, and S. Schneider, J. Raman Spectrosc. **31,** 359 (2000).

19. A. Tao, F. Kim, C. Hess, J. Goldberger, R. R. He, Y. G. Sun, Y. N. Xia, and P. D. Yang, Nano Lett. **3,** 1229 (2003).

20. K. Kneipp, G. Kneipp, I. Itzkan, R. R. Dasari, and M. S Feld, Chem. Rev. **99,** 2957 (1999).

21. L. Zeiri, B. V. Bronk, Y. Shabtai, J. Czégé, and S. Efrima, Colloids Surfaces A. **208,** 357 (2002).

22. R. M. Jarvis, and R. Goodacre, Anal. Chem. **76,** 40 (2004).

23. A. Sengupta, M. L. Laucks, and E. J. Davis, Appl. Spectrosc. **59,** 1016 (2005).

24. M. L. Laucks, A. Sengupta, K. Junge, E. J. Davis, and B. D. Swanson, Appl. Spectrosc. **59,** 1222 (2005).

25. Y. - P. Zhao, D. X. Ye, G. C. Wang, and T. M. Lu, Proc. SPIE. **5219,** 59 (2003).

26. S. B. Chaney, S. Shanmukh, R. A. Dluhy, and Y.- P. Zhao, Appl. Phys. Lett. **87,** 031908.1 (2005).

27. S. Shanmukh, L. Jones, J. Driskell, Y.-P. Zhao, R. Dluhy, and R. A. Tripp, Nano Lett. 6, 2630 (2006).

28. K. Kneipp, and J. Flemming, J. Mol. Struct. **145,** 173 (1986).

29. L. Zeiri, B.V. Bronk, Y. Shabtai, J. Eichler, and S. Efrima, Appl. Spectrosc. **58,** 33 (2004).

30. K. J. Rothschild, J. R. Andrew, W. J. DeGrip, and H. E. Stanely, Science **191,** 1176 (1976).

31. E. Podstawka, Y. Ozaki, and L. M. Proniewicz, Appl. Spectrosc. **58,** 570 (2004).

32. K. C. Schuster, E. Urlaub, and J. R. Gapes, J. Microbiol. Methods **42,** 29 (2000).

33. J. S. Suh, and M. Moskovits, J. Am. Chem. Soc. **108,** 4711 (1986).

34. C. E. Taylor, S. D. Garvey, and J. E. Pemberton, Anal. Chem. **68,** 2401 (1996).

35. J. M. DiRienzio, K. Nakamura, and M. Inouye, Annu. Rev. Biochem. **47,** 481 (1978).

36. J.-H. Ryu, and L.R. Beuchat, J. Appl. Microbiol **95,** 1304 (2003).

37. K. Schuster, I. Reese, E. Urlaub, J. R. Gapes, and B. Lendl, Anal. Chem. **72,** 5529 (2000).

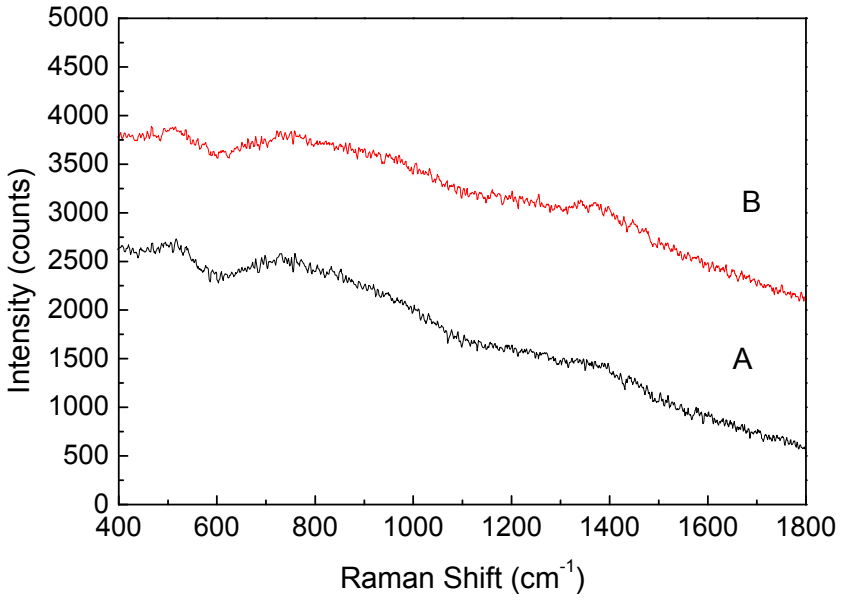

Fig. 4.1. Raman spectra of (A) TSB medium; (B) *E. coli* O157 (10^8 CFU/ml) in TSB. Incident laser powers of 69 mW and collection time of 10 s were used to obtain these spectra. Spectra were vertically offset (30%) for clarity.

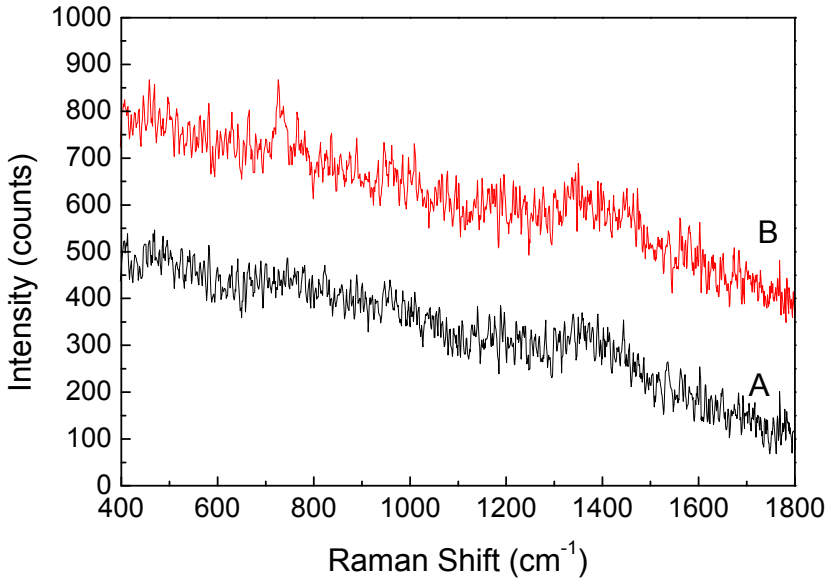

Fig. 4.2. Raman spectra of (A) PBS; (B) *E. coli* O157 (10^8 CFU/ml) in PBS. Incident laser powers of 69 mW and collection time of 10 s were used to obtain these spectra. Spectra were vertically offset (30%) for clarity.

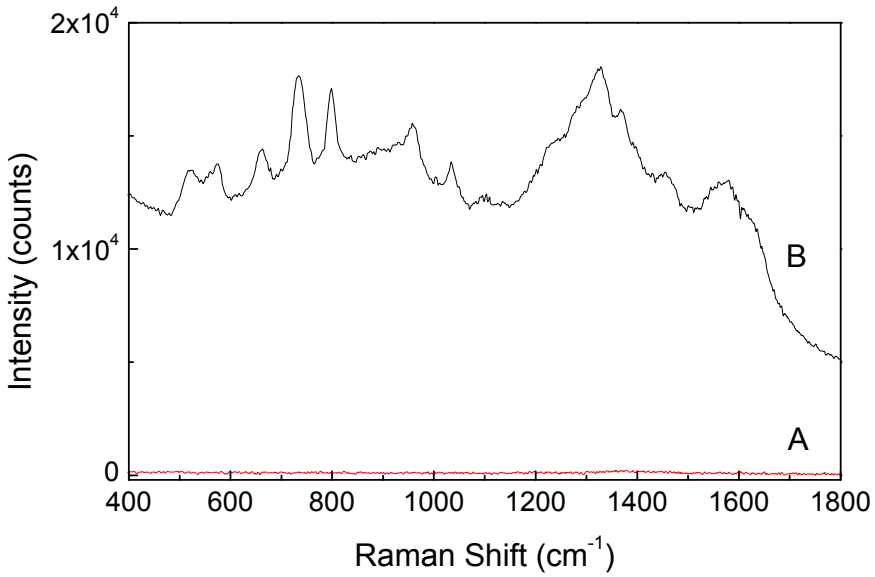

Fig. 4.3. Raman spectra of (A) DI water; (B) *E. coli* O157 in DI water. Incident laser powers of 69 mW and collection time of 10 s were used to obtain these spectra. Spectra were vertically offset (10%) for clarity.

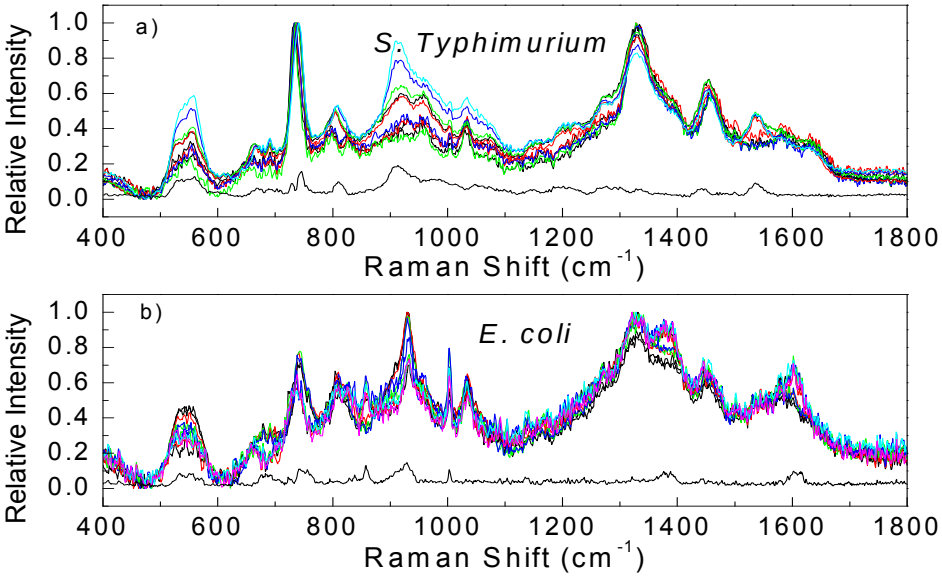

Fig. 4.4. SERS spectra of (a) *S. typhimurium* and (b) *E. coli* O157:H7 normalized to the peak intensity of the most intense peak are overlapped in order to demonstrate the SERS signal reproducibility from different areas of the same substrate. Spectra were collected from several spots on different substrates. Incident laser powers of 35 mW and collection time of 10 s were used to obtain these spectra. The standard deviation spectrum for each species is shown at the bottom of each panel.

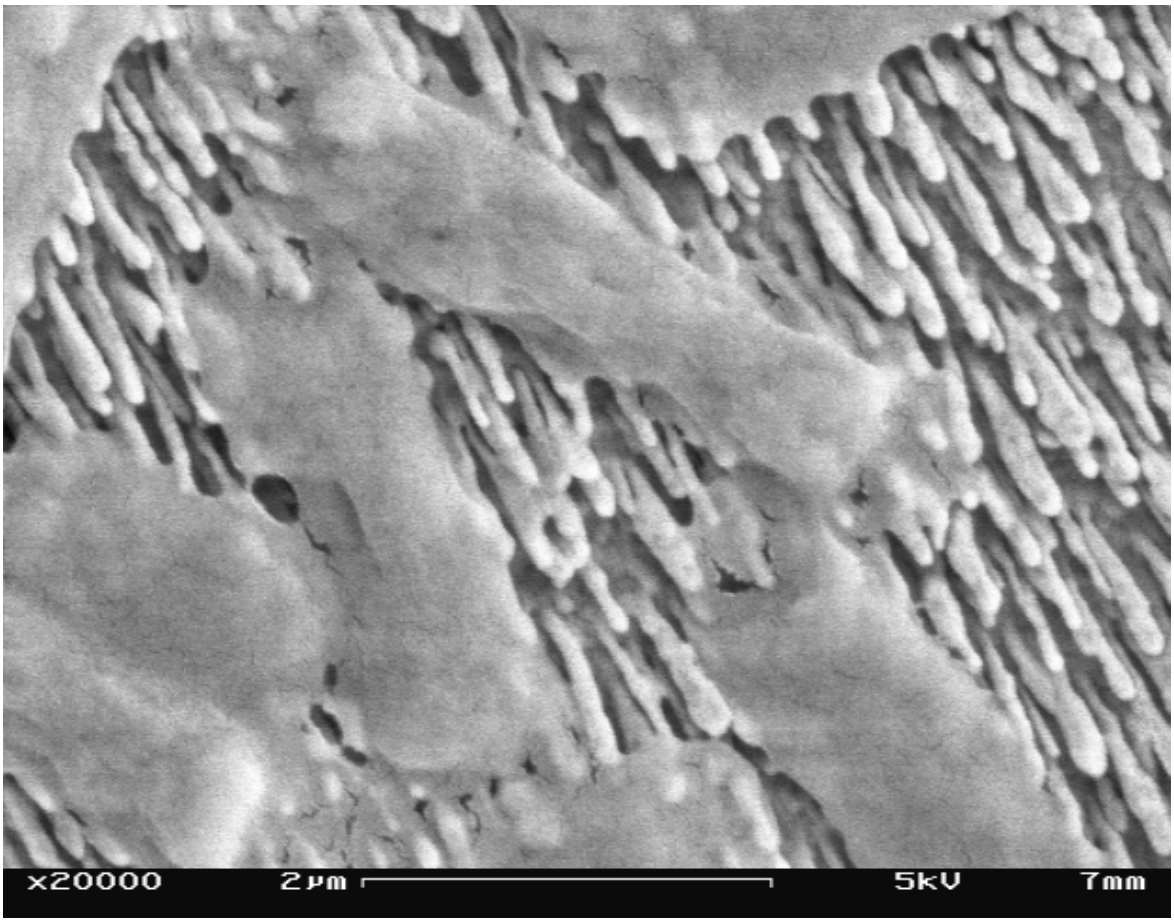

Fig. 4. 5. A SEM image of *E. coli* bacteria on a silver nanorod array substrate. The scale bar represents 2 μm. Since the cells did not appear to have lysed, the shifts observed in the SERS spectra are a product of cell wall biochemistry or other chemical components external to the cell.

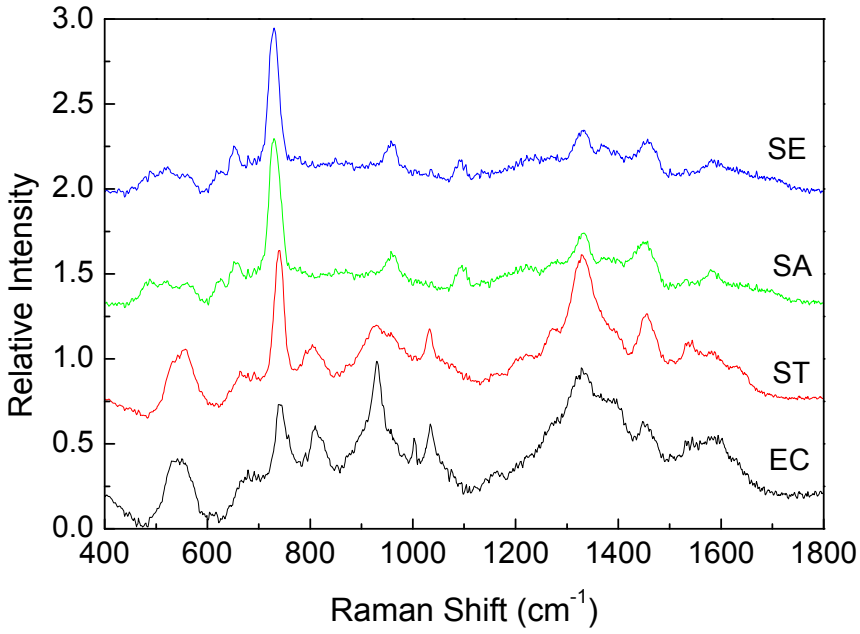

Fig. 4.6. SERS spectra of four bacterial species obtained on silver nanorod array substrates. EC = *E. coli* O157:H7; ST = *Salmonella. typhimurium*; SA = *Staphylococcus aureus* and SE = *Staphylococcus epidermidis*. Incident laser powers of 24 mW and collection time of 10 s were used to obtain these spectra. Spectra were offset vertically for display clarity.

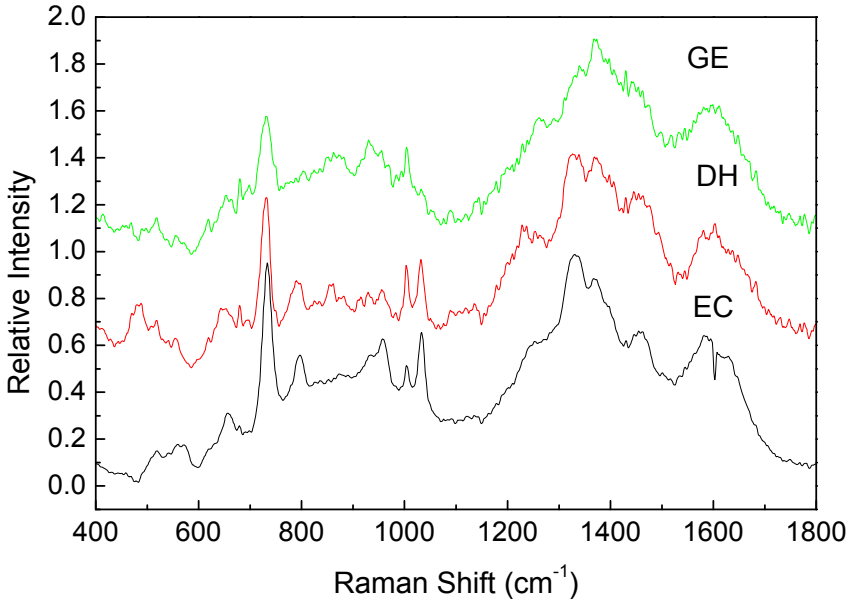

Fig. 4.7. SERS spectra of the *E. coli* strains. EC = *E. coli* O157:H7; DH = *E. coli* DH 5σ; GE = generic *E. coli*. Incident laser powers of 69 mW and collection time of 10 s were used to obtain these spectra. Spectra collected from multiple spots for each strain were baseline corrected and normalized to the most intense band. Spectra were offset vertically for display clarity.

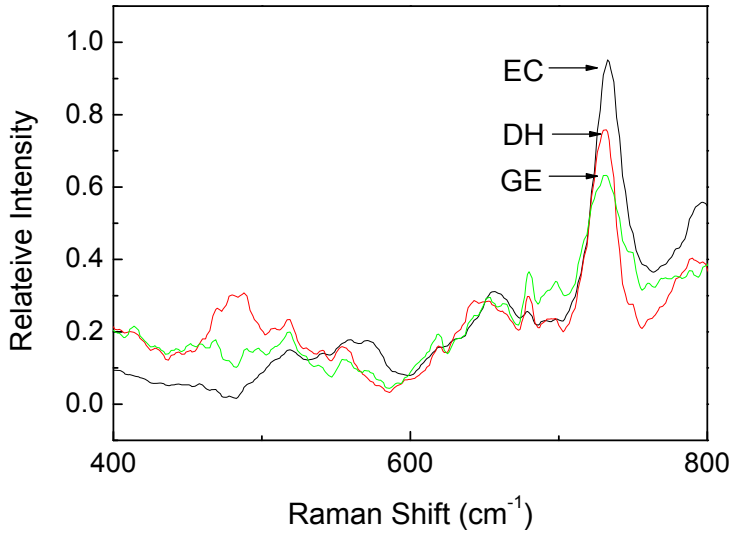

Fig. 4.8. The average SERS signal of generic *E. coli* (GE), *E. coli* O157:H7 (EC) and *E. coli* DH 5α (DH) between 400-800 cm^{-1}. Incident laser powers of 69 mW and collection time of 10 s were used to obtain these spectra. Spectra collected from multiple spots for each strain were baseline corrected and normalized to the most intense band.

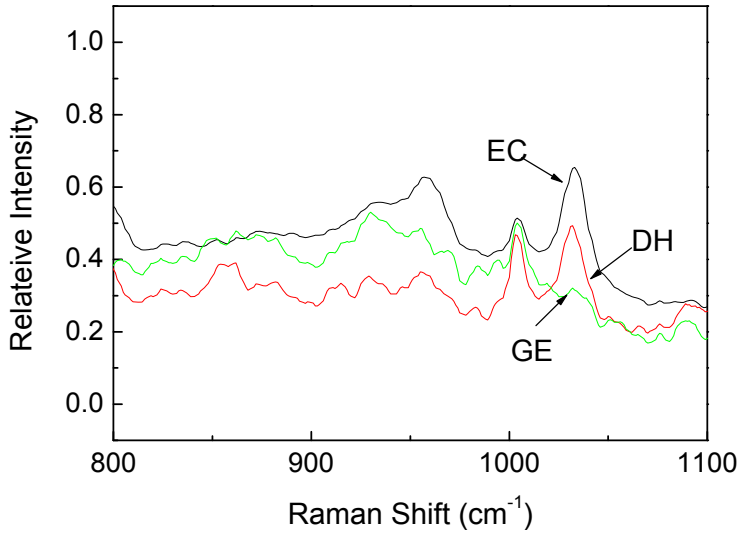

Fig. 4.9. The average SERS signal of generic *E. coli* (GE), *E. coli* O157:H7 (EC) and *E. coli* DH 5α (DH) between 800-1100 cm^{-1}. Incident laser powers of 69 mW and collection time of 10 s were used to obtain these spectra. Spectra collected from multiple spots for each strain were baseline corrected and normalized to the most intense band.

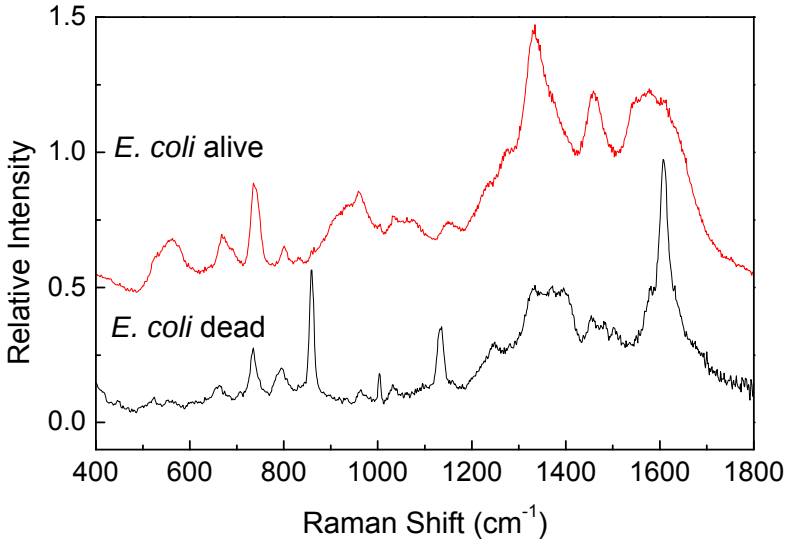

Fig. 4.10. SERS spectra of viable *E. coli* O157:H7 and nonviable E. coli O157:H7. Incident laser powers of 14 mW and collection time of 10 s were used to obtain these spectra. Spectra were offset vertically for display clarity.

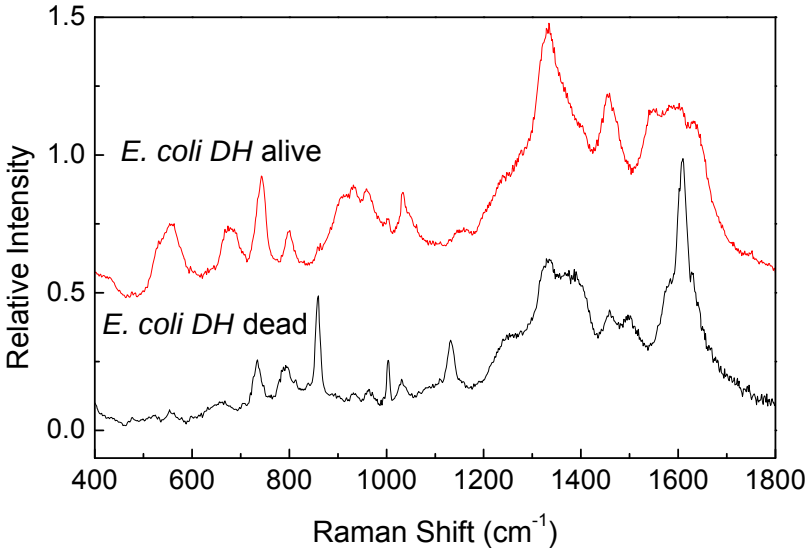

Fig. 4.11. SERS spectra of viable and nonviable *E. coli* DH 5α. Incident laser power of 14 mW and collection time of 10 s was used to obtain these spectra. Spectra were offset vertically for display clarity.

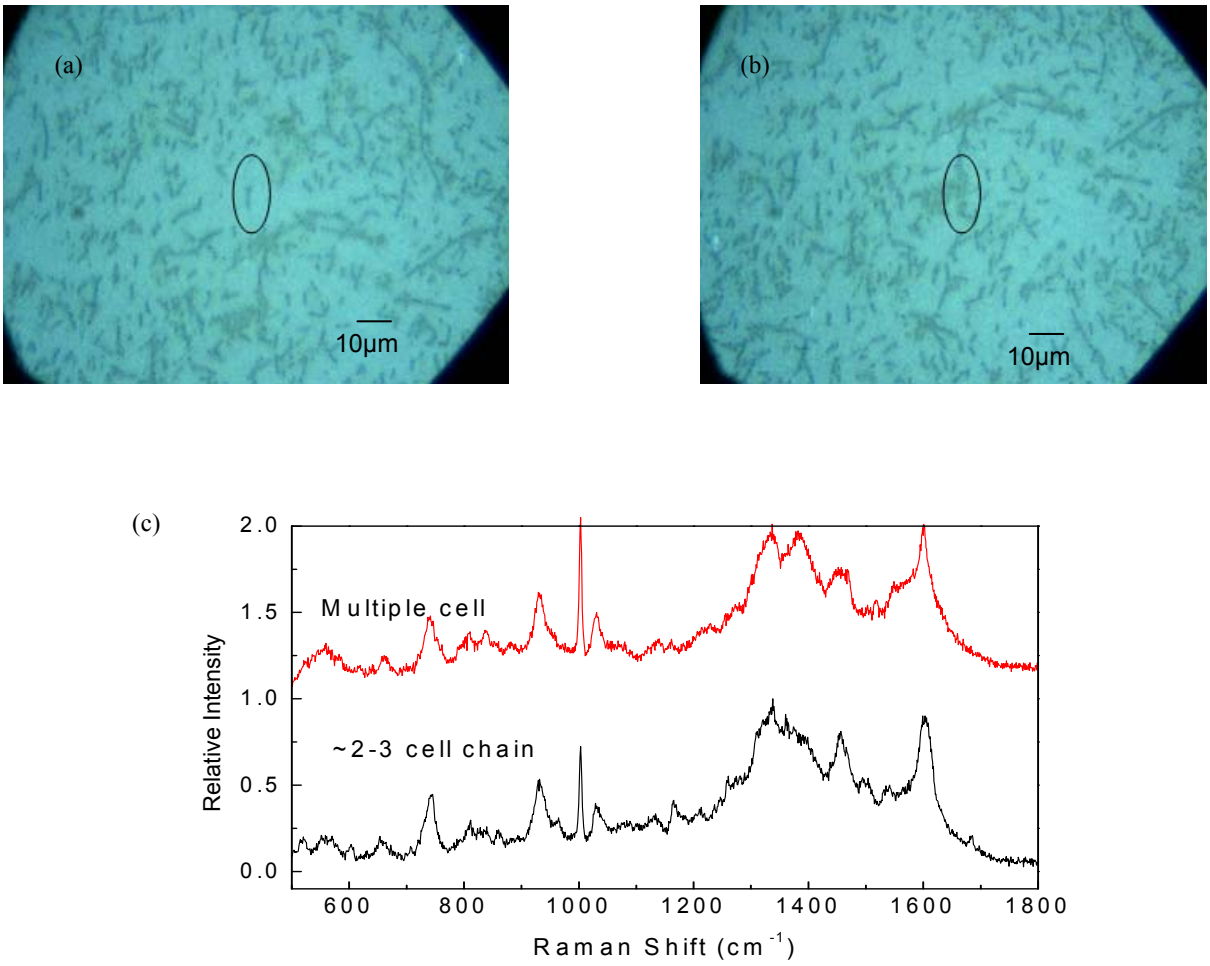

Fig. 4.12. Raman microscope measurements. Bacteria imaging under 50× microscope objective, (a) single *E. coli* O157:H7 two-three cell chain contributing to the SERS spectrum (b) a multiple cell cluster contributing to the SERS spectrum. SERS spectra of single *E. coli* O157:H7 two-three cell chain and a multiple cell cluster are offset vertically for display clarity. Incident laser powers of 12 μW and collection time of 10 s were used to obtain these spectra.

CHAPTER 5

SURFACE- ENHANCED RAMAN SPECTRA OF MIXED CELL CULTURE: CLASSIFICATION BY PRINCIPLE COMPONENT ANALYSIS[1]

[1]HsiaoYun Chu, Yaowen Huang, and Yiping Zhao. To be submitted to *Applied Spectroscopy.*

ABSTRACT

Surface-enhanced Raman scattering (SERS) spectra of two different mixed cultures consisting of *E.coli* O157:H7 and *Staphylococcus aureus*; *E.coli* O157:H7 and *Salmonella typhimurium*, as well as their respective pure cell culture were measured from silver nanorod array substrates. SERS spectra showed some differences in relative intensity and slight spectral shifts between different pure cell cultures and also between a mixed culture and pure culture. Spectra were also analyzed using a chemometric technique, principle component analysis (PCA). PCA was applied to group these microorganisms based on their spectral fingerprints. The resultant PCs score plots showed correct grouping of these microorganisms, including discrimination between two pure cultures in each case. PCA analysis of both mixed cultures along with their respective pure culture, resulted in each cases three different clusters corresponding to the two pure cultures and the mixed culture. These results indicate that SERS spectra can be utilized to identify a pure culture in a mixed cell population via its spectral fingerprint as demonstrated by principle component analysis on the whole SERS spectra.

INTRODUCTION

Accurate and rapid bacterial identification has always been crucial in clinical medicine, environmental monitoring, food safety and quality control. The ideal microbial detection method for routine purposes would require minimum sample preparation, would analyze samples directly (i.e. would not require reagents), would be rapid, would be automated and relatively inexpensive. With recent developments in analytical instrumentation, these requirements can be fulfilled by physico-chemical spectroscopic methods, often referred to as "whole organism fingerprinting", [1] and "metabolic fingerprinting". [2] Popular techniques include mass spectrometry [3, 4] and vibrational spectroscopic methods such as Fourier transform infrared spectroscopy and Raman spectroscopy.[5-7] Raman spectroscopy shows great promise since it is a reproducible and versatile technique that has already been used in many bacterial studies to obtain information-rich spectra. The drawback of the method is the weakness of the inelastic scattering process with typically only ~1 in 10^8 incident photons Raman scattered; thus the spectral acquisition for biological samples can take several minutes. Fortunately, some 10^3-10^6-fold of enhancements can be achieved by using the surface-enhanced Raman scattering (SERS) method.[8] In addition to signal enhancement, SERS has a fluorescence-quenching effect, [9] and this is extremely useful when examining microorganism, which often exhibit a high fluorescence background under excitation in the near-infrared to visible regions.

Several studies using SERS for identification of bacteria have been reported.[10-14] The Raman spectra in these studies were obtained from either isolated pure bacterial cultures or a single bacterial colony. Since the similar chemical composition in microorganisms often transform into very similar spectra, visual examination to classify SERS spectra from different species often found little difference, and could be somewhat subjective. Raman spectra usually

contain many overlapping bands and rapidly generate large data sets, thus data interpretation is difficult by simply visual inspection. An alternative approach to analyze these vibrational measurements in the formulation of mathematical models is essential for the discrimination and characterization of microorganisms.

Multivariate data such as the spectra data generated from a SERS experiment consist of the results of observations of many different variables (wavenumbers) for a number of objects (e.g. samples of different microorganisms). Each variable may be regarded as constituting a different dimension, such that if there are n variables (Raman bands) each object may be said to reside at a unique position in an abstract entity referred to as n-dimensional hyperspace.[15] This hyperspace is obviously difficult to visualize, thus the purpose of multivariate analysis is to simplify or reduce dimensionality. In other words, multivariate analysis summarizes a large body of data by means of relatively few parameters, which enable a graphical display with minimal loss of information. This graphical display would then assist human interpretation of the data. Chemometrics is the use of mathematical and statistical methods to improve the understanding of chemical information and to correlate quality parameters or physical properties to analytical instrument data. [16] Chemometric techniques can highlight the minute spectral differences and can objectively differentiate between similar spectra.

Within chemometrics, there are two main strategies to analyze multivariate data, unsupervised learning and supervised learning algorithms. In general an unsupervised (objective) method such as principal component analysis (PCA) is used to look at the 'natural' differences and similarities between these spectra and require no prior knowledge of the identity of the samples. The central idea of PCA is to reduce the dimensionality of a dataset consisting of a large number of interrelated variables while retaining as much as possible of the variation present

in the dataset. [17] For most Raman spectra, the number of samples in the analysis is very small compared to the number of variables (wavenumbers). In this case, multivariate analysis by PCA is appropriate. PCA can detect structure in these data and can 'cluster' samples into groups by producing scores plots. By contrast, supervised (subjective) methods are 'calibrated' with some known answer from existing knowledge of the sample, prior knowledge is required. With a set of well-characterized samples, a model can be developed so that it can predict the identity of unknown samples. [18] A combination of objective and subjective methods can also be used. Pre-selecting spectral regions based on visual inspection of the spectra and using these regions in cluster analysis is a common approach.

Application of chemometrics to SERS has been limited due to the irreproducibility limitations of some SERS substrates. With the development of stable oblique angle deposition (OAD) fabricated SERS substrates, it is necessary to explore the efficiency of chemometrics as applied to SERS spectra. The aim of the present study was to combine SERS spectra and chemometrics method for the discrimination of bacteria. We evaluated the possibility of using Raman spectra to discriminate single species from a mixed cell population. SERS spectra from pure *E.coli* O157:H7, *Staphylococcus aureus*, and *Salmonella typhimurium* samples, as well as mixed populations (*E.coli* O157:H7+ *Staphylococcus aureus* and *E.coli* O157:H7+*Salmonella typhimurium*) were recorded. This approach was to assess the SERS technique on an inhomogeneous sample. PCA was employed for the classification of bacterial species.

EXPERIMENTAL METHODS

Bacterial Samples

The following bacteria were used in the analyses: *Escherichia coli* O157:H7 (ATCC 43888), *Staphylococcus aureus* (ATCC 6538) (American Type Culture Collection) (Rockville, MD) and *Salmonella typhimurium* 1925-1 (poultry isolate) (Department of Food Science and Technology, The University of Georgia). Bacterial cells were grown in trypticase soy broth (TSB, Difco, Detroit, Mich) over night at 37 °C with 240 rpm shaking. This growth procedure routinely yielded a stock culture containing ~10^9 CFU/ml in stationary phase. Bacterial populations were determined by the conventional surface plate count method using plate count agar (PCA, Difco). Following incubation, the cultures were washed three times with sterilized deionized (DI) water before re-suspending in DI water. Desired dilutions were made in sterilized DI water. Two different types of mixed cell cultures were prepared by mixing equal amount of *E. coli* O157:H7 (10^8 CFU/mL) and *Staphylococcus aureus* (10^8 CFU/mL); also equal amount of *E. coli* O157:H7 (10^8 CFU/mL) and *Salmonella typhimurium* 1925-1(10^8 CFU/mL).

SERS Substrates

The SERS active substrate used to obtain spectra was silver nanorod arrays fabricated by OAD technique using a custom-designed electron beam/sputtering evaporation (E-beam) system (Torr International, New Windsor, NY) that has been previously described. [19] Glass microscopic slides (Gold Seal® Catalog No.3010) were used as the base platform for silver nanorod arrays deposition. The glass slides were cleaned with piranha solution (80% sulfuric acid, 20% hydrogen peroxide) and rinsed with DI water. The substrates were then dried with a stream of nitrogen gas before loading into the E-beam system. A base layer of Ti (20nm) and silver film (500 nm) were first evaporated onto the glass slides at normal angle to the surface at a rate of

~1.0 Å/s and 3.0-4.0 Å/s, respectively. The substrates were then rotated with computer controlled motors to 86˚ with respect to the surface normal. Ag nanorods were grown at this oblique angle in which the deposition rate was ~3.0 Å/s and the deposition pressure was approximately 1×10^{-6} Torr. The film thickness was monitored by a quartz crystal microbalance positioned at normal incidence to the vapor source direction. These deposition conditions produced optimal SERS substrates with average nanorods length of 868 ± 95 nm and the average diameter of 99 ± 29 nm. The average density of the nanorods was approximately 13 ± 0.5 rods/μm^2 with an average tilting angle of ~73° with respect to the substrate normal. Prior to data collection, the substrates were stored in a relatively clean environment at room temperature to avoid any changes in surface morphology due to temperature or atmospheric humidity.

SERS Measurements

SERS spectra were acquired using a HRC-10HT Raman analyzer system (Enware Optronics Inc., Irvine, CA). This system consists of a diode laser, spectrometer, integrated Raman probe head for both excitation and collection, and separate excitation and collection fibers. The excitation source was a frequency stabilized, narrow linewidth near IR diode laser with a wavelength of 785nm. The excitation laser beam coupled to a 100 μm fiber was focused onto the substrate through the Raman probe head and was unpolarized at the sample. The focal length of the Raman probe was 6 mm and the diameter of the laser spot was 100 μm. The Raman signal from the substrate was collected by the same Raman probe head and was coupled to a 200 μm collection fiber, which delivered the signal to the spectrometer equipped with a charge coupled device (CCD) detector. The laser power at the sample varied and was monitored with a power meter (λ = 785 nm, Thorlabs Inc., Newton, NJ). The spectra were acquired with a 10s collection time. A 2.0-μL aliquot of bacterial samples was applied to the Ag nanorod array

substrate and allowed to bind at room temperature prior to spectrum acquisition. SERS spectra were collected from multiple spots across the substrate and from multiple substrates. Generally, solution spot sizes were 2 mm in diameter meaning concentrations of a culture suspension containing ~10^8 CFU/ml corresponded to the excitation of roughly 500 cells on the laser spot.

Data analysis

Enwave Raman analyzer software (Enware Optronics Inc. Irvine, CA) was used for instrument control and data collection. The spectral coverage is ~200 to 2400 cm^{-1} with 785 nm excitation. ASCII data were exported from the Raman analyzer software into Origin software 7.0 version (OriginLab Corporation, Northampton, MA) for spectra processing, including spectra plotting, baseline correction, normalization and peak detection.

Principle component analysis (PCA) was carried out by Unscrambler version 9.7 (Camo, AS, Norway). Prior to PCA analysis, each SERS spectrum was smoothed using the Savitsky-Golay method with first derivative, a second order polynomial and nine-point smoothing. Spectra were normalized with respect to it most intense peak. Principle components plots were used to visualize the differences between the spectra of each sample.

RESULTS and DISSCUSSION

Surface Enhanced Raman Spectroscopy of the Samples

To assess the ability of SERS to distinguish Raman signature of a pure cell sample from a mixed culture, two different types of mixed cell cultures were evaluated. First, the mixture of closely related species that belongs to the Gram positive class, *E. coli* O157:H7 and *Salmonella typhimurium*; second, the mixture of Gram positive and negative species, *S. aureus and E. coli* O157:H7.

The average SERS spectra of pure cell samples and the mixed culture containing *E. coli* O157:H7 and *Salmonella typhimurium* are shown in Figure 5.1. The similarities among the spectra of the pure cultures of *E. coli* O157:H7 and *S. typhimurium* to the mixture are not surprising since both species share similar chemical composition and cellular structure. The main bands in the spectra of these samples may be associated with carbohydrate (~550, 1030 cm^{-1}) [20] and protein (~1450 cm^{-1}). [20] The strong SERS band at ~735 cm^{-1} and the broad band at ~1330 cm^{-1} have been attributed to the nucleic acid base adenine [21, 22, 23]. However, polysaccharides, protein and phospholipids also have been assigned to these bands and are significant components of cell membrane structures. [24, 25] Despite the similarities in these spectra, some differences can still be observed upon closer inspection. Figures 5.2 and 5.3 highlight regions within the spectra where differences in intensity and slight spectral shifts can be seen. The Average SERS spectra of the mixture containing *S. aureus* and *E. coli* O157:H7 and SERS spectra of the respective pure culture are shown in Figure 5.4. Since *S. aureus* and *E. coli* O157:H7 belong to different Gram types and have evident differences in the cell envelope components we expected to have more pronounced spectral variation. Based on our data, this does not seem to be the case. Though there are visible spectral differences in terms of ratio of band intensities between *S. aureus* and *E. coli* O157:H7 (Fig.5.5), the main bands (~550, 735, 1030, 1330, and 1450 cm^{-1}) appear common to both pure cell samples and the mixture sample.

Since molecules and functional groups that are in the immediate proximity of the metal surface will predominate in a SERS measurement. Molecular components of the cell wall and membrane should favor over nucleic acids that locate internally in SERS band assignment. The similarities of spectra from different bacteria and from mixed culture suggest that SERS possibly comes from a small number of molecules which are present in all bacteria cell surface. For

example, the ubiquitous component peptidoglycan found in the bacterial cell walls, surface polysaccharide; such as lipopolysaccharide (a component in the outer membrane of Gram negative bacteria) and capsular polysaccharide. Because the strength of the local electromagnetic field at the substrate surface has its maximum in the direction normal to the surface, vibrational mode from change in the polarizability of the adsorbates that are perpendicular to the surface will be preferentially enhanced than adsorbates that are parallel to the substrate surface. In addition to the effect of molecular orientation on SERS spectral feature, intermolecular forces and selective molecular adsorption on the metal surface also explain the possibility that certain Raman active molecules could completely dominate the spectrum of the mixture. Nevertheless, considering the chemical heterogeneity of the bacterial surface, one can not entirely rule out that some minute secondary differences are present, though not discernible from the spectra.

Although resources for standard Raman spectra of biological materials are slowly becoming available and can be useful, it is not always the case that peaks expressed in a Raman spectrum will also be observed in the SERS spectrum of the same sample. It is noteworthy that, at this point, all the reported peak assignments for bacterial SERS spectra remain tentative.

Principle Component Analysis and Bacteria Classification

Visual inspection of spectra with great similarity for classification could be trying, subjective and unrealistic. To classify and identify microorganisms based on vibrational spectra, it is not necessary to identify all band intensities and frequencies in a spectrum and assign them to specific molecular compounds. Spectra can be evaluated as spectroscopic fingerprints of the samples.[26] Principal component analysis (PCA) can highlight the minute spectral differences and can objectively differentiate between similar spectra. PCA is a method of recasting the multi-

dimensional data onto a new set of axes or orthogonal basis vectors that are typically called principal components (PC). The PC containing the greatest variance is labeled PC 1, while the axis containing the second most variance is labeled PC 2. PCs model the most statistically significant variations in the dataset and are primarily used to reduce the dimensionality of the sample matrix prior to the use of clustering methods. To explore the data and identify individual groups based on differences in the SERS spectra, PCA was employed to 'cluster' samples into groups.

Figure 5.6A shows the PCA analysis performed using spectral data from two pure cell samples of the same Gram type in the 400-1800 cm^{-1} range. The plot gives information about patterns in the samples. The score plot for (PC1, PC2) is especially useful, since these two components summarize more variation in the data than any other pair of components. Samples with close scores along the same PC are similar (they have close values for the corresponding variables). Conversely, samples for which the scores differ much are quite different from each other. Looking at PC1, the negative value for PC1 suggests samples are likely to be *E. coli* O157:H7 and the positive score for PC1 suggest that those samples are likely to be *S. typhimurium*. This score plot indicates that two separated clusters for *E. coli* O157:H7 and *S. typhimurium*, respectively. We then investigated a mixed cell sample containing *E. coli* O157:H7 and *S. typhimurium* in equal ratios. The addition of new samples gives a different plot (Fig. 5.6B). Three relatively isolated clusters divide similar spectra into three groups. One of the clusters refers to SERS spectra of *E. coli* O157:H7 (coded EC), is clearly away from the other clusters. Another cluster associated with spectra of *S. typhimurium* (coded ST) is located closer to the third cluster (spectra of mix cell samples, coded M).

Figure 5.7A shows the PCA analysis performed using spectral data from two pure cell samples of different Gram types. One tightly formed cluster constituting the pure *S. aureus* cell samples (coded SA) is well separated from *E. coli* O157:H7 samples (coded EC). Again, spectral data from mixed cell samples containing equal ratios of *S. aureus* and *E. coli* O157:H7 were compared with the spectra from the pure cell samples in the 400-1800 cm^{-1} range. Spectra from *E. coli* O157:H7 was grouped into a well isolated cluster clearly away from the other samples; the rest of the spectra could be relatively extracted into two clusters. While spectra of *S. aureus* were grouped tightly together, spectra from mixed culture (coded M) seem to fall into two sub-clusters (Fig 5.7B) with one sub-cluster situates close to the *S. aureus* cluster.

It should be noted that for a combined dataset, PCA does not look for the subsets of data. In stead; the features in the whole dataset of thousands of points are resolved into a few significant principle components, which can express the entire dataset with their scores for each spectrum. In the PCA process, the mean of all spectra is calculated and each spectrum is subtracted from the mean, leaving the variations from the mean. When PCA was performed for the data set of pure cells, PCA derived the PCs necessary to describe the variations from the mean for the entire data. When PCA was done for the data set of pure cells and mixture combined, the mean and variations were different from the set of pure cells data. PCA would derive the PCs necessary to discriminate three types of identities ascribed to the two different pure cells and the one mixture containing these two respective pure cells. We did not attempt to examine whether we can identify the individual spectral characteristics of single cell species in a spectral set of a mixture. This objective can be achieved by forming standard sets of each pure cell samples and testing the individual spectrum from the mixture sample against these standard calibration sets. The aim of the present work was to test the possibility of using SERS spectra to

check whether a sample belongs to a single species or contains both species (is the sample homogeneous or heterogeneous). The results from PCs plots clearly demonstrate the potential of SERS technique to distinguish different species and to differentiate pure cell sample from mixed cell samples even when there is great similarity among their Raman signatures.

CONCLUSIONS

This study demonstrates that the combination of SERS bacterial fingerprint with the PCA method, the classification of different bacterial species can be objectively achieved in less than a minute. These initial results further indicate that this approach could be useful for the early screening and discrimination of pure bacterial species from a heterogeneous mixed culture environment. This is an important step towards the application of SERS technique in a real life sample matrix where multi bacterial species often coexist.

ACKNOWLEDGEMENTS

This research was supported by funding from the National Science Foundation (ECS0304340 and ECS070178).

REFERENCES

1. R. Goodacre, E. M. Timmins, R. Burton, N. Kaderbhai, A. Woodward, D. B. Kell, and P. J. Rooney, Microbiology **144,** 1157 (1998).
2. O. Fiehn, Plant Mol. Biol. **48,** 155 (2002).
3. J. O. Lay, Trends Anal. Chem. **19,** 507 (2000).
4. S. Vaidyanathan, J. J. Rowland, D. B. Kell, and R. Goodacre, Anal. Chem. **73,** 4134 (2001).
5. D. Naumann, D. Helm, and H. Labischinski, Nature **351,** 81 (1991).
6. K. Maquelin, L.-P. Choo-Smith, T. Van Vreeswijk, H. P. Endtz, B. Smith, R. Bennett, H. A. Bruining, and G. J. Puppels, Anal. Chem. **72,** 12 (2000).
7. K. Maquelin, L. P. Choo-Smith, H. P. Endtz, H. A. Bruining, and G. J. Puppels, J. Clin. Microbiol. **40,** 594 (2002).
8. M. Moskovits, Rev. Mod. Phys. **57,** 783 (1985).
9. K. Kneipp, A. S. Haka, H. Kneipp, K. Badizadegan, N. Yoshizawa, C. Boone, K. E. Shafer-Peltier, J. T. Motz, R. R. Dasari, and M. S. Feld, Appl. Spectrosc. **56,** 150 (2002).
10. S. Efrima, and B.V. Bronk, J. Phys. Chem. B **120,** 5947 (1998).
11. A. A. Guzelian, J. M. Sylvia, J. A. Janni, S. L. Clauson, and K. M. Spencer, Proc. SPIE **4577,** 182 (2002).
12. A. Sengupta, M. L. Laucks, and E. J. Davis, Appl. Spectrosc. **59,** 1016 (2005).
13. M. L. Laucks, A. Sengupta, K. Junge, E. J. Davis, and B. D. Swanson, Appl. Spectrosc. **59,** 1222 (2005).
14. M. Kahraman, M. M. Yazici, F. Sahin, O.F. Bayrak and M. Culha, Appl. Spectrosc. **61,** 479 (2007)

15. R. Goodacre, Vib. Spectrosc. **32,** 33 (2003).

16. B.K. Lavine, Anal. Chem. **70,** 209R (1998).

17. I.T. Jolliffe, Principal Component Analysis (Springer-Verlag,New York, 1986), 2nd ed., P.1.

18. D. I. Ellis, and R. Goodacre, Analyst **131,** 875 (2006).

19. S. B. Chaney, S. Shanmukh, R. A. Dluhy, and Y.- P. Zhao, Appl. Phys. Lett. **87,** 031908.1 (2005).

20. K. C. Schuster, E. Urlaub, and J. R. Gapes, J. Microbiol. Methods **42,** 29 (2000).

21. E. Podstawka, Y. Ozaki, and L. M. Proniewicz, Appl. Spectrosc. **58,** 570 (2004).

22. K. Kneipp, and J. Flemming, J. Mol. Struct. **145,** 173 (1986).

23. L. Zeiri, B.V. Bronk, Y. Shabtai, J. Eichler, and S. Efrima, Appl. Spectrosc. **58,** 33 (2004).

24. R. M.; Jarvis, and R. Goodacre, Anal. Chem. **76,** 40 (2004).

25. K. J. Rothschild, J. R. Andrew, W. J. DeGrip, and H. E. Stanley, Science **191,** 1176 (1976).

26. K. Maquelin, C. Kirschner, L.-P. Choo-Smith, N. van den Braak, H. P. Endtz, D. Naumann and G. J. Puppels, J. Microbiol. Methods, **51,** 255 (2002).

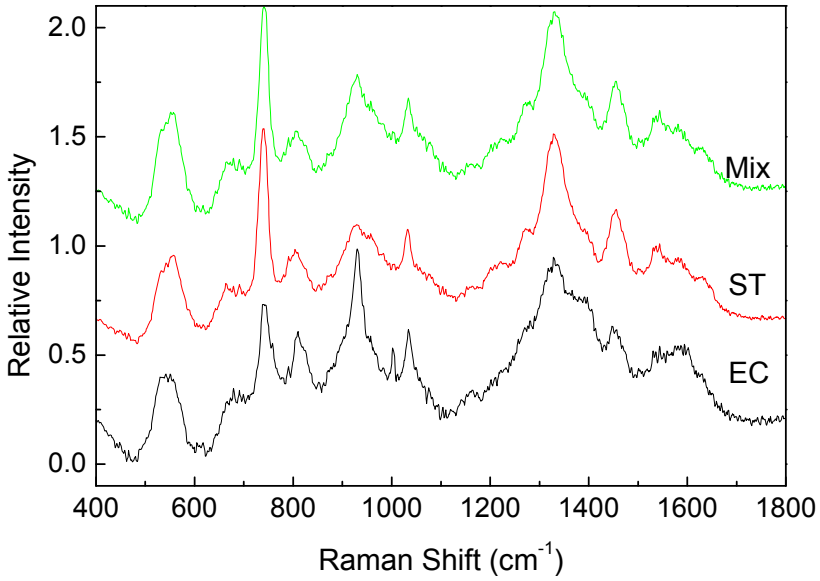

Fig. 5.1. Typical SERS spectra of two bacterial species and its mix culture obtained on silver nanorod array substrates. EC, *E. coli* O157:H7; ST, *S. typhimurium*; Mix, mix culture of *E. coli* O157:H7 and *S. typhimurium*. Incident laser powers of 28 mW and collection time of 10 s were used to obtain these spectra. Spectra were offset vertically for display clarity.

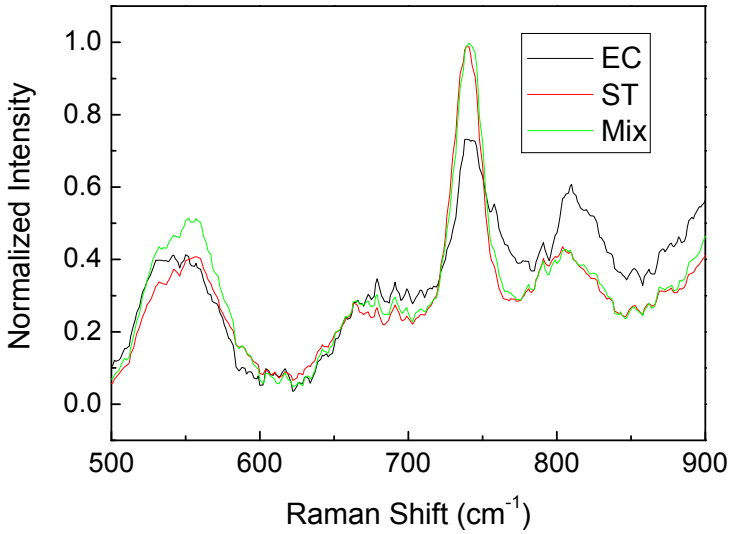

Fig. 5.2. The average SERS response for each of the samples between 500-900 cm^{-1}. EC, *E. coli* O157:H7; ST, *S. typhimurium*; Mix, mix culture of *E. coli* O157:H7 and *S. typhimurium*. Incident laser powers of 28 mW and collection time of 10 s were used to obtain these spectra.

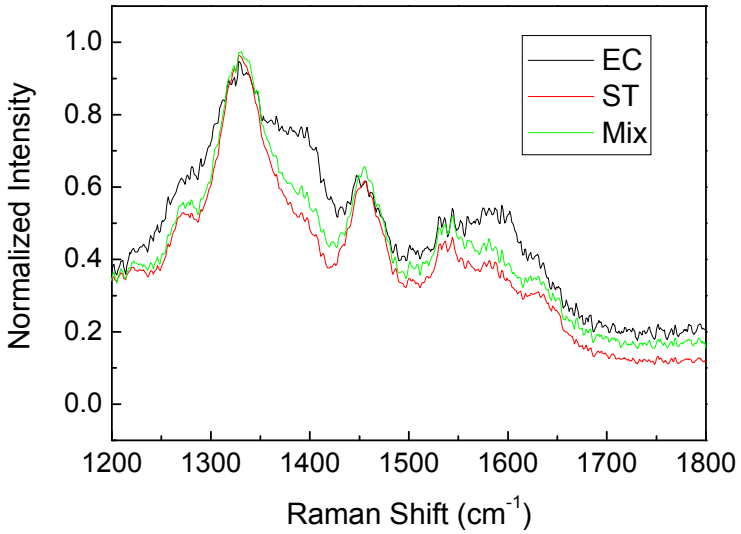

Fig. 5.3. The average SERS response for each of the samples between 1200-1800 cm^{-1}. EC, *E. coli* O157:H7; ST, *S. typhimurium*; Mix, mix culture of *E. coli* O157:H7 and *S. typhimurium*. Incident laser powers of 28 mW and collection time of 10 s were used to obtain these spectra.

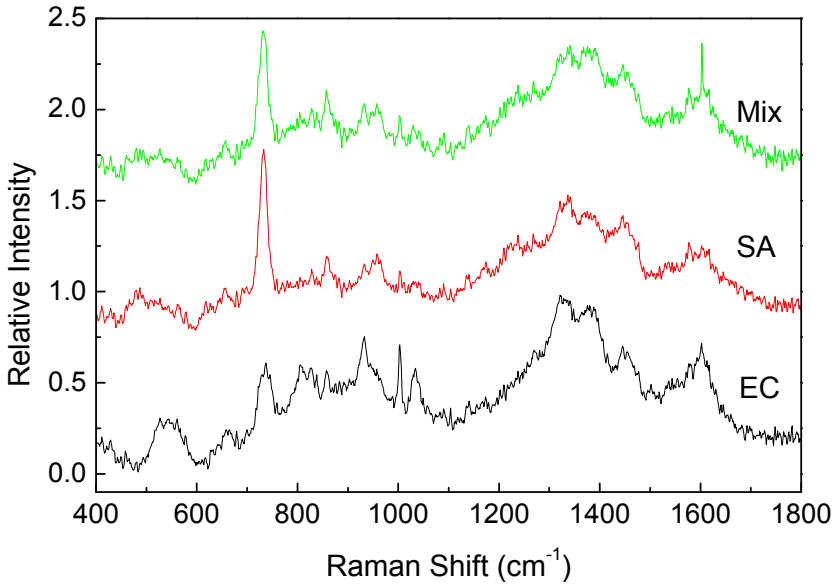

Fig. 5.4. Typical SERS spectra of two bacterial species and its mix culture obtained on silver nanorod array substrates. EC, *E. coli* O157:H7; SA, *Staphylococcus aureus*; Mix, mix culture of *E. coli* O157:H7 and *Staphylococcus aureus*. Incident laser powers of 24 mW and collection time of 10 s were used to obtain these spectra. Spectra were offset vertically for display clarity.

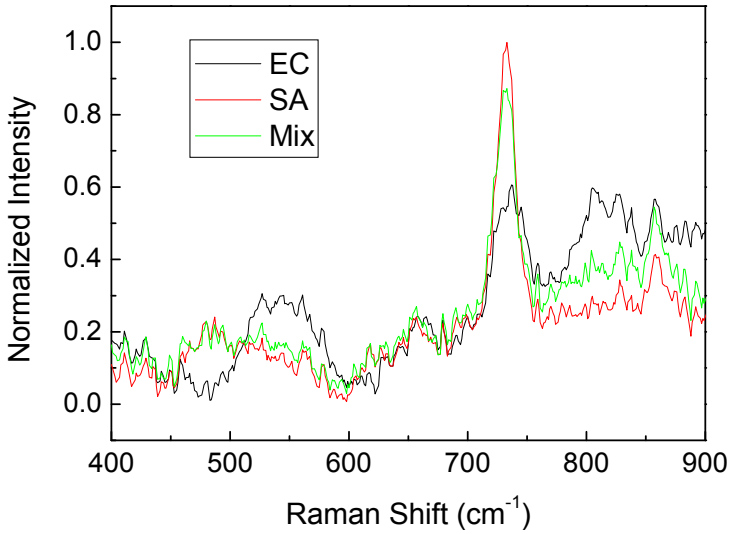

Fig. 5.5. The average SERS response for each of the samples between 400-900 cm^{-1}. EC, *E. coli* O157:H7; SA, *Staphylococcus aureus*; Mix, mix culture of *E. coli* O157:H7 and *Staphylococcus aureus*. Incident laser powers of 24 mW and collection time of 10 s were used to obtain these spectra.

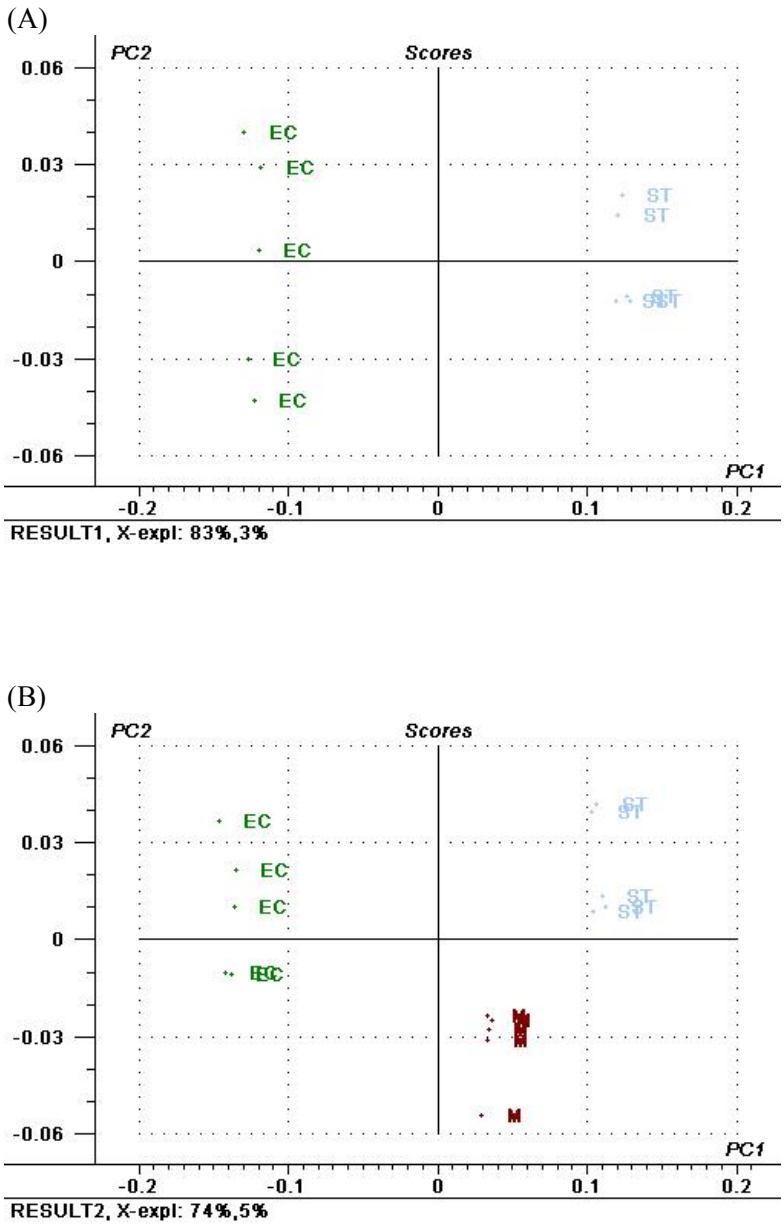

Fig. 5.6. (A) PCA scores plot of *E. coli* O157:H7 (EC); and *S. typhimurium* (ST) pure cell samples; (B) PCA scores plot of pure cell samples and their mixed cell samples (M). The PCA model was constructed using the spectral range from 400-1800 cm^{-1}.

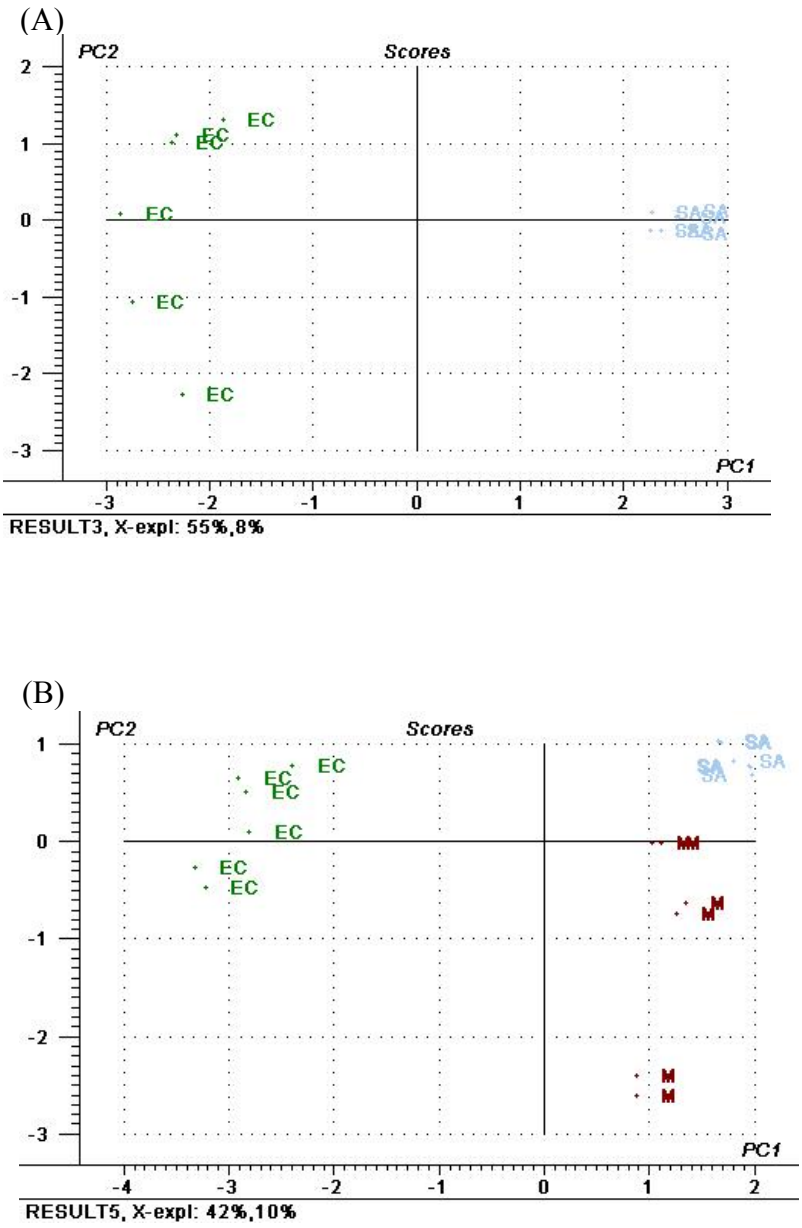

Fig. 5.7. (A) PCA scores plot of *E. coli* O157:H7 (EC); and *S. aureus* (SA) pure cell samples; (B) PCA scores plot of pure cell samples and their mixed cell samples (M). The PCA model was constructed using the spectral range from 400-1800 cm^{-1}.

CHAPTER 6

SUMMARY AND CONCLUSIONS

Surface enhanced Raman spectroscopy offers considerable potential in the area of molecular identification and trace element analysis, which has significant applications in both biological and chemical analysis. We have created a portable SERS probe which can be easily incorporated with a fiber Raman system. We demonstrated the concentration dependent of Raman intensities on the OAD fabricated silver nanorod array using BPE as molecular probe and observed a sensitivity of 14 attomole for BPE. Furthermore, we tested the response time and stability of the in situ SERS signal of BPE in a water solution on the silver nanorod substrate. Our present results indicate that SERS probe can be integrated into a fiber Raman system for in situ measurements and can act as a portable and remote sensor for accurate and rapid real-time SERS measurements. This is an important development for practical SERS applications because of the possibility of using low-power laser, inexpensive substrate and compact size sensor for field applications.

In order to evaluate these SERS substrates as potential bioanalytical sensors for bacterial identification, spectra from various pathogenic bacteria on the substrate were obtained. Good signal-to-noise and reproducible Raman spectra of bacteria were demonstrated. The bacterial SERS spectra show clear distinction between different species (*Salmonella typhimurium*, *E. coli* O157:H7, *S. aureus* and *S. epidermidis*) and strains (*E. coli* O157:H7, generic *E. coli* and *E.coli* DH 5α). Major Raman band attributing to bacterial cell surface components such as carbohydrate, protein and phospholipids were observed. The ability to distinguish between nonviable and viable cells was presented. The ability to obtain high quality Raman spectra of single bacterial cell on silver nanorod array substrates was also demonstrated with very low laser power (12 μW) and short collection time (10s).

SERS spectra of two different mixed cultures consisting of *E.coli* O157:H7 and *S. aureus*; *E.coli* O157:H7 and *S. typhimurium*, as well as their respective pure cultures were measured. Principle component analysis was applied to group these microorganisms based on their spectral fingerprints. The resultant PCs score plots showed correct grouping of these microorganisms, including discrimination between two pure cultures and the mixed culture in each case. The combination of bacterial SERS fingerprints and PCA method enable the objective classification of different bacterial species. These initial results further indicate that this approach could be useful for the early screening and discrimination of pure bacterial species from a heterogeneous mixed culture environment.

This work clearly demonstrates the great potential of the silver nanorod substrate as a real-time multiplexing SERS-based sensor for chemical and biological applications. The SERS method is of practical interest for microbiological analysis, as it requires only a very simple sample preparation procedure consisting of washing the cells and drying on a SERS substrate. No chemical reagents are necessary to specifically label target microorganisms. The speed, specificity and ease of implementation of SERS technique represents a valuable alternative to current bacterial diagnostic tools and provides the possibility of portable pathogen sensor for on-site food inspection.

CHAPTER 7

FUTURE RESEARCH

From a problem-solving standpoint, SERS is not fully developed at present. Much future research work needs to be done on the applicability of this technique to real samples.

Priority should be given to the development of standardized SERS-active substrates that are of consistent quality and suitable for long-time storage. Since not all compounds are SERS-active, it would be very advantageous to develop substrates that are selective for a particular type of analytes. Substrates that exhibit high affinity and or specific interaction with target molecules could expand the specificity of SERS technique for analytical application in multi-components real samples. Using submicron or nano-scale size fiber tip as a SERS substrate to exact position the tip to localize the target bacteria or biological molecules also possess great potential.

Additional separation technique, such as centrifugation and filtration, also needs to be developed and incorporated into a bacterial detection procedure to allow substantial isolation of bacterial cells (~ 1 μm) from larger biological cells or molecular impurities in real sample matrix which often confound the bacterial SERS signals.

The molecular level challenges are evident for SERS methodology as well. A combination of model compounds and genetically engineering mutants can be used to help identify the molecular origins of the observed vibrational signals.

In operational settings, detection and identification of bacteria can be done by comparing a measured SERS spectrum of a target against a SERS signature library. Therefore, a comprehensive, reproducible and robust SERS spectral library is key to a successful SERS-based detection method. The signature library should at least contain priority pathogens, near neighbors to the pathogens, a variety of biological and non-biological background interferent materials. The signatures must be reproducible and exhibit minimal variability induced by sensor uncertainty, biological growth conditions and sample preparation conditions.

Consequently, standardized SERS-active substrates need to be incorporated and measurement under various controlled growth parameters from all reference library materials need to be included.

APPPENDICES

APPENDIX A

References for chapter 4

1. P.S. Mead, L. Slutsker, V. Dietz, L.F. McCaig, J.S. Bresee, C. Shapiro, P.M. Griffin, and R. V. Tauxe, "Food-related illness and death in the United States" Emerging infectious diseases. **5,** 607 (1999).
2. C. A. Batt, in Listeria, Listeriosis, and Food Safety, T. Ryser and E. H. Marth, Eds. (Marcel Dekker, New York, 1999), 2nd ed., p. 261.
3. S. Vaidyanathan, D. B. Kell, and R. Goodacre, "Flow-injection electrospray ionization mass spectrometry of crude cell extracts for high-throughput bacterial identification" J. Am. Soc. Mass Spectrom. **13,** 118 (2002).
4. W. H. Nelson, R. Manoharan, and J. F. Sperry, "UV resonance Raman studies of bacteria" Appl. Spectrosc. Rev. **27,** 67 (1992).
5. Q. Wu, T. Hamilton, W. H. Nelson, S. Elliott, J. F. Sperry, and M. Wu, "UV Raman spectral intensities of E.coli and other bacteria excited at 228.9, 224 and 248.2 nm" Anal. Chem. **73,** 3432 (2001).
6. T. A. Alexander, P. M. Pellegrion, and J. B. Gillespie, "Near-infrared surface-enhanced Raman scattering mediated detection of single optically trapped bacterial spores" Appl. Spectrosc. **57,** 1340 (2003).
7. M. Fleischmann, P. J. Hendra, A. J. McQuillan, "Raman spectra of pyridine adsorbed at a silver electrode" Chem. Phys. Lett. **26,** 163 (1974).
8. M. Moskovits, "Surface-enhanced spectroscopy" Rev. Mod. Phys. **57,** 783 (1985).
9. A. Campion, and P. Kambhampati, "Surface-enhanced Raman scattering" Chem. Soc. Rev. **4,** 241 (1998).

10. K. Kneipp, A. S. Haka, H. Kneipp, K. Badizadegan, N. Yoshizawa, C. Boone, K. E. Shafer-Peltier, J. T. Motz, R. R. Dasari, and M. S. Feld, "Surface-enhanced Raman spectroscopy in single living cells using gold nanoparticles" Appl. Spectrosc. **56,** 150 (2002).
11. Z. Q. Tian, B. Ren, and D. Y. Wu, "Surface-enhanced Raman scattering: from noble to transition metals and from rough surface to ordered nanostructures" J. Phys. Chem. B **106,** 9463 (2002).
12. A.A. Stacy and R.P. Van Duyne, "Surface enhanced raman and resonance raman spectroscopy in a non-aqueous electrochemical environment: tris(2,2′-bipyridine)ruthenium(II) adsorbed on silver from acetonitrile" Chem. Phys. Lett. **102,** 365 (1983).
13. G. J. Kovacs, R. O. Loutfy, P. S. Vincett, C. Jennings, and R. Aroca, "Distance dependence of SERS enhancement factor from Langmuir-Blodgett monolayers on metal island films: evidence for the electromagnetic mechanism" Langmuir **2,** 689 (1986).
14. K. T. Carron, X. Gi, and M. L. Lewis, "A surface enhanced Raman spectroscopy study of the corrosion-inhibiting properties of benzimidazole and benzotriazole on copper" Langmuir **7,** 2 (1991).
15. L. M. Sudnik, K. L. Norrod, and K. L. Rowlen, "SERS-active Ag films from photoreduction of Ag+ on TiO2" Appl. Spectrosc. **50,** 422 (1996).
16. S. M. Nie, and S. R. Emory, "Probing single molecules and single nanoparticles by surface-enhanced Raman scattering" Science **275,** 1102 (1997).

17. T. R. Jensen, M. D. Malinsky, C. L. Haynes, and R. P. Van Duyne, "Nanosphere lithography: tunable localized surface plasmon resonance spectra of silver nanoparticles" J. Phys. Chem. B **104,** 10549 (2000).
18. G. Suer, U. Nickel, and S. Schneider, "Preparation of SERS-active silver film electrodes via electrocrystallization of silver" J. Raman Spectrosc. **31,** 359 (2000).
19. A. Tao, F. Kim, C. Hess, J. Goldberger, R. R. He, Y. G. Sun, Y. N. Xia, and P. D. Yang, "Langmuir-Blodgett silver nanowire monolayers for molecular sensing using surface-enhanced Raman spectroscopy" Nano Lett. **3,** 1229 (2003).
20. K. Kneipp, G. Kneipp, I. Itzkan, R. R. Dasari, and M. S Feld, "Ultrasensitive chemical analysis by Raman spectroscopy" Chem. Rev. **99,** 2957 (1999).
21. L. Zeiri, B. V. Bronk, Y. Shabtai, J. Czégé, and S. Efrima, "Silver metal induced surface enhanced Raman of bacteria" Colloids Surfaces A. **208,** 357 (2002).
22. R. M. Jarvis, and R. Goodacre, "Discrimination of bacteria using surface-enhanced Raman spectroscopy" Anal. Chem. **76,** 40 (2004).
23. A. Sengupta, M. L. Laucks, and E. J. Davis, "Surface-enhanced Raman spectroscopy of bacteria and pollen" Appl. Spectrosc. **59,** 1016 (2005).
24. M. L. Laucks, A. Sengupta, K. Junge, E. J. Davis, and B. D. Swanson, "Comparison of psychro-active marine bacteria and common mesophillic bacteria using surface-enhanced Raman spectroscopy" Appl. Spectrosc. **59,** 1222 (2005).
25. Y. - P. Zhao, D. X. Ye, G. C. Wang, and T. M. Lu, "Designing nanostructures by glancing angle deposition" Proc. SPIE. **5219,** 59 (2003).

26. S. B. Chaney, S. Shanmukh, R. A. Dluhy, and Y.- P. Zhao, "Aligned silver nanorod arrays produce high sensitivity surface-enhanced Raman spectroscopy substrates" Appl. Phys. Lett. **87,** 031908.1 (2005).
27. S. Shanmukh, L. Jones, J. Driskell, Y.-P. Zhao, R. Dluhy, and R. A. Tripp, "Rapid and sensitive detection of respiratory virus molecular signatures using a silver nanorod array SERS substrate" Nano Lett. 6, 2630 (2006).
28. K. Kneipp, and J. Flemming, "Surface enhanced Raman scattering of nucleic acids adsorbed on colloidal silver particles" J. Mol. Struct. **145,** 173 (1986).
29. L. Zeiri, B.V. Bronk, Y. Shabtai, J. Eichler, and S. Efrima, "Surface-enhanced Raman spectroscopy as a tool for probing specific biochemical components in bacteria" Appl. Spectrosc. **58,** 33 (2004).
30. K. J. Rothschild, J. R. Andrew, W. J. DeGrip, and H. E. Stanely, "Opsin structure probed by Raman spectroscopy of photoreceptor membranes" Science **191,** 1176 (1976).
31. E. Podstawka, Y. Ozaki, and L. M. Proniewicz, "Part I: surface enhanced Raman spectroscopy investigation of amino acids and their homodipeptides adsorbed on colloidal silver" Appl. Spectrosc. **58,** 570 (2004).
32. K. C. Schuster, E. Urlaub, and J. R. Gapes, "Single-cell analysis of bacteria by Raman microscopy: spectral information on the chemical composition of cells and on the heterogeneity in a culture" J. Microbiol. Methods **42,** 29 (2000).
33. J. S. Suh, and M. Moskovits, "Surface- Enhanced Raman spectroscopy of amino acids and nucleotide bases adsorbed on silver" J. Am. Chem. Soc. **108,** 4711 (1986).

34. C. E. Taylor, S. D. Garvey, and J. E. Pemberton, “Carbon contamination at silver surface: surface preparation procedures evaluated by Raman spectroscopy and X-ray photoelectron spectroscopy” Anal. Chem. **68,** 2401 (1996).

35. J. M. DiRienzio, K. Nakamura, and M. Inouye, “The ourter membrane proteins of gram-negative bacteria: biosynthesis, assembly, and functions” Annu. Rev. Biochem. **47,** 481 (1978).

36. J.-H. Ryu, and L.R. Beuchat, “Development of method to quantify extracellular carbohydrate complexes produced by *Escherichia coli* O157:H7” J. Appl. Microbiol **95,** 1304 (2003).

37. K. Schuster, I. Reese, E. Urlaub, J. R. Gapes, and B. Lendl, “Multidimensional information on the chemical composition of single bacterial cells by confocal Raman microspectroscopy” Anal. Chem. **72,** 5529 (2000).

APPENDIX B

References for chapter 5

1. R. Goodacre, E. M. Timmins, R. Burton, N. Kaderbhai, A. Woodward, D. B. Kell, and P. J. Rooney, "Rapid identification of urinary tract infection bacteria using hyperspectral whole-organism fingerprinting and artificial neural networks" Microbiology **144,** 1157 (1998).
2. O. Fiehn, "Metabolomics-the link between genotypes and phenotypes" Plant Mol. Biol. **48,** 155 (2002).
3. J. O. Lay, "MALDI-TOF mass spectrometry and bacterial taxonomy" Trends Anal. Chem. **19,** 507 (2000).
4. S. Vaidyanathan, J. J. Rowland, D. B. Kell, and R. Goodacre, "Discrimination of aerobic endospore-forming bacteria via electrospray-ionization mass spectrometry of whole cell suspensions "Anal. Chem. **73,** 4134 (2001).
5. D. Naumann, D. Helm, and H. Labischinski, "Microbiological characterizations by FT-IR spectroscopy" Nature **351,** 81 (1991).
6. K. Maquelin, L.-P. Choo-Smith, T. Van Vreeswijk, H. P. Endtz, B. Smith, R. Bennett, H. A. Bruining, and G. J. Puppels, "Raman spectroscopic method for identification of clinically relevant microorganisms growing on solid culture medium" Anal. Chem. **72,** 12 (2000).
7. K. Maquelin, L. P. Choo-Smith, H. P. Endtz, H. A. Bruining, and G. J. Puppels, "Rapid identification of Candida species by confocal Raman microspectroscopy" J. Clin. Microbiol. **40,** 594 (2002).
8. M. Moskovits,"Surface-enhanced spectroscopy" Rev. Mod. Phys. **57,** 783 (1985).

9. K. Kneipp, A. S. Haka, H. Kneipp, K. Badizadegan, N. Yoshizawa, C. Boone, K. E. Shafer-Peltier, J. T. Motz, R. R. Dasari, and M. S. Feld, "Surface-enhanced raman spectroscopy in single living cells using gold nanoparticles" Appl. Spectrosc. **56,** 150 (2002).
10. S. Efrima, and B.V. Bronk, "Silver colloids impregnating or coating bacteria" J. Phys. Chem. B **120,** 5947 (1998).
11. A. A. Guzelian, J. M. Sylvia, J. A. Janni, S. L. Clauson, and K. M. Spencer, "SERS of whole cell bacteria and trace levels of biological molecules" Proc. SPIE **4577,** 182 (2002).
12. A. Sengupta, M. L. Laucks, and E. J. Davis, "Surface-enhanced Raman spectroscopy of bacteria and pollen" Appl. Spectrosc. **59,** 1016 (2005).
13. M. L. Laucks, A. Sengupta, K. Junge, E. J. Davis, and B. D. Swanson, "Comparison of psychro-active marine bacteria and common mesophillic bacteria using surface-enhanced Raman spectroscopy" Appl. Spectrosc. **59,** 1222 (2005).
14. M. Kahraman, M. M. Yazici, F. Sahin, O.F. Bayrak and M. Culha, "Reproducible surface-enhanced Raman scattering spectra of bacteria on aggregated silver nanoparticles" Appl. Spectrosc. **61,** 479 (2007)
15. R. Goodacre, "Explanatory analysis of spectroscopic data using machine learning of simple, interpretable rules" Vib. Spectrosc. **32,** 33 (2003).
16. B.K. Lavine, "Chemometrics" Anal. Chem. **70,** 209R (1998).
17. I.T. Jolliffe, Principal Component Analysis (Springer-Verlag,New York, 1986), 2nd ed., P.1.

18. D. I. Ellis, and R. Goodacre, “Metabolic fingerprinting in disease diagnosis: biomedical applications of infrared and Raman spectroscopy” Analyst **131,** 875 (2006).
19. S. B. Chaney, S. Shanmukh, R. A. Dluhy, and Y.- P. Zhao, “Aligned silver nanorod arrays produce high sensitivity surface-enhanced Raman spectroscopy substrates” Appl. Phys. Lett. **87,** 031908.1 (2005).
20. K. C. Schuster, E. Urlaub, and J. R. Gapes, “Single-cell analysis of bacteria by Raman microscopy: spectral information on the chemical composition of cells and on the heterogeneity in a culture” J. Microbiol. Methods **42,** 29 (2000).
21. E. Podstawka, Y. Ozaki, and L. M. Proniewicz, “Part I: surface enhanced Raman spectroscopy investigation of amino acids and their homodipeptides adsorbed on colloidal silver” Appl. Spectrosc. **58,** 570 (2004).
22. K. Kneipp, and J. Flemming, “Surface enhanced Raman scattering of nucleic acids adsorbed on colloidal silver particles” J. Mol. Struct. **145,** 173 (1986).
23. L. Zeiri, B.V. Bronk, Y. Shabtai, J. Eichler, and S. Efrima, “Surface-enhanced Raman spectroscopy as a tool for probing specific biochemical components in bacteria” Appl. Spectrosc. **58,** 33 (2004).
24. R. M.; Jarvis, and R. Goodacre, “Discrimination of bacteria using surface-enhanced Raman spectroscopy” Anal. Chem. **76,** 40 (2004).
25. K. J. Rothschild, J. R. Andrew, W. J. DeGrip, and H. E. Stanley, “Opsin structure probed by Raman spectroscopy of photoreceptor membranes” Science **191,** 1176 (1976).
26. K. Maquelin, C. Kirschner, L.-P. Choo-Smith, N. van den Braak, H. P. Endtz, D. Naumann and G. J. Puppels, “Identification of medically relevant microorganisms by vibrational spectroscopy” J. Microbiol. Methods, **51,** 255 (2002).